Linking the Valley: Early Bronze Age Pottery and Obsidian Networks in the Araxes River Basin

Mez, Natalie Eva

Linking the Valley

Early Bronze Age Pottery and Obsidian Networks in the Araxes River Basin

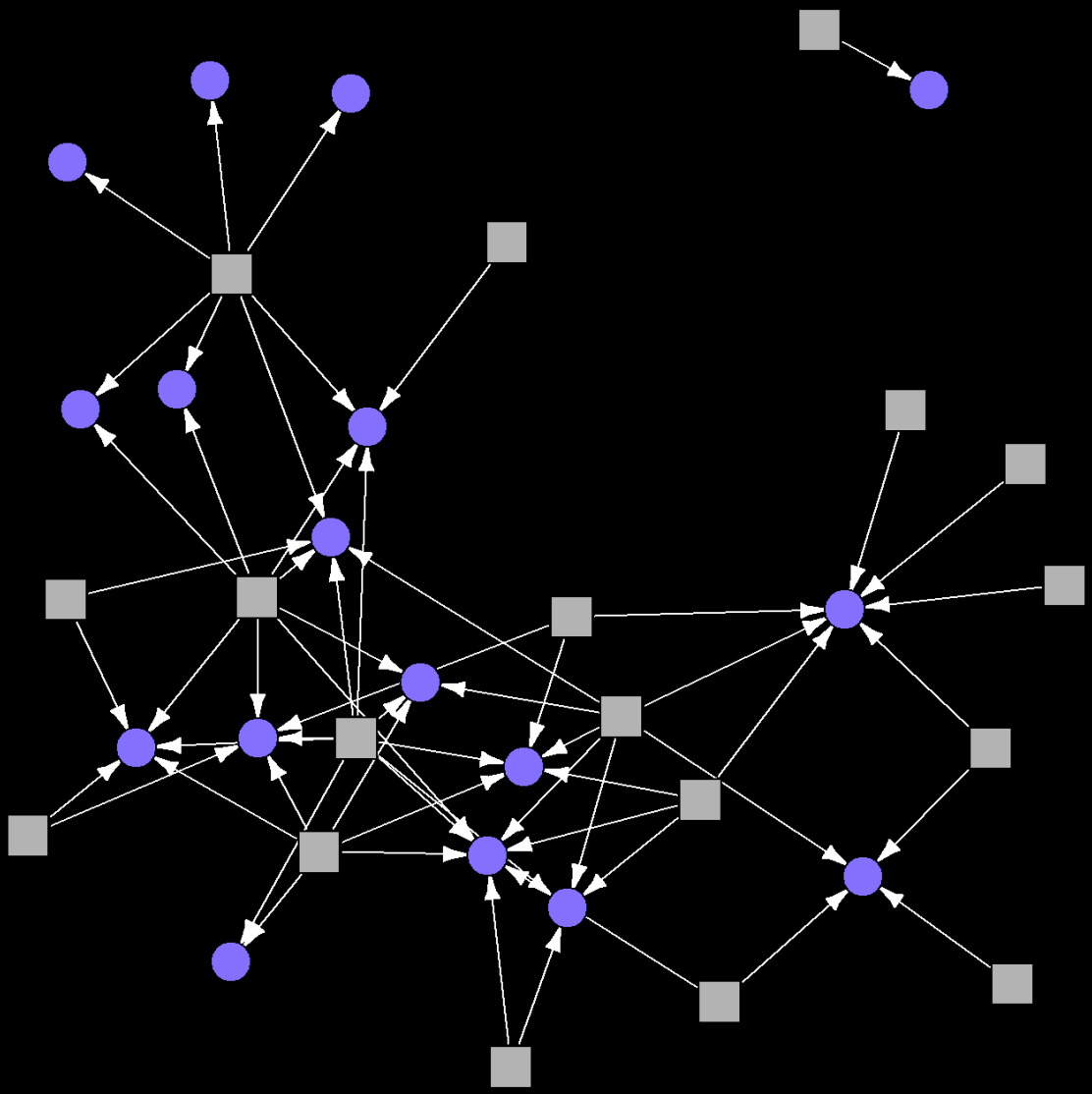

Natalie Eva Mez

Cover figure:

Bimodal network representation of obsidian provenance data (Figure by N. Mez).

Natalie Eva Mez

Student number: s3245551

Linking the Valley

Early Bronze Age Pottery and Obsidian Networks in the Araxes River Basin

Master Thesis Archaeological Science

Final Version

Course code: 1084VTSY

Supervisor: Dr. Lambers

Leiden University, Faculty of Archaeology

Frankfurt am Main, 15.06.2023

Table of Contents

List of Figures

List of Tables

List of Appendices

Acknowledgments

Like the sites in my material culture networks, I am also a single node embedded in a web of relationships. Here, I wish to express my gratitude to the many people in my academic an personal support networks.

First and foremost, I want to thank Karsten Lambers for his patience and constructive criticism throughout this lengthy thesis journey. Sepideh Maziar is to thank for sparking my interest in the archaeology of the Caucasus in the first place and for the helpful meetings we had, where she shared not only data but also advice. I also want to thank Judith Thomalsky for giving me access to her unpublished article and an insightful talk.

Lucky as I am, all my dear friends in Leiden, Frankfurt, and elsewhere supported me throughout this process with their humor and empathy. Some of them contributed to this work directly: I have to thank Stephanie for being my academic twin in general, but also specifically for her support in thorough proofreading. I also have to thank Irini for her invaluable feedback and proofreading. I want to thank Victoria for proofreading and many discussions about our theses. Juan-Marco is to thank for his willingness to discuss the perks and pitfalls of network analysis with me.

The biggest thank you goes to my parents, Shelley and Hans-Christian. They enabled me to pursue a graduate degree in Leiden – I am forever grateful for their support. I also want to thank my brother Christian for humoring me the best. Last, I must thank my husband Omar, for his endless kindness and patience.

1. Introduction

Less than two decades ago, American anthropologist Smith (2005, p. 231) stated that "the most spatially extensive material culture horizon in Bronze Age southwest Asia is absent from almost all major Western synthetic discussions of the ancient Near East." In contrast to the intensively studied city-states in Mesopotamia, the contemporaneous Kura-Araxes horizon consists of, at times, understudied villages (Batiuk et al., 2022, p. 238). Nowadays, a considerable body of research deals with the archaeology of the Caucasus, including the Kura-Araxes (Sagona, 2018).

Figure 1.1 Physical map of the Caucasus (Figure by M. Kurtubadze, accessible via https://eurasiangeopolitics.files.wordpress.com/2014/08/russia-nc-north-caucasus-physical.png).

Kura-Araxes describes an Early Bronze Age cultural horizon prevalent from the mid-4th to mid-3rd millennium BCE. The phenomenon is defined by characteristic black-burnished ceramics and material culture elements like fire installations and metal ornaments (Longford, 2015, p. 6). The Kura-Araxes

interfluve in the South Caucasus (Figure 1.1) was determined as the origin based on a combination of radiocarbon dating and pottery analysis. From there, it spread to Iran, Anatolia, and the distant Levant (Sagona, 2018, p. 214). In most research, the expansion is seen as a migration, although precise modalities are still under debate (Rothman, 2015, p. 9192). Critical issues in Kura-Araxes research are inter-site material culture similarity (Iserlis, 2010; Palumbi & Chataigner, 2014), the spread's causes (Rothman, 2016), and periodization (Badalyan, 2014).

Due to its availability, the research has had a strong emphasis on pottery. The studies on ceramics provided a means to trace the Kura-Araxes cultural horizon (Palumbi, 2008). Also, insights on ceramic technology (Iserlis et al., 2015), diet (Manoukian et al., 2022), and ritual (Sagona, 1998) were inferred from the pottery assemblages. A dearth of quantitative methods is observable when investigating the Kura-Araxes pottery. Obsidian is not as defining for the Kura-Araxes phenomenon as the omnipresent ceramics, but the vast majority of lithic material found in the Kura-Araxes homeland was obsidian (Batiuk et al., 2022, p. 292). No written sources provide information on this cultural horizon (Maziar, 2021, p. 43). For obsidian, quantitative approaches are more abundant (Barge et al., 2018).

The present research positions itself in this niche as it takes a quantitative approach to reinvestigate Kura-Araxes sites along the Araxes River Basin. The similarities in pottery decoration and shared obsidian sources are selected as proxies for possible past interactions among sites. This study aims to contribute to the critical theme of "unity and disunity" (Palumbi & Chataigner, 2014) in Kura-Araxes research by investigating aspects of similarity and diversity among Araxes Valley sites.

For the Araxes Valley, there are substantial results regarding the obsidian provenance and homogeneity of pottery décor: In her 2021 study, Maziar investigated social networks along the Araxes River Basin from the Neolithic to the Early Bronze Age. Without performing quantitative analyses, she compares the pottery decorations and obsidian provenance data at different sites based on published research, personal communication, and her fieldwork (Maziar, 2021, p. 54). Her qualitative comparison investigates how strongly geographical proximity affects the social networks in the study area (Maziar, 2021, p. 42).

Maziar (2021) concludes that the shared use of obsidian sources north and south of the Araxes hints at possible communication routes (p. 55). On the contrary, the pottery style shows no detectable connection between the sites (Maziar, 2021, p. 55). Generally, she observes that the network structures are localized (Maziar, 2021, p. 54). This study builds on Maziar's (2021) previous research by conducting network analysis based on pottery and obsidian finds. The results obtained from this study are used to reevaluate her findings critically. Thus, her results are reviewed through SNA while

Besides providing points of comparison for the network's interpretation, Maziar's (2021) study serves as an example of the methodological hurdles faced when applying SNA: The data has to be extracted from various publications and streamlined, a suitable network representation has to be chosen, the research aims to have to be translated into network terms to make them investigable, and, finally, the quantitative measures have to be interpreted archaeologically.

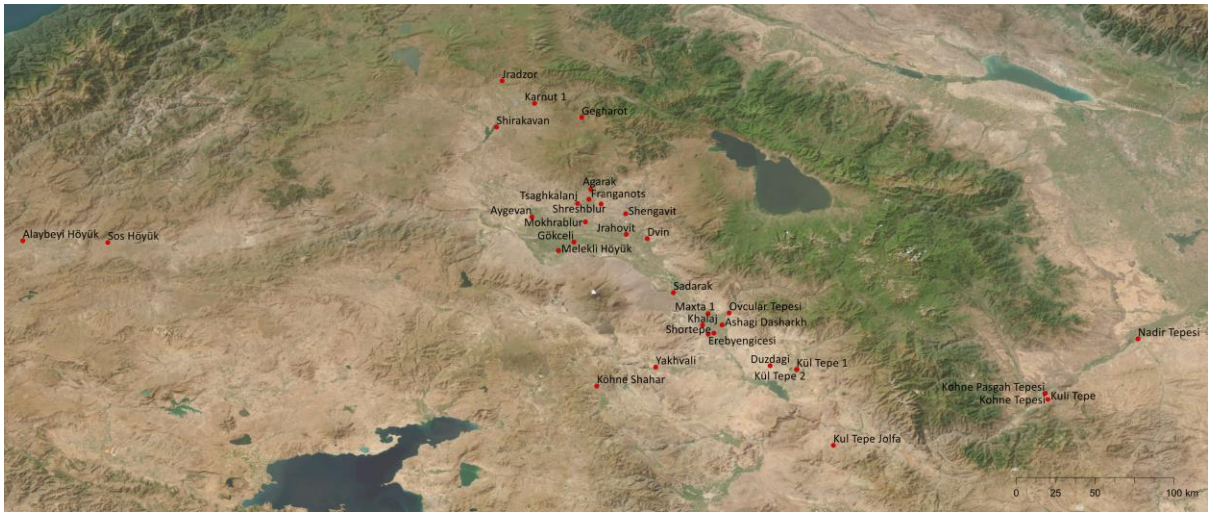

Figure 1.2 Map of sites in the database, larger version provided in Appendix 1 (Figure by N. Mez).

The datasets used in the present study constitute nominal, binarized information on pottery decoration and obsidian provenance. This data was collected almost exclusively from published research. The sites studied are located in the Araxes River Basin (Figure 1.2). Iranian localities are included south of the river, along the Khoda Afarin and Jolfa Plains. As northern tributaries of the Araxes, the Ksakh and Hrazdan Rivers connect the surroundings of Mount Aragats to the Araxes Basin (Batiuk et al., 2022, p. 298). Thus, these areas can be considered extensions of the Araxes Valley, and more sites north of the Araxes in Armenia are covered in the study area. Besides northwestern Iran and Armenia, archaeological sites in Nakhichevan (Azerbaijan) and Erzurum (Turkey) are added to the dataset. Nakhichevan is north of Iran, with the Araxes River forming the borderline. The Pasinler Plain in Erzurum marks the western extension of the Araxes River basin. Only one site from the neighboring Erzurum Plain was included.

In several instances, ceramics and obsidian were found at the same site. However, more research on ceramics is available for this study than on obsidian. Investigating obsidian provenance requires specialized equipment depending on the choice of analytical technique, i.e., X-ray fluorescence spectrometers (Orange et al., 2021b). Therefore, the obsidian network contains fewer sites than the pottery network. Regarding the sites where ceramics and obsidian were found, one must differentiate

between the surveyed and excavated sites. For the surveyed sites, the surface finds mainly consist of ceramic sherds and obsidian tools (Maziar & Zalaghi, 2021). Meanwhile, the excavations provided more types of archaeological evidence, such as architecture, metalwork, faunal and botanical remains (Marro et al., 2009), and burials (Işıklı, 2019). Regarding the chronological frame of the thesis, the later Kura-Araxes period from ca. 2900 to 2400 BCE is investigated exclusively.

The methodology combines the Jaccard similarity statistic with Social Network Analysis (SNA). This approach is executed in the R software environment. Before the network analysis, the pottery style and obsidian provenance data are subjected to the Jaccard similarity measure. These quantified inter-site similarities are used as the basis for the networks. This approach is scientifically relevant and innovative in multiple ways. Generally, SNA has been proven helpful for investigating questions concerning homogeneity in material culture (Dawson, 2020, p. 75). SNA combined with visibility networks in geographical information systems (GIS) (Earley-Spadoni, 2015) and least-cost path networks (Fabian, 2018) of Caucasian sites were used effectively in archaeological research. Regarding the selected materials, ceramics (Birch & Hart, 2021) and obsidian finds (Ladefoged et al., 2019) have been successfully demonstrated as the basis for SNA in a multitude of studies (Mills, 2017, p. 388).

Specifically, for the Kura-Araxes cultural horizon, SNA is absent from the current state of research, although geographic networks of obsidian exchange and procurement have been addressed (Barge et al., 2018). SNA can systematically compare many sites in different regions of the Kura-Araxes cultural horizon within a single methodological framework instead of point-by-point comparisons between settlements. Community detection algorithms, a tool for SNA, can group the sites in the networks that are connected densely (Traag et al., 2019). Whether these groups, based on intra-site similarities, appear to be heavily influenced by location can inform about processes underlying the assimilation of material culture and resource use, i.e., the central question of Kura-Araxes migration. In this study, SNA allows a methodical comparison of various data sources, such as pottery and obsidian data. This comparison is possible because the same measurements and community detection algorithms are applied to these similarity networks.

SNA, combined with a sufficiently documented workflow, provides a quantitative approach and a defined vocabulary to make the research outcomes more comprehensible, reproducible, and replicable. Furthermore, some researchers discuss investigations with network science terminology, even though they do not perform network analysis (Maziar, 2021). Such an approach makes applying SNA to these case studies appear sensible. Besides SNA, quantifying inter-site similarity through calculating Jaccard indices is new to Kura-Araxes pottery and obsidian research. So far, descriptive statistics have been

employed to investigate pottery assemblages for individual sites (Palumbi, 2008). Moreover, this study highlights the benefits and pitfalls of applying SNA to previously conducted research.

Wehner (2019) describes two basic assumptions regarding material culture similarity networks. First, similarity structures inform about the degree of convergence and, thus, about the existence and intensity of social interaction. Second, the interaction causes convergence (Wehner, 2019, p. 101). He points out that similarity in this context only implies interaction potentials (Wehner, 2019, p. 91). In other words, material culture similarity may indicate the likelihood of past interactions between settlements, not serve as proof of them. The nature of these "interactions" highly depends on the archaeological context. On the regional scale, trade (Sagona, 2018, p. 272), migration (Palumbi & Chataigner, 2014, p. 254), and seasonal transhumance (Orange et al., 2021b, p. 928) are all possible points of contact between Kura-Araxes communities.

This thesis defines similarity as "the measure of resemblance, what corresponds to the number of elements shared by two or more entities. The higher this number is, the higher the similarity is" (Achino et al., 2017, p. 85). This definition allows similarity to be analyzed through a quantitative approach. Dissimilarity is conceptualized as complementary to similarity (Carlson, 2017, p. 297). Connectivity is a central concept in archaeological network research, commonly defined as "the social and geographical interdependence of small-scale, locally specific phenomena […] with a dynamic network of relations enjoyed by them with the wider world" (Skeates, 2009, p. 556). This definition is vague and must be sharpened into specific phenomena the case study may address.

For the present research, the methodology can only address similarities in pottery style and obsidian procurement. What is insightful in this case study is not primarily the connectivity but rather the similarity patterns. In network terms, connectivity means a connection between any two nodes in the graph, while disconnectivity means a pair of nodes without a connection (Voloshin, 2009, p. 15). These connections result from the data selection and methodological choices; therefore, the connectivity in the network is as intense as the research design makes it. Because the similarity networks are based on shared features, the fact that nodes in the networks are connected is not revelatory, as this information is already available during data collection. The insightful aspect is how and to which extent the nodes are connected.

This thesis aims to reveal similarity patterns among sites along the Araxes River Basin during the Kura-Araxes period. Therefore, the following archaeological research question is investigated:

- *How similar are the sites regarding pottery décor and obsidian source use, and what do these similarities imply about regional homogeneity and possibly migration?*

The related subquestions are:

- *What are the characteristics of the pottery and obsidian similarity networks?*
- *How do the network structures differ for the sites shared between the pottery and obsidian networks?*

Creating and discussing these networks is only part of the challenge. The fundamental issue lies in applying SNA to the case study. Therefore, a second methodological research question is pursued:

- *To what limits can SNA be applied to regional archaeological studies, such as Maziar (2021), which were not intended for SNA?*

The related subquestions are:

- *Which research design and data selection changes were necessary to adapt Maziar's case study?*
- *How do the results of the SNA relate to Maziar's findings?*

Following this introduction, Chapter 2 presents the thematic and methodological background. Chapter 2.1 briefly overviews the Kura-Araxes cultural tradition relevant to this study, while Chapter 2.2 introduces SNA in archaeological research. Chapter 3 discusses the materials and methods used in this thesis. Chapter 3.1 introduces the site clusters, based on their locations, that are the basis for further analysis. Chapter 3.2 presents the collected and processed data on the pottery decorations at Araxes Valley sites. Following this, Chapter 3.3 presents the data on the obsidian finds and sources. These two sections also address the limitations of the datasets.

Next, the selected methodology is described in Chapter 4. The individual steps in the workflow and methodological choices are explained in the five subchapters. The six segments in Chapter 5 present the results corresponding to the subchapters in the methods section. Subsequently, Chapter 6.1 discusses the possible impact of location and geographical proximity on the case study. Chapter 6.2 presents the patterns and trends observed in the networks and the interpretation thereof. This segment is followed by Chapter 6.3, which discusses the results compared to Maziar's investigation specifically and Kura-Araxes research generally. Chapter 6.4 places the results in context with other studies on archaeological similarity networks. The last section, Chapter 6.5, discusses the biases and limitations of the present work. Finally, Chapter 7 answers the research questions and showcases potential avenues for future research that have emerged throughout this study.

2. Background

2.1 Kura-Araxes Cultural Horizon

This segment briefly introduces the archaeological context in which the study area is embedded. After addressing the terminology and chronology, a brief overview of the geography and research history in the Araxes River Basin is provided. Subsequently, assumptions about Kura-Araxes society are touched upon. Last, selected aspects of Kura-Araxes material culture are presented, with particular attention given to ceramic and obsidian finds.

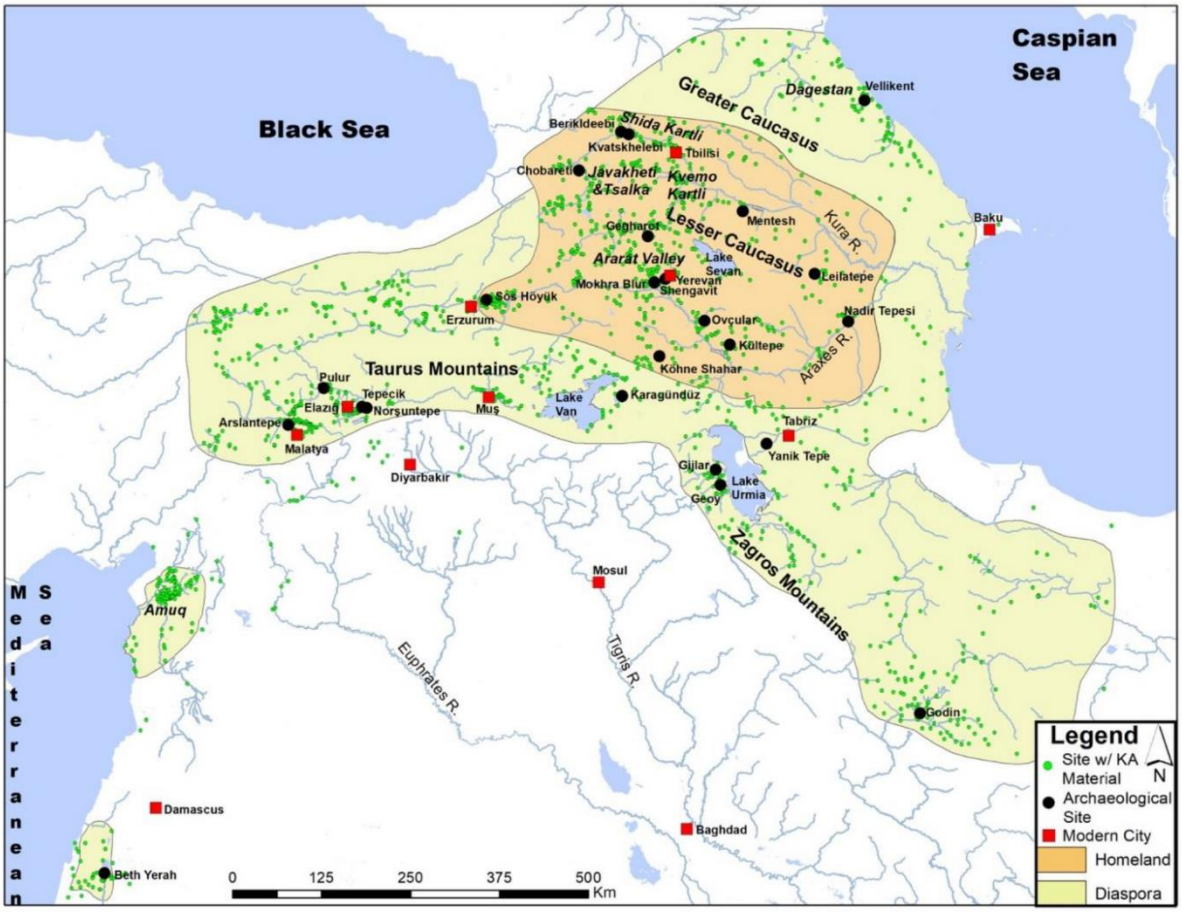

Figure 2.1 Map of Kura-Araxes extension (Batiuk et al., 2022, Figure 1).

The Kura-Araxes cultural horizon is not understood as a uniform society but rather a multitude of sites sharing commonalities despite their local variations (Rothman, 2018, p. 127). Batiuk et al. (2022) provide an up-to-date and in-depth elaboration on the Kura-Araxes phenomenon. Soviet archaeologist Kuftin coined the expression in the 1940s, highlighting the geographic origin of the cultural tradition between the rivers Kura and Araxes (Sagona, 2018, p. 215). Although this name might be the most popular nowadays, other terms for the same phenomenon co-exist. Alternatives for the supra-

regional level are Early Transcaucasian Culture and, less frequently, Outer Fertile Crescent (Palumbi, 2008, p. 8). Local names for the cultural tradition are based on specific sites, such as Shengavitian in Armenia, Karaz in Anatolia, Khirbet Kerak in Israel, and Yanik in northwestern Iran (Rothman, 2016, pp. 217–218).

The Araxes River is one of the natural routes connecting eastern Anatolia with the South Caucasus, making the Araxes Valley a vital crossing point (Yardimciel et al., 2018, p. 70). Besides the Kura, the Araxes is the largest river in the South Caucasus, extending over 1072 kilometers. The river flows southward from its sources in Erzurum into the Ararat Plain. As the Araxes continues southeastward, it enters Nakhichevan marking the borders with Armenia and Iran. It returns eastward through the Karadağ and Talysh ranges before emptying into the Azerbaijan Kura (Palumbi, 2008, p. 4). Batiuk et al. (2022, p. 238) and Sagona (2018, p. 214) consider the sites in the Araxes Valley south of the river at the edge of the Kura-Araxes homeland. Contrarily, Maziar (2021) conceptualizes this part of the study area as a Kura-Araxes diaspora (p. 47).

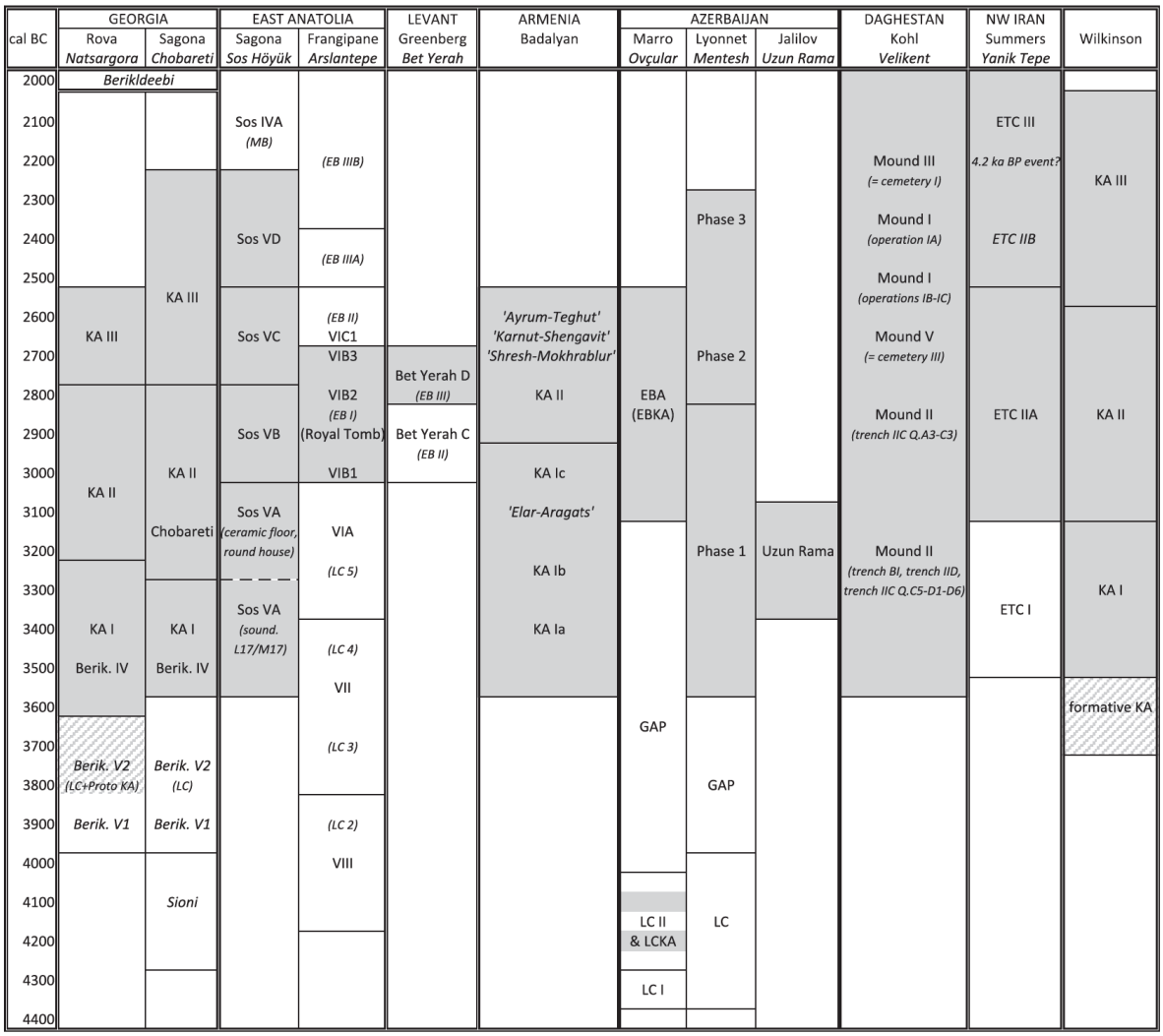

Figure 2.2 Periodization of the Kura-Araxes phenomenon (Palumbi & Chtaigner, 2014, Figure 1).

Despite varying perspectives concerning the homeland – diaspora dichotomy, the overall borders of the geographical expansion of the Kura-Araxes cultural tradition are expressed consensually (Figure 2.1). The periodization is a matter of discussion, as shown by the differing subdivisions in Figure 2.2. In the southern Caucasus, the Kura-Araxes spanned a timeframe from the mid-4th millennium to the mid-3rd millennium BCE (Rova, 2020, p. 361). The Kura-Araxes cultural horizon is placed within the Early Bronze Age; however, these two terms are not to be equalized (Sagona, 2018, p. 225).

Marro and Bakhshaliyev attest to the coexistence of Late Chalcolithic and Kura-Araxes pottery traditions in the Middle Araxes Basin, challenging the usual periodization (Marro et al., 2009, p. 54). This hypothesis is debated because the ceramics are more similar to the pottery of the 3rd millennium BCE, i. e. the dimple decoration and the lack of radiocarbon dates (Palumbi & Chataigner, 2014, p. 250). In this thesis, these ceramics under debate are excluded. Generally, inconsistent pottery typologies and a dearth of radiocarbon dates make fine-grained chronological analysis difficult (Sagona, 2018, p. 224).

The period investigated in this study covers the late 4th to mid-3rd millennium BCE. Across the study area, this timeframe is divided differently. At Sos Höyük, this period corresponds to phases mid-VB and VC; at Gegharot, it is described as EB II, and at Nadir Tepesi simply as Kura-Araxes (Batiuk et al., 2022, p. 242). For the northern part of the Araxes Valley, the timeframe corresponds to Kura-Araxes II according to Badalyan's periodization. Maziar proposes a subdivision with Kura-Araxes II from 2900 to 2700-2600 BCE and Kura-Araxes III from 2700-2600 to 2400 BCE for the southern Araxes Basin (Maziar, 2019, p. 55).

Figure 2.3 Small mound site, Kohne Tepesi, south of the Araxes (Zalaghi et al., 2021, Figure 4).

Figure 2.4 Large mound site, Köhne Shahar (Alizadeh et al., 2015, Figure 2)

The total number of documented Kura-Araxes sites ranges from more than 700 (Sagona, 2018, p. 216) to over 1000 (Rothman, 2018, p. 127). Kura-Araxes settlements are usually small mounds (Figure 2.3), their size ranging between 1 and 2 ha. These villages are often single-period sites, and many are erected on virgin soil or follow an occupational gap in the stratigraphy (Sagona, 2018, p. 218). However, more extensive settlements exist (Figure 2.4), like the 6 ha site of Köhne Shahar (Abedi & Omrani, 2015, p. 56). The architecture is circular in northwestern Iran (Figure 2.5), Nakhichevan, and the Ararat Plain. These round mudbrick houses were built on stone foundations and varied in size (Sagona, 2018, p. 235). Fortifications are unusual for Kura-Araxes sites, but massive walls were discovered at Shengavit, Köhne Shahar, and Sos Höyük (Sagona, 2018, p. 241).

Figure 2.5 Round mudbrick architecture at Kohne Pasgah Tepesi (Maziar, 2010, Figure 10).

This brief research history on Kura-Araxes sites in the Araxes Valley includes the major excavations and surveys. An overview of all sites and their associated publications is provided in Table 3.2 and Table 3.5. From 1994 to 2000, Sagona excavated at Sos Höyük west of the Araxes Basin (Sagona, 2000, p. 329). 41.34 km further to the west, Mehmet Işıklı conducted salvage excavations at Alaybeyi Höyük from 2016 to 2017 during a gas pipeline construction project (Işıklı, 2019, p. 144). 337.25 km to the east, north of the river in Nakhichevan, Ristvet, Baxşaliev, and Aşurov revisited Maxta 1 in 2006. Since 2008, a long-term Azerbaijani excavation project has been ongoing (Ashurov et al., 2020, pp. 40–41). Another Kura-Araxes site in Nakhichevan, Ovçular Tepesi, is only 10.3 km from Maxta 1. During Soviet times, much of the Kura-Araxes layers at Ovçular Tepesi were removed (Maziar, 2019, p. 60). However, recent excavations yielded some Kura-Araxes material (Marro et al., 2009). 48.67 km down the river, Abibullaev first excavated Kültepe 1 between 1955 and 1964 (Maziar, 2019, p. 59). Marro and Bakhshaliyev continued the excavations from 2012 to 2018 (Marro et al., 2019). In the 1980s, Aliyev excavated Kültepe 2, only 250 m from Kültepe 1 (Maziar, 2019, p. 60). In 2006, Bakhshaliyev and Ristvet conducted new excavations as part of their Nakhichevan survey (Ristvet et al., 2011).

More Kura-Araxes settlements are located in the remaining part of the northern Araxes Basin. Nevertheless, systematic information is missing, and the Nagorno-Karabakh area is hardly accessible because of the political conflict between Armenia and Azerbaijan (Maziar, 2019, p. 60). Further to the north, the Early Bronze Age sites in Armenia surrounding Mount Aragats are comprehensively published. Key excavated sites included in this study are Agarak (Ashtarak), Karnut 1, Franganots, Jradzor, Shirakavan, and Tsaghkalanj, most of which were excavated in the 1970s and 1980s by Armenian archaeologists (Badalyan & Avetisyan, 2007).

In the southern part of the Araxes Basin, Alizadeh excavated Nadir Tepesi in 2006 (Alizadeh et al., 2018), the only excavated Kura-Araxes site in the Mughan Plain (Maziar, 2019, p. 60). 164.31 km further to the west, in the Jolfa Plain, Abedi and Omrani excavated Kul Tepe Jolfa in 2014 (Abedi & Omrani, 2015). The western neighbor to the Jolfa Plain is the Khoda Afarin Plain, where Maziar and Zalaghi excavated Kohne Pasgah Tepesi (Maziar, 2010) and Kohne Tepesi in 2006, only ca. 270 m apart (Zalaghi et al., 2021). To understand the Early Bronze Age settlement patterns in the southern part of the Araxes River Basin (Maziar & Zalaghi, 2021, p. 37), the Araxes Valley Archaeological Project was carried out in 2013 (Maziar & Zalaghi, 2021). The project consisted of a survey of 110 km along the Araxes from the Khoda Afarin to the Jolfa Plain (Maziar, 2019, p. 60). It yielded only one site, Kuli Tepe, securely assigned to the Kura-Araxes period (Maziar & Zalaghi, 2021, p. 43).

Substantial altitudinal differences characterize the archaeological sites along the Araxes Valley. Most of the settlements are located in the alluvial zone of the Araxes Valley, with altitudes ranging from

about 600 to 900 m asl, or on higher mountain valleys, gorges, and plateaus, with altitudes ranging from about 1700 to 2200 m asl. Shengavit (990 m asl), Gegharot (2100 m asl) (Batiuk et al., 2022, p. 299), Ovçular Tepesi (876 m asl) (Maziar, 2015, p. 33) and Duzdağı are located on terraces or natural hills along the Araxes Valley (Batiuk et al., 2022, p. 299). In contrast, Jrahovit (ca. 800 m asl), Dvin (ca. 900 m asl) (Haroutunian, 2016, p. 101), Mokhrablur, Aygevan, Maxta, Kültepe 1 are settlement mounds in valley bottoms, floodplains, and alluvial plains. The sites in Nakhichevan are located at about 800 m asl (Batiuk et al., 2022, p. 299). Shreshblur is located at ca. 900 m asl, Franganots at ca. 1000 m asl, and Shirakavan at ca. 1500 m asl (Haroutunian, 2016, p. 101). The sites of Kohne Pasgah Tepesi (330 m asl) and Kultepe Jolfa (968 m asl) at the eastern end of the Araxes are much lower than the surrounding areas (Batiuk et al., 2022, p. 306). Far to the west, Sos Höyük in the Erzurum Plain is located at an 1800 m asl (Maziar, 2015, p. 33).

According to Maziar (2015), elevation does not appear to have been a determining factor for settlement choices south of the Araxes in northwestern Iran. She proposes that this is caused by different communities inhabiting the sites or the same groups having flexible subsistence strategies (p. 33). Haroutunian (2016) observes that the altitudes of settlement locations did not shift from the EB I to EB II for the Armenian settlements. Additionally, he notes an increase in sites in northeastern Armenia, closer to copper and obsidian sources (Haroutunian, 2016, p. 102). Although the region is rich in mineral deposits and other natural resources (Batiuk et al., 2022, p. 285), many of these, besides obsidian, are hard to integrate into provenance and consumption networks. Despite the knowledge about salt mines exploited during the Early Bronze Age (Marro, 2021), it is impossible to retrieve information about where the salt from the mine was consumed. Metals can be traced, but many sources, as well as re-use, make provenance analysis challenging.

Regarding social stratification, Palumbi and Chataigner (2014) describe the Kura-Araxes communities as lacking centralized common institutions, suggested by the collective burial practices (p. 253). According to Sagona (2018), the Kura-Araxes house is a center for economic, craft, and ritual activity. He relates this interpretation to a kin-ship-based society (p. 280). The communities inhabiting these villages combined agricultural and pastoral activities in their subsistence strategies (Palumbi & Chataigner, 2014, p. 253). Longford (2015) sees this as a reason to reconsider transhumant pastoralism as an explanation for the Kura-Araxes expansion. She suggests that the spread was fueled by communities searching for new farmland (Longford, 2015, p. 171). Sagona (2018) lists the most popular yet debated explanations for the expansion: overgrazing of pastures and population pressure, climate change, search for metal ores, access to more trade networks, displacement due to intrusions from the North Caucasus into the homeland (p. 272).

Kura-Araxes pottery of the South Caucasus was initially brown, gray, or mottled black. The color scheme with black exteriors and red interiors became prevalent by the end of the fourth millennium BCE (Palumbi & Chataigner, 2014, p. 249). The pottery is handmade, slab or coil constructed, and probably fired in a pit (Rothman, 2016, p. 221). Most Kura-Araxes pottery is grit-tempered, and the surface is burnished (Figure 2.6). Distinctive morphological traits are rail-rims and so-called Nakhichevan lugs (Figure 2.7). Incised, relief or grooved decorations form geometric motifs of varying complexity (Marro et al., 2009, p. 54). Palumbi describes frequent Kura-Araxes vessel shapes as "truncated, conical necked jars with ovoid bodies, large S-shaped bowls, and circular lids" (Palumbi, 2017, p. 115). Lids are found on closed and open forms (Palumbi, 2017, p. 115). Petrographic studies show the use of local clay sources for the production of Kura-Araxes vessels in host areas like Anatolia (Kibaroğlu et al., 2011, p. 3082), the Levant (Iserlis, 2010) and the Araxes Valley (Maziar, 2021). For the manufacture of the Kura-Araxes pottery, household production is assumed. This production mode might be one of the causes of diversity in decorations and shapes as more potters are involved than would be in workshop production (Batiuk et al., 2022, p. 283).

Figure 2.6 Sherd of a burnished jar with dimple decoration, Kohne Pasgah Tepesi collection CC BY 4.0 (Figure by S. Maziar).

Figure 2.7 Sherd of a burnished bowl with a Nakhichevan handle, Kohne Tepesi collection CC BY 4.0 (Figure by S. Maziar).

The reliance on pottery to investigate the possible migration patterns has been criticized as a "pots equal peoples" approach (Rothman, 2016, p. 221). In the present study, migration is not equated with similarity in ceramics. Similar pottery and obsidian procurement are used as proxies for interactions, the nature of which cannot be determined unambiguously. Furthermore, Palumbi challenges the assumption that the typical red-black burnished ware necessarily identifies Kura-Araxes sites. He stresses how such wares emerged contemporaneously in Eastern Anatolia and the Upper Euphrates region (Palumbi, 2008, p. 311). Additionally, in northwestern Iran, the Iron Age pottery is grey-black

(Sattarnezhad et al., 2020, p. 121), similar to Kura-Araxes sherds, making a chronological assessment of surveyed sites based on surface sherds even more challenging.

Besides pottery, other forms of material culture are also considered part of the Kura-Araxes cultural package. Fixed hearths in the houses, often circular with a tri-leaf-shaped hole (Figure 2.8), appear frequently. Also, portable hearth stands (andirons) in rectangular or horseshoe shapes, often with zoo- or anthropomorphic designs, are found at many sites. Metal objects made from arsenical bronze (Figure 2.9) were often discovered in burials. Common metal artifacts are clothing pins with spiral heads, spiral bracelets, and coiled earrings or hair rings (Longford, 2015, p. 6).

Figure 2.8 Hearth from Shengavit (Sagona, 2018, Figure 5.7).

Figure 2.9 Bronze pendants and beads from Gegharot (Badalyan et al., 2014, Figure 11).

Over 20 deposits of high-quality obsidian are known to exist in Armenia's volcanic formations (Badalyan, 2021, p. 431). Obsidian was an essential raw material for Kura-Araxes societies. Over 90% of chipped stone objects were made from it. The remaining lithic assemblage was made from flint (Badalyan, 2021, p. 430). Various productive processes used obsidian tools, including potting, cooking, butchery, farming, leather-, wood-, and cloth-working (Batiuk et al., 2022, p. 291). As for pottery manufacture, household production is also assumed for the lithic industry. The obsidian toolkit comprises blades, scrapers, cutters, and gravers. The most studied artifact group is arrowheads. Batiuk et al. (2022) attribute arrowhead specialization to individual experts instead of special workshops (p. 292). Obsidian was added as a temper during pottery manufacture (Batiuk et al., 2022, p. 291) and used as jewelry, figurines eyes, and part of the burial assemblage (Badalyan, 2021, p. 430).

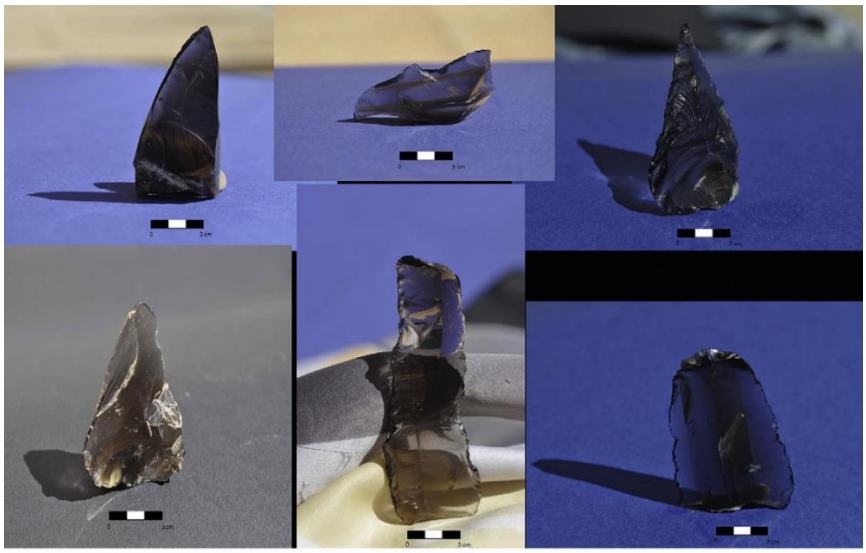

Figure 2.10 Obsidian finds from Kul Tepe Jolfa (Khademi Nadooshan et al., 2013, Figure 5).

The presence of obsidian at many Kura-Araxes sites and known deposits in the region has enabled scientists to trace past distribution through provenance analysis. Maziar (2021) has demonstrated that obsidian paired with pottery data aids in investigating possible networks (p. 54). Besides, provenance studies based on individual sites (Khademi Nadooshan et al., 2013), local areas (Orange et al., 2021a), and large-scale regional studies (Orange et al., 2021b) were conducted.

This segment dealing with the archaeological context highlighted how the materials used in this thesis are part of an archaeological phenomenon spanning hundreds of villages across a millennium and a large region. The relevance of ceramics and obsidian in Kura-Araxes research was emphasized. Next, it is necessary to clarify the main points of applied SNA to comprehend this study's methodological choices and workflow.

2.2 Social Network Analysis in Archaeology

This section gives a concise introduction to SNA and its basic concepts in general. Regarding archaeological SNA, the main focus is material culture networks that investigate similarity, as this approach is taken in the thesis. The Jaccard similarity coefficient will be described in brief. Finally, the limitations and potential pitfalls of this methodology are addressed.

Networks, especially in graph theory and sociology, have been studied for a long time. However, network science's emergence mainly occurred at the beginning of this century. Although networks can belong to different spheres, such as nature or technology, the same organizing principles influence them, resulting in similar structures that can be investigated using the same mathematical tools (Barabási, 2016, Section 1.3). SNA is a type of network science that targets relationships between people based on mutual interests or affiliations (Schubert et al., 2019, p. 1).

Nowadays, researchers from various disciplines use network science to tackle complexity, regardless of the specificities of their domain (Prignano et al., 2017, p. 2). Network analysis has a scientific impact on biology, computer science, and social sciences (Barabási, 2016, Section 1.6). The use of SNA in archaeological research stems from previous applications in close fields like geography or anthropology (Mills, 2017, p. 380). In the 1960s and subsequent decades, early network research in archaeology focused on spatial approaches in graph theory and geography. In the following decades, similar research was conducted.

A sociogram, the output of SNA, is the visual representation of a network. It consists of nodes (or vertices), primarily circles, and edges (or links), usually as lines. The nodes are social units (Boyd & Rocconi, 2021, p. 2), and the edges between two nodes can represent every kind of relationship (Schubert et al., 2019, p. 1). There are different types of network structures. Decentralized networks have multiple centers. In centralized networks, the nodes cluster around a main center, and a random distribution of nodes in the absence of any clusters is called a distributed network (Dawson, 2020, p. 75). In this study, the network nodes represent sites and obsidian sources, and the edges represent pottery decoration features and provenanced obsidian finds.

An essential distinction between networks is whether they are directed or undirected. A directed sociogram represents the connection between pairs of nodes according to the direction of the relationship. Undirected sociograms do not distinguish between source and target nodes in a connected pair, a dyad (Boyd & Rocconi, 2021, p. 2). For the obsidian provenance network, the obsidian must have reached the sites from the source in whatever manner. Therefore, the network can be directed. The

pottery similarity network is undirected because there is no known direction regarding shared pottery features. For comparability, the obsidian choice similarity network is undirected as well.

Moreover, the edges can be weighted or unweighted. The edges vary in strength according to their weight in a weighted network (Collar et al., 2015, p. 21). In the similarity networks produced in this study, the edge weights correspond to the Jaccard indices between the site pairs. In an unweighted network, all edges have the same strength. These edge weights are a type of edge attributes, which are data that describe the properties of a node or edge and are called node/edge attributes (Düring, 2015, pp. 2–3). These node and edge attributes can be stored in additional columns in the matrices holding the information. For this case study, a node attribute is the location-based cluster a site is located in, and an edge attribute is the weight of a connection between two sites indicated by the Jaccard index.

Networks can be unimodal, consisting of only one type of node, or bimodal, i.e., with two different types of nodes. In the present study, the pottery and obsidian similarity networks are unimodal, as the settlements are the only type of nodes. The obsidian provenance network is bimodal, as the settlements are the first type of node and the obsidian sources the second. Unimodal networks are based on adjacency matrices (Table 2.1). These square matrices hold the nodes and frequency of connections as edge weights. The node names or IDs are the row and column names. The resulting sociogram visualizes how all possible node pairs are connected by the number of shared connections (Boyd & Rocconi, 2021, p. 2). Bimodal networks are based on a different form, the incidence matrix (Table 2.2). These non-square matrices contain nodes and edges; each frequency between them is either one or zero. The row names are the nodes of the first type, and the column names are the nodes of the second type (Boyd & Rocconi, 2021, pp. 2–3).

Table 2.1 Example of an adjacency matrix.

Nodes	Node 1	Node 2	Node 3
Node 1	3	0	1
Node 2	1	2	0
Node 3	0	0	0

Table 2.2 Example of an incidence matrix.

	Type 2 nodes		
Type 1 nodes	Node A	Node B	Node C
Node 1	1	0	1
Node 2	1	1	0
Node 3	0	0	0

SNA has risen in popularity in archaeological research during the last two decades. Methodological developments influenced this upsurge. Combining a wide array of techniques, such as GIS or agent-

based models, has become more feasible; handling large datasets has become more manageable; and tools for creating complicated computer graphics of networks have become available (Mills, 2017, p. 381). Mills (2017) provides a more in-depth history of SNA in archaeological research. Furthermore, Brughmans and Peeples (2023) recently published a comprehensive textbook for SNA in archaeology.

SNA has been proven helpful for investigating questions concerning homogeneity and connectivity in material culture (Dawson, 2020). Although using material culture as the base for edges within the network can be a complex proxy for past interaction, many studies have employed this approach. The methodologies measure inter-site similarities through these material culture edges (Collar et al., 2015, p. 13). Questions of identity, social hierarchies, and the spread of innovations are a few research aims that can be addressed through material culture networks. These networks can be based on data about many artifacts, considering their raw material sources, technology, and designs. For different kinds of material culture, SNA can be based on presence/absence data (Mills, 2017, p. 387). Networks based on provenance are usually bimodal, as one set of nodes represents the sites and the other set of nodes the sources of raw material (Mills, 2017, pp. 387–388).

Due to the abundance in many archaeological contexts, networks are frequently created from pottery data. Ceramic provenance was used to investigate exchange (Mills, 2017, p. 388). Small-scale interactions between members of a learning community were studied with networks of pottery technology attributes (Mills, 2017, p. 388). Obsidian is another popular material for network analysis. A key characteristic of obsidian is its relative homogeneity within and heterogeneity between sources, giving it great interpretative potential in provenance networks (Mills, 2017, p. 388).

Following Prignano et al.'s terminology, Archaeological Similarity Networks (ASN) are a type of material culture network. In these inter- or intra-site assemblage networks, general social proximity, and possible past relations are inferred from their degree of similarity (Prignano et al., 2017, p. 1). In the unimodal ASN, the nodes usually represent assemblages at different sites, and the edges are based on the co-presence of objects or features between the assemblages. These relationships can also be visualized in a bimodal network, with the first type of node being the sites and the second type being the objects/features. The edges would signify the presence of an object/feature at a site, somewhat like in provenance networks (Prignano et al., 2017, p. 5).

Discretizing the archaeological record into categories is necessary before quantifying assemblage similarity. The frequencies of categorical attributes determine how strong an edge is, apart from the fact that they either appear or do not in the assemblage (Prignano et al., 2017, p. 5). For this study, the pottery decoration and the obsidian sources have been assigned to categories based on their descriptive terms/names. These occurrences are used as the basis for the Jaccard calculations. There is no

general answer to the most appropriate similarity measure. Nevertheless, the chosen similarity measure strongly influences the following SNA (Prignano et al., 2017, p. 7).

The Jaccard similarity coefficient, or Jaccard index, is the most popular approach to measuring the similarity between asymmetrical sets through binary attributes (Schmidt et al., 2022). The Jaccard index is calculated through "the ratio of the number of common to all unique non-zero attributes for a pair of entities" (Habiba et al., 2018, p. 65). The similarity is numerically expressed on a scale from zero to one. Zero means no similarity between the compared objects, and one means maximum similarity (Schmidt et al., 2022). Similarity measures can be converted into dissimilarities in the same manner as dissimilarity indices can be turned into similarities. This conversion is accomplished by subtracting the (dis)similarity index from the highest possible score (Carlson, 2017, p. 297).

$$\text{Jaccard}(x, y) = \frac{|S_x \cap S_y|}{|S_x \cup S_y|}$$

Figure 2.11 Jaccard formula (Habiba et al., 2018, p. 65).

With the Jaccard coefficient, an entity has more significant similarity if both attributes are present and less similarity if one is absent from either. Because the attributes absent in both sets are ignored, the Jaccard index is a convenient solution to handle scarce datasets, which are often an issue in archaeological studies (Habiba et al., 2018, p. 65). If not ignored, the absent values in both datasets would positively skew the similarity.

The Jaccard index is not the only similarity measure used in ASN. The Brainerd-Robinson coefficient is another prevalent measure for comparing archaeological assemblages in general and, therefore, often used as the basis for archaeological SNA (Prignano et al., 2017, p. 9). The Jaccard index is designed for binary data (Sacco, 2021, p. 102), whereas the Brainerd-Robinson coefficient is suitable for non-binary data (Habiba et al., 2018, p. 64). Because the data collected as binary presence/absence data can be processed efficiently with the Jaccard index, it was chosen as a similarity measure for this study. Alone or combined with similarity measures, the network density can be reduced by removing edges below a threshold as long as it does not become disconnected (Prignano et al., 2017, p. 6).

Nonetheless, similarity remains a fundamental issue in archaeological network research. If parts of the archaeological record are considered similar, they are used as an edge in the network. However, the perceived similarity is subjective and quantifying similarity remains challenging even if typological groups are fractionated into specific characteristics (Schubert et al., 2019, p. 2). The problem of subjective similarity cannot be alleviated in this study, as it is, to a certain extent, a fundamental issue of archaeological research.

Despite the promising insights SNA offers, there are pitfalls besides similarity to mind. First and foremost, because SNA can be used to investigate a multiplicity of relational research questions, they can also be affected by a multiplicity of inherent biases. Furthermore, the identified connections were not necessarily relevant in the past (Dawson, 2020, p. 76). Prignano et al. (2017) list source heterogeneity, incompleteness, and proxies for non-measurable interactions as general challenges of archaeological research (p. 3) that affect the application of SNA. Another issue concerning archaeological network analysis is that many archaeologists do not publish their datasets and a detailed workflow alongside their articles. Thus, archaeological networks often do not circulate much (Prignano et al., 2017, p. 3). This study's complete datasets, workflows, and codes are provided to mitigate this issue.

Schubert et al. (2019) point out more fallacies that may occur in archaeological network analysis. A concern mentioned is the ignorance of geographical considerations such as travel effort (Schubert et al., 2019, p. 2). Additionally, selecting the spatial scope of the network leads to biases, as by excluding settlements, possible ties might be severed (Prignano et al., 2017, p. 4). Prignano et al. (2017) remark on how archaeological networks are affected by temporal changes, as links can strengthen or weaken; connections can appear and disappear (p. 4).

Moreover, archaeological data is an incomplete representation of the past based on the archaeologist's interpretation. Consequently, edges are often only connected by a few occurrences. Furthermore, the absence of a feature does not mean it was never present. It simply shows that it has not been recorded. Therefore, the weak links in archaeological networks may be subjected to changes through new research, making them more unstable (Schubert et al., 2019, p. 2).

2.3 Chapter Summary

This chapter introduced the background of the thesis. The present study focuses on sites in and close to the Araxes River Basin, an essential corridor for movement throughout the region's history. The sites are located on different terrains and altitudes and were occupied from the late 4th to mid-3rd millennium BCE. Usually, the Kura-Araxes settlements are small mound sites with circular mudbrick architecture. The kinship-based and unstratified communities combine agricultural and pastoral activities in their subsistence strategies. The characteristic black and red burnished pottery is decorated in varying techniques, and the imagery ranges from simple to complex geometric motifs. Obsidian is the

primary material for the Kura-Araxes lithics. The obsidian tools, as well as the ceramics, are crafted locally in household production.

This cultural horizon is investigated using SNA. Our case study's network connections are based on intra-site similarities in ceramic décor/obsidian source choice. These similarities are calculated through the Jaccard coefficient. Different types of networks are part of this study: unimodal and bi-modal, weighted or unweighted edges, and directed and undirected. Other archaeologists employed SNA of ceramic similarity and obsidian provenance to answer questions related to social proximity and raw material procurement systems. However, similarity-based SNA bears several risks, i.e., misinterpretation of absences, irrelevant connections, and shortcomings in addressing geographical factors. With this knowledge of the Kura-Araxes cultural horizon and SNA in archaeology, the archaeological and methodological context for the case study is set, and we can turn to the characteristics and limitations of the datasets.

3. Materials

3.1 Location-based Site Clusters

All the sites included in the network are located in the Araxes River Basin and its adjacent areas in Iran, Armenia, Azerbaijan, and Turkey. These current political boundaries only partially reflect geographic realities that could have influenced daily life in the past. In particular, Gökçeli and Melekli Höyük are located in Anatolia, although they are much closer to the Armenian settlements than to the other two Turkish sites, Alaybeyi and Sos Höyük. The sites in northwestern Iran are also located on different terrains, sometimes far from each other. Therefore, all sites are grouped into location-based clusters determined by proximity. These clusters will be compared to communities based on similarities in the network structures to juxtapose homogeneity in material culture and spatial patterns.

Other factors besides proximity influence mobility in this area. According to Chataigner and Barge (2008), snow is abundant above 2000 m asl during winter. However, these areas are pasture lands during summer (Chataigner & Barge, 2008, p. 374). Paleo-environmental studies determined steppe-type vegetation, enabling visibility and ease of movement within plains and valleys. Additionally, there were many crossing points to traverse the rivers, which were often narrow streams (Chataigner & Barge, 2008, p. 374). Therefore, in Clusters 3 and 6, sites south and north of the Araxes were grouped. Otherwise, the sites in a cluster are on the same riverside. The main aspect challenging travel in this area lies in the steep river valleys (Chataigner & Barge, 2008, p. 374) and altitudinal variations pointed out in Chapter 2.1. For the studied sites, the altitudes range from 330 m asl at Kohne Pasgah Tepesi in the east (Batiuk et al., 2022, p. 306) to 1800 m asl at Sos Höyük in the west (Maziar, 2015, p. 33).

Figure 3.1 Map of location-based site clusters (Figure by N. Mez).

Table 3.1 Location-based site clusters.

Location cluster	Sites	No.	Modern regions
1	Alaybeyi Höyük Sos Höyük	2	Anatolia
2	Gegharot Jradzdor Karnut 1 Shirakavan	4	Armenia
3	Agarak Aygevan Dvin Franganots Gökçeli Jrahovit Melekli Höyük Mokhrablur Shengavit Shreshblur Tsaghkalanj	11	Anatolia, Armenia
4	Köhne Shahar Yakhvali	2	Northwestern Iran
5	Ashagi Dasharkh Erebyengicesi Khalaj Maxta 1 Ovçular Tepesi Sardarak Shortepe	7	Nakhichevan
6	Duzdağı Kültepe 1 Kültepe 2 Kul Tepe Jolfa	4	Nakhichevan, northwestern Iran
7	Kohne Pasgah Tepesi Kohne Tepesi Kuli Tepe Nadir Tepesi	4	Northwestern Iran

Several site clusters are visible based on their locations on the map in Appendix 1 (Figure 3.1). The two sites in Cluster 1 are located in the neighboring Erzurum, and Pasinler plains in Anatolia (Işıklı, 2019). Cluster 2 features sites in the Shirak Plain (Badalyan & Avetisyan, 2007) and the nearby Tsaghahovit Plain in Armenia (Badalyan et al., 2014). The sites in Cluster 3 are all located in the Ararat Plain, in Anatolia and Armenia. Cluster 4 comprises two sites in the Shahar (Alizadeh et al., 2015) and Maku valleys (Kleiss & Kroll, 1979) located in the foothills of the Zagros Mountains in northwestern Iran. Cluster 5 features the sites at the Arpaçay-Araxes confluence on the Sharur Plain in Nakhichevan, Azerbaijan (Ashurov, 2002). The sites in Cluster 6 are located on the Nakhichevan Plain (Ristvet et al.,

2011). Cluster 7 contains sites in the Khoda Afarin Plain (Maziar & Zalaghi, 2021). Nadir Tepesi and Kul Tepe Jolfa are not close to other sites but are grouped with the sites in the nearest cluster to prevent pre-determined isolation. Nadir Tepesi in the Mughan Plain is connected to the Khoda Afarin Plain through the Araxes Valley and therefore included in Cluster 7. Kul Tepe Jolfa is added to Cluster 6 as it lies closest to it, and the Araxes Valley provides a corridor between the Jolfa and Nakhichevan plains (Abedi et al., 2014).

The clusters have different sizes: the most extensive features 11 sites, and the second largest seven. Three remaining clusters contain four sites, and two have two sites each. The imbalanced cluster sizes can introduce biases in network metrics. This bias may overrepresent larger site clusters, overshadowing patterns within smaller clusters. Additionally, due to sampling bias, smaller clusters may have fewer opportunities for connections because of their relatively lower representation.

3.2 Pottery from Araxes Basin Sites

After detailing these spatial divisions, the temporal frame is revisited. The studied layers at these sites date to the Kura-Araxes II period (ca. 2900 to 2400 BCE), as mentioned in Chapter 2.1. The Kura-Araxes I sites in the study area are disregarded to reduce the risk of integrating non-contemporaneous data in the network representations. If the sites were occupied during multiple Kura-Araxes periods, the ceramics were only taken from levels corresponding to Kura-Araxes II. Apart from the salt mine Duzdağı (Marro, 2021), all investigated sites are interpreted as villages of varying sizes and are primarily mounds. More general information about the sites can be found in the publications listed in Table 3.2.

The data had to be extracted from published research, as online repositories exist only for the ceramic assemblages from Shengavit (Rothman, 2022) and the ArAGATS project (Khatchadourian et al., 2023). These databases were not used because the ceramic data cannot be filtered according to decoration and downloaded for efficient processing. The recent establishment of a crowd-sourced online database of sites with Kura-Araxes material (Batiuk et al., 2022) was also unusable for this study. The brief information provided for the sites varies in detail and cannot be exported from the website, thus being accessible but hardly interoperable. Most importantly, the database does not include pottery or obsidian data.

The pottery sherds are distributed among different countries and institutions. Since this approach only requires digital data, no direct access to the material is needed, although it would have been preferable. The decorative features were recorded from site reports, monographs, and papers. As the data is published, it was processed and edited to some degree. In most cases, the data was not presented in tabular form but had to be extracted from text passages. Some of the publications were only available in Azerbaijani. Therefore machine-translated versions of the documents were relied upon, possibly causing errors. Only for Kuli Tepe was raw data provided (Maziar & Zalaghi, 2021, p. 43).

Especially in Armenia, relevant excavations were conducted many decades ago. Therefore, the original excavation reports are not accessible and cannot be machine-translated. Badalyan's (2014) article was used as the primary source for these sites. However, it is unclear if he appropriately represented the diversity in decorative techniques and motifs at the different sites (Badalyan, 2014). Therefore, the pottery similarity network might overemphasize the similarity between Mokhrablur, Shreshblur, and Jrahovit and between Shengavit, Dvin, and Aygevan.

The number of sites in the network is lower than that mentioned in Maziar's (2021) article because the ceramics are not published sufficiently for several settlements or the publications are still in preparation. There are data gaps when it comes to the sites Angeghakot, Narinkala, Uyts, Goris, and Amazd in the Syunik region of Armenia (Kroll, 2006), Shah Tepesi, Khan Tepesi, and Pasgah Tepesi in northwestern Iran (Alizadeh et al., 2018), and Şorsu, Zirinclik and Uçan ağıl in Nakhichevan (Marro & Stöllner, 2021), only to name a few.

The site's pottery assemblages will be compared based on the decoration techniques and motifs. Comparing the quantities would intensify the biases based on the type of fieldwork, as excavations yield higher amounts of pottery than surveys. Furthermore, the site sizes vary considerably, i.e., from 0.2 ha for Kohne Tepesi (Zalaghi et al., 2021, p. 76) to 6 ha for Kul Tepe Jolfa (Abedi et al., 2014, p. 33). This bias also affects the comparison of entire assemblages. However, it is reduced as the quantitative element is taken out. In some cases, the precise number of recovered Kura-Araxes sherds is not stated, making even the inclusion of percentages impossible.

Apart from sherd numbers, vessel shapes, sizes, morphological features, surface treatments, firing conditions, and colors were also not collected in the databases. The surface treatment, firing conditions, and color are reflected in the ware groups. The information collected on decoration techniques and motifs is recorded as binary presence/absence data. Zero means a decorative feature is absent or was not recorded, whereas one means that this particular feature is present at the site. The cultural interpretation of the motifs and the vessel functions are not addressed, as they fall outside this study's scope.

Maziar's (2021) research only draws comparisons based on the decoration (p. 43). Taking the same perspective makes it possible to compare the results obtained from the SNA to her original work. In this sense, decoration refers to features unrelated to function or manufacture, aside from the techniques used to create the motifs (Batiuk et al., 2022, p. 256). Nevertheless, the relation to Maziar's (2021) study is not the only reason for this choice. Focusing on the decoration techniques and motifs is also necessary because the detail of documentation in the publication varies a lot. Therefore, although many features could be considered, recorded features have limited overlap. To create an adequate network representation, one would have to keep only the sites published to the same degree of detail. The resulting network would exclude many sites of interest.

The non-decorative features almost always published, like the manufacturing technique or the temper, do not carry great interpretative potential regarding similarity as the pottery in the dataset is nearly always handmade and grit-tempered. Batiuk et al. (2022) acknowledge that the means of pottery production vary too little to infer relevant variations (p. 256). Nonetheless, the slow-wheel (Abedi & Omrani, 2015, p. 64) and mixed or chaff temper were also recorded at a few sites (Maziar, 2010, p. 173). The terminology regarding vessel shapes and morphological features is inconsistent, making many datasets hard to compare. Not focusing on preassigned decorative groups but collecting all decorative techniques and motifs as individual features is an attempt to avoid circular reasoning.

Reflecting on the possible causes for pottery similarities and their implications helps comprehend the explanatory potential of ceramic similarity networks. Pottery similarities between close and distant sites are caused by multiple factors, i.e., trade, migration or mobility, societal customs like cooking, serving food, storing practices, and transmitting knowledge about pottery-making (Mills et al., 2013, p. 9). This knowledge can be transmitted vertically from generation to generation or horizontally between peer groups (de Groot, 2019, p. 602). This information exchange through economic relations or population movement can be affected by geospatial proximity, as it is often more costly to interact with distant locations (de Groot, 2019, p. 602).

Nonetheless, sites close to each other may have strikingly different ceramic assemblages. These differences may be caused due to an adherence to traditions or the signaling of group identities through cultural practices (de Groot, 2019, p. 603). The similarity of ceramic decorations has further implications because the decors and motifs were used as social markers, thus, ideologically charging the imagery (Mills et al., 2013, p. 9). There is no way of knowing the nature of those relationships causing similarities, but the plausibility of the options can nonetheless be discussed. As stated in Chapter 1, trade (Sagona, 2018, p. 272), migration or cultural diffusion (Palumbi & Chataigner, 2014, p. 254), and

seasonal transhumance (Orange et al., 2021b, p. 928) are all potential types of interaction between Kura-Araxes communities.

Trade is an interaction unlikely directly related to pottery décor due to the use of local clays (Maziar, 2021) and household production of ceramics (Batiuk et al., 2022, p. 283). However, through trade with other goods or resources like obsidian or metals, people could have come into contact with non-local pottery and might have been influenced by the imagery. Despite the household production of obsidian artifacts (Maziar & Glascock, 2017, p. 36), for obsidian, trade is a more conceivable type of interaction, especially when the material is procured from (multiple) distant sites.

As a form of mobility, periodical or seasonal transhumance is highly likely to have affected Kura-Araxes communities. According to ethnographic evidence, the hot and arid summer climate forces inhabitants of the Araxes Valley to move their herds to pasturelands in higher altitudes (Chataigner & Barge, 2008, p. 378). Herders might have encountered different communities along the way or at their destination. Therefore, transhumance might explain commonalities in adjacent areas. Migration could explain similarities at close and distant sites and is most often used to understand the shared features among this vast area (Palumbi & Chataigner, 2014, p. 255).

I would deem conquest or colonization, which could theoretically cause material culture assimilation, unlikely for the rather de-centralized, unstratified, and small Kura-Araxes communities (Palumbi & Chataigner, 2014, p. 253). Furthermore, recurring interactions between neighboring sites through collaborative activities like raw material extraction, i.e., salt mining, or management of agricultural and pasture lands as well as recreational or cultic gatherings are also plausible explanations for material culture similarities, yet hard to detect in the Kura-Araxes archaeological record.

Table 3.2 Sites included in the ceramics network.

Site	Location	Modern region	Fieldwork	Ceramics publication
Agarak	3	Armenia	Excavation	Badalyan & Avetisyan, 2007
Alaybeyi Höyük	1	Anatolia	Excavation	Işıklı, 2019
Ashagi Dasharkh	5	Nakhichevan	Survey	Ashurov, 2002
Aygevan	3	Armenia	Excavation	Badalyan, 2014
Duzdağı	6	Nakhichevan	Excavation	Marro, 2021
Dvin	3	Armenia	Excavation	Badalyan, 2014
Erebyengicesi	5	Nakhichevan	Excavation	Ashurov, 2002
Franganots	3	Armenia	Survey	Badalyan & Avetisyan, 2007
Gegharot	2	Armenia	Excavation	Hayrapetyan, 2008
Gökçeli	3	Anatolia	Survey	Marro & Özfirat, 2003

Jradzor	2	Armenia	Survey	Badalyan & Avetisyan, 2007
Jrahovit	3	Armenia	Excavation	Badalyan, 2014
Karnut 1	2	Armenia	Excavation	Badalyan & Avetisyan, 2007
Khalaj	5	Nakhichevan	Excavation	Seyidov et al., 2010
Kohne Pasgah Tepesi	7	NW Iran	Excavation	Maziar, 2010
Köhne Shahar	4	NW Iran	Excavation	Alizadeh et al., 2015
Kohne Tepesi	7	NW Iran	Excavation	Zalaghi et al., 2021
Kültepe 1	6	Nakhichevan	Excavation	Marro et al., 2019
Kültepe 2	6	Nakhichevan	Excavation	Ristvet et al., 2011
Kul Tepe Jolfa	6	NW Iran	Excavation	Abedi et al., 2014
Kuli Tepe	7	NW Iran	Survey	Maziar & Zalaghi, 2021
Maxta 1	5	Nakhichevan	Excavation	Ashurov et al., 2020
Melekli Höyük	3	Anatolia	Survey	Marro & Özfirat, 2003
Mokhrablur	3	Armenia	Excavation	Badalyan, 2014
Nadir Tepesi	7	NW Iran	Excavation	Alizadeh et al., 2018
Ovçular Tepesi	5	Nakhichevan	Excavation	Marro et al., 2009
Sadarak	5	Nakhichevan	Survey	Bakhshaliyev & Seyidov, 2013a
Shengavit	3	Armenia	Excavation	Badalyan, 2014
Shirakavan	2	Armenia	Excavation	Badalyan & Avetisyan, 2007
Shortepe	5	Nakhichevan	Excavation	Bakhshaliyev & Seyidov, 2013b
Shreshblur	3	Armenia	Excavation	Badalyan, 2014
Sos Höyük	1	Anatolia	Excavation	Sagona, 2000
Tsaghkalanj	3	Armenia	Excavation	Badalyan & Avetisyan, 2007
Yakhvali	4	NW Iran	Survey	Kleiss & Kroll, 1979

The pottery network includes 34 sites (Table 3.2) spread across modern-day Anatolia, Armenia, Nakhichevan, and northwestern Iran. Most sites were excavated, but eight are only known through prospection. Inspired by Palumbi's (2008) approach, wares at the sites studied are grouped into four categories. Palumbi separates the Kura-Araxes period assemblages by the end of the 4th millennium BCE into three ware groups: Monochrome Ware, Red-Black Burnished Ware, and Black Burnished Ware. He notes that the temper used for the three groups does not seem to differ much, as it is usually grit or mixed grit and organic (Palumbi, 2008, p. 205). So Palumbi distinguishes the burnished wares only by their color scheme. Palumbi added whatever term was used in the excavation reports regarding the unburnished ceramics at the Kura-Araxes sites (Palumbi, 2008, p. 176).

1. Red Black Burnished Ware:

   The Red Black Burnished Ware (RBBW) is often called Kura-Araxes ware. It appeared around 3100 BCE. This ware is characterized by a black exterior and red interior in open and closed vessels

(Palumbi, 2008, p. 205). The surface is burnished. Sagona emphasizes that this ware should not be equated with the RBBW from the Upper Euphrates (Sagona, 2018, pp. 256–257).

2. Black Burnished Ware:

   The second type of pottery, described as a standard Kura-Araxes ware, is the Black Burnished Ware (BBW). It differs from the Red Black Burnished ware by the interior color being black or grey-black instead of reddish (Batiuk et al., 2022, p. 256). BBW has an exceptionally bright sheen achieved by careful polishing (Palumbi, 2008, p. 205).

3. Monochrome Burnished Wares:

   Besides RBBW and BBW, some monochrome burnished wares (Batiuk et al., 2022, p. 256) in colors other than black or red-black are attested. Most monochrome burnished sherds in the database are red on their exterior and interior (Badalyan & Avetisyan, 2007), although brown sherds were also excavated (Maziar, 2010, p. 171).

4. Unburnished Wares:

   The umbrella category of unburnished ware is vast and designed to include all the unburnished ceramics discovered. Collecting all unburnished wares at the selected sites would create many categories that are hard to compare because different terminology was used.

The table containing the coordinates for the sites (Appendix 2) and the wares in the ceramic assemblage (Appendix 3) are also included. The preconceived notion that these ware groups do not meaningfully enhance the network structure was confirmed in Chapter 5.2. Therefore, they can be excluded confidentially.

Table 3.3 Decorative features collected in the ceramics dataset.

Decoration techniques	
Terms	Examples
Nakhichevan lug	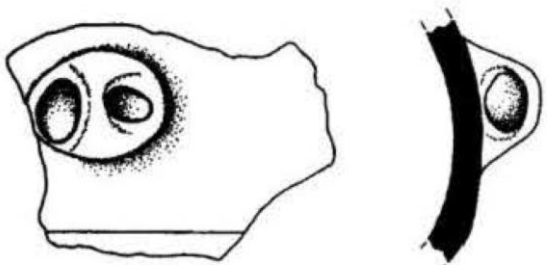

Figure 3.2 (Marro & Özfirat, 2003, Plate 7.1).

Dimple

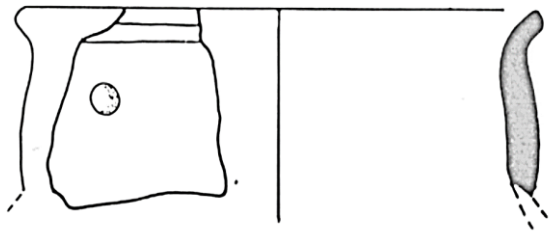

Figure 3.3 (Sagona, 2000, Figure 14.4).

Application

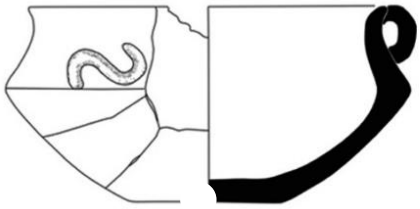

Figure 3.4 (Abedi & Omrani, 2015, Figure 10.4).

Groove

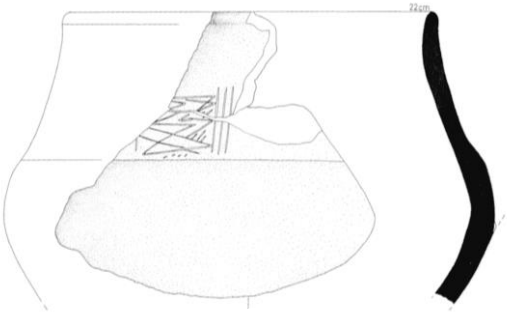

Figure 3.5 (Marro et al., 2009, Plate 1.3).

Excision

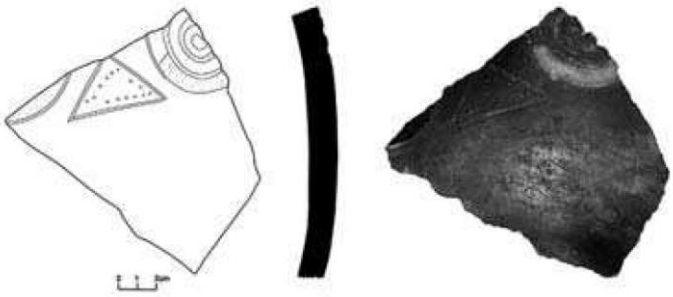

Figure 3.6 (Abedi et al., 2014, Figure 41.10).

Incision/ Scraped	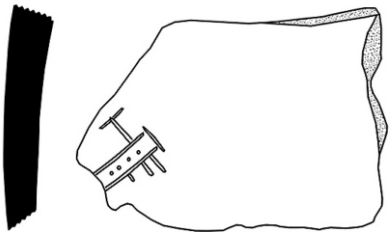

Figure 3.7 (Abedi & Omrani, 2015, Figure 7.12).

Painted	

Figure 3.8 (Alizadeh et al., 2015, Figure 14.5).

Relief/ Embossed	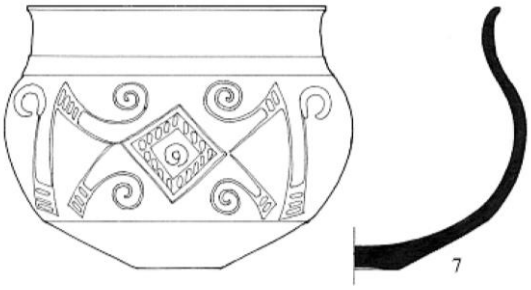

Figure 3.9 (Badalyan et al., 2014, Figure 3.7).

Comb-scraped	Technique recorded at Kuli Tepe, but no Kura-Araxes example pictured in source publications.

Decoration motifs

Terms	Examples
Concentric circles	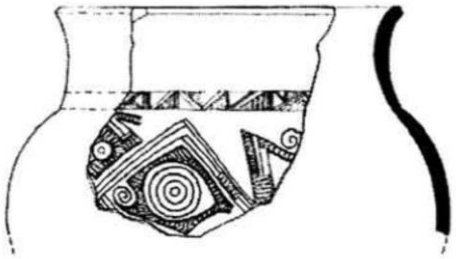

Figure 3.10 (Badalyan & Avetisyan, 2007, Plate 8.1).

Ladder

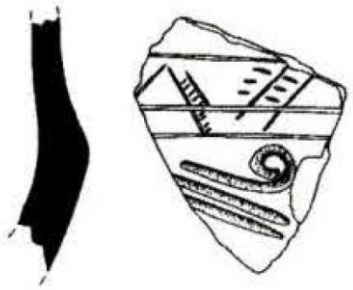

Figure 3.11 (Marro & Özfirat, 2003, Plate 6.7).

Spiral/
Loop

Figure 3.12 (Ashurov, 2020, p. 145).

Horizontal line

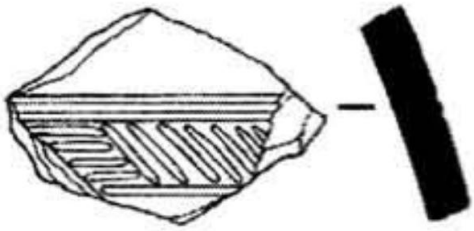

Figure 3.13 (Badalyan & Avetisyan, 2007, Plate 2.11).

Crosshatched lines

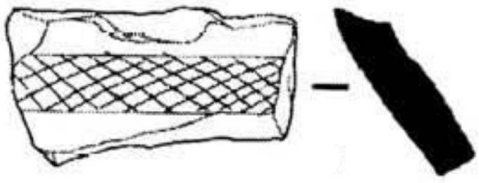

Figure 3.14 (Badalyan & Avetisyan, 2007, Plate 5.5).

Parallel lines

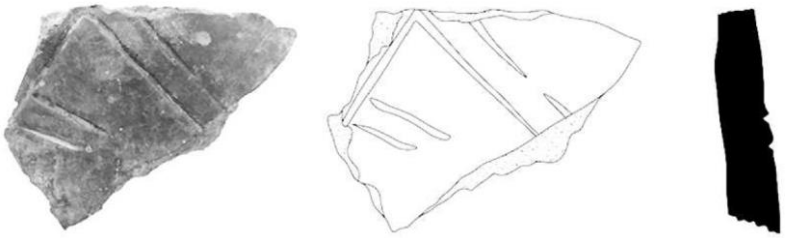

Figure 3.15 (Alizadeh et al., 2015, Figure 18.6).

Triangle

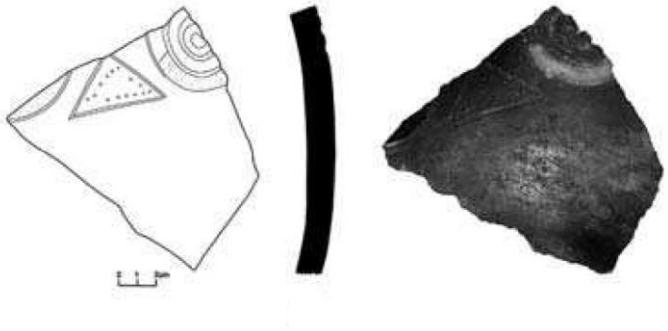

Figure 3.16 (Abedi et al., 2014, Figure 41.10).

Hatched chevrons

Figure 3.17 (Işıklı, 2019, Plate 9 d).

Zigzag

Figure 3.18 (Zalaghi et al., 2021, Figure 23 B).

Anchor/
Ram's horns

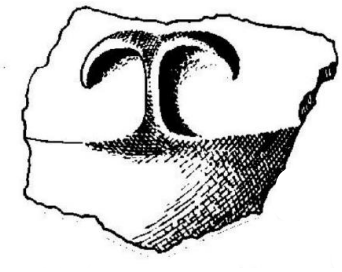

Figure 3.19 (Ashurov, 2002, Plate 10.1).

Geometric motif

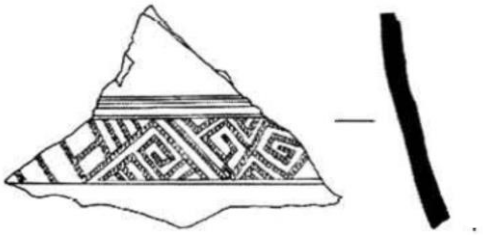

Figure 3.20 (Badalyan & Avetisyan, 2007, Plate 5.1).

Plant motif

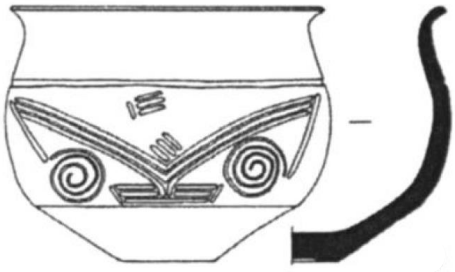

Figure 3.21 (Badalyan, 2014, Figure 5.9).

Snake motif

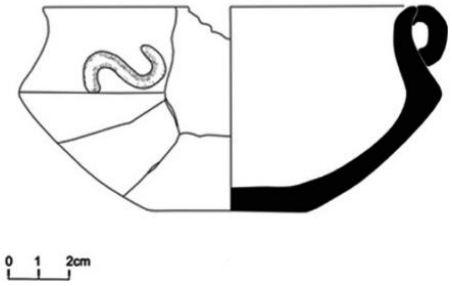

Figure 3.22 (Abedi & Omrani, 2015, Figure 10.4).

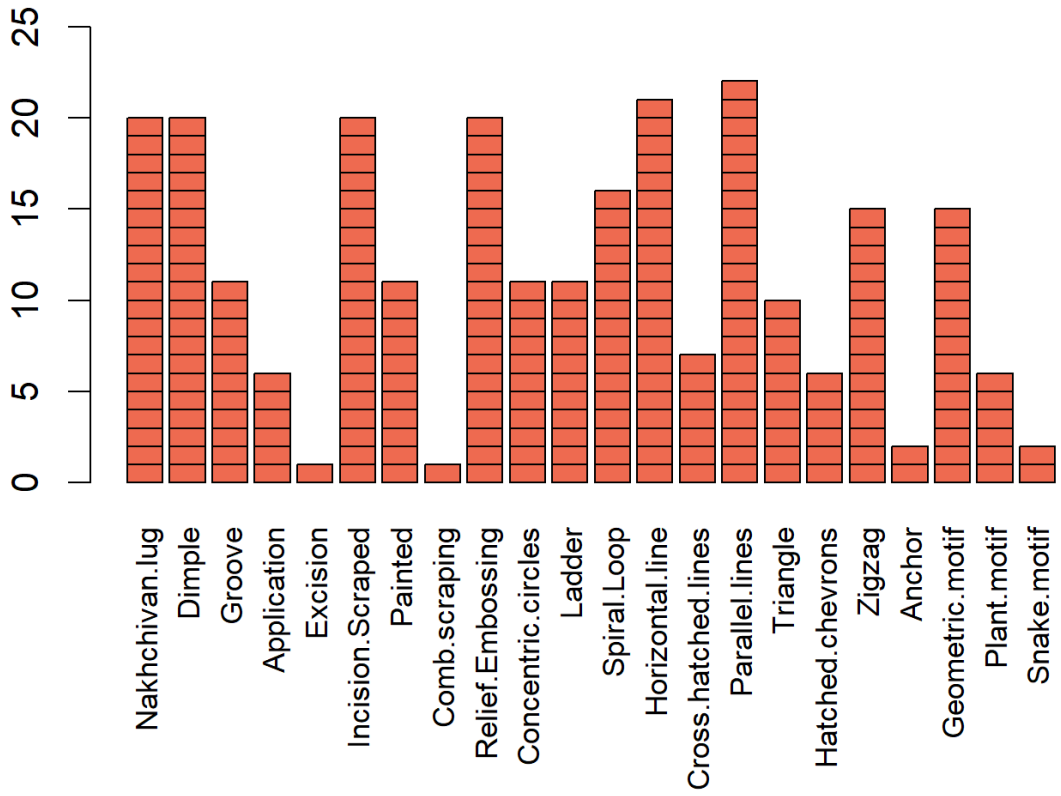

Figure 3.23 Bar plot of decorative features in the unfiltered pottery dataset (Figure by N. Mez).

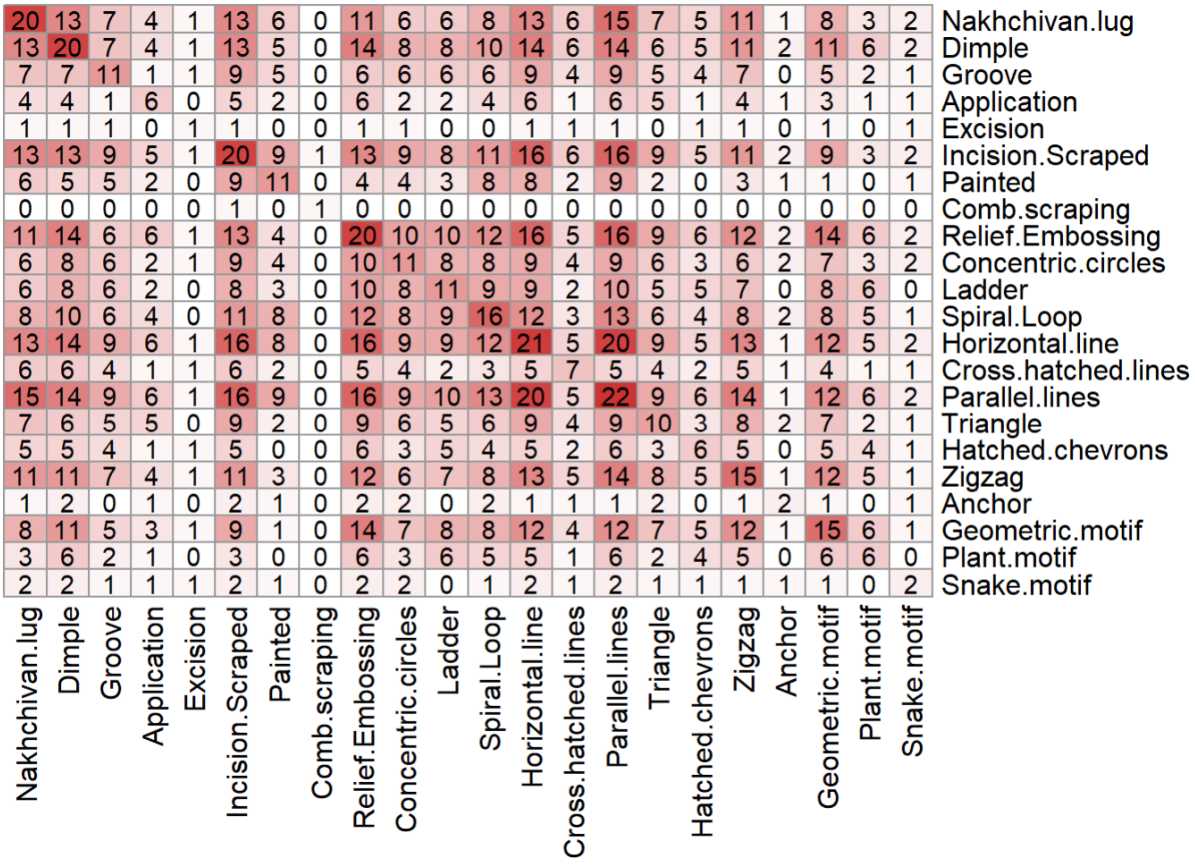

Figure 3.24 Heatmap displaying co-occurrences of pottery decorations (Figure by N. Mez).

Twenty decorative features (Figure 3.23) were recorded: nine decorative techniques and 11 motifs. The most common decoration techniques are “Relief” (n = 21), “Nakhichevan lug” (n = 21), “Incision” (n = 20), and “Dimple” (n = 20). The Nakhichevan lug is a morphological trait, not a decorative technique. Nevertheless, due to its characteristic shape, one could regard it as a decorative feature that is a core element of the Kura-Araxes ceramic repertoire. Therefore, it is included in the analysis. Comb-scraping appears only at Kuli Tepe, as it is rather untypical for the Kura-Araxes (Marro et al., 2009, p. 54). Excisions are also rare, recorded only once. Regarding the decoration motifs, “Parallel lines” (n = 22) and “Horizontal line” (n = 21) are the most frequent. “Spiral” (n = 16), “Zigzag” (n = 15), and “Geometric motifs” (n = 15) frequently appear as well. “Anchor/ram’s horns” and “Snake motif” only appear twice in the dataset. The incidence matrix listing which decorative features were identified at which sites is included in Appendix 5.

The heatmap in Figure 3.24 shows that horizontal and parallel lines co-occur 20 times, which might be caused by their likeness as parallel lines are at times positioned horizontally. Co-occurrences between motifs and techniques sometimes result from the motifs being created with said techniques. In the case of parallel and horizontal lines, they are often made by incisions. The same reasoning applies to horizontal lines and parallel lines in combination with relief. Geometric motifs are primarily created using the relief technique, linking these two features 14 times. Otherwise, notable co-occurrences between features are: Nakhichevan lugs and parallel lines appearing 15 times together and dimples co-occurring 14 times each with horizontal and parallel lines and relief decoration.

Table 3.4 Terms for features grouped into categories.

Type of feature	Grouped feature terms	New category name
Technique	Incisions, scrapes	Incision/Scraped
	Applications, modeled, and plastic designs	Application
	Reliefs, embossings	Relief/Embossing
Motif	Spirals, loops, curls	Spiral/Loop
	Vegetal emblems, plant motifs	Plant motif

Besides the issue of insufficient publication, the main hurdle and source of uncertainties is the lack of a fixed nomenclature. Multiple terms for what I perceived as the same technique or motive were unified (Table 3.4). This process could have caused the misinterpretation or misassignment of decorative

features. The category “Geometric motifs” encompasses all patterns too complex to be segmented into individual motifs. Besides the variety in terminology, the complexity of the motifs makes it highly demanding to synthesize the studies.

The only term I added is “Zigzag”. Otherwise, I did not use new expressions to re-describe the pottery. The term “Square” is mentioned only by Hayrapetyan (2008), and I could not identify the motif in the provided figures, so I excluded this term. However, the complex motifs can be described in different ways. What one researcher describes as triangles, someone else could consider zigzags. Sometimes the same researchers differ in their descriptive choices, i.e., Badalyan and Avetisyan (2007) refer to decoration as plastic design, what is termed embossed in Badalyan’s (2014) more recent article. In this study, I follow Badalyan’s (2014) terminology as the publication is more recent and an elementary component of many subsequent discussions about ceramic decorations (Sagona, 2018, pp. 260–261).

As there is no corpus containing detailed information on Kura-Araxes pottery decorations and motifs from sites in various regions, the data collection and preparation posed a significant challenge. Badalyan (2014) defined different groups of Kura-Araxes pottery in Armenia and their chrono-spatial occurrence, but he did not create a fine-grained typology. Ashurov (2002) created a typology for the vessel functions in the Nakhichevan region (p. 42). A supra-regional typology with decorations compartmentalized into motifs would be a suitable basis for SNA. However, this work has not been done for the Kura-Araxes ceramics yet.

3.3 Obsidian from Araxes Basin Sites

The pottery and obsidian datasets share spatiotemporal boundaries. Therefore, all the settlements in the obsidian provenance network are also located in the Araxes Valley and connected areas. The timeframe under investigation corresponds to the dating for the ceramic database, from ca. 2900 to 2400 BCE. However, information on obsidian provenance is mainly given for the entire Early Bronze Age occupation, possibly including multiple Kura-Araxes phases. This issue is only resolved for sites unoccupied in the Kura-Araxes I period. The provenance attribution is only usable when associated with the Kura-Araxes occupation, as procurement systems might change over time. This unprecise temporal resolution might affect the network’s usefulness negatively.

The obsidian samples from the selected sites were not analyzed comprehensively in a single research project but independently by many scholars. An extensive literature search yielded the provenance information, as the PAST-OBS and SCOPE projects featuring recent multiperiod investigations on

obsidian procurement in the southern Caucasus and northwestern Iran are still in preparation and mostly inaccessible (Orange et al., 2021b, p. 934). Thus, the data is processed from a variety of published research or articles in preparation. The number of settlements in the obsidian network is a subset of the sites in the pottery network. This size difference is caused by the more limited availability of obsidian provenance, as it requires more cost, specialized equipment, and references for source characterization compared to macroscopic pottery analysis.

As for the pottery dataset, sample numbers were not collected for the obsidian database. The reasoning behind this choice is the same: The sample sizes are probably not representative due to the different site sizes and research intensity. The source information is given as binary presence/absence data. Zero means absent or undetected, and one means that a sample from a site was attributed to this source. The artifact types were not recorded in the database, since they are not required to investigate procurement. If artifact types were included in the network analysis, it could not be compared to Maziar's (2021) findings, as it would investigate different issues.

The obsidian network includes 17 sites (Table 3.5) spread across modern-day Anatolia, Armenia, Nakhichevan, and northwestern Iran. All sites were excavated except for Kuli Tepe, which was only surveyed. Because the obsidian dataset contains fewer sites than the pottery dataset, Cluster 4 is absent from the obsidian network. From Cluster 1, only Sos Höyük and from Cluster 5, only Ovçular Tepesi remain in the obsidian dataset.

Table 3.5 Sites included the obsidian network.

Site	Location	Modern region	Fieldwork	Obsidian publication
Agarak	3	Armenia	Excavation	Juharyan, 2018
Aygevan	3	Armenia	Excavation	Badalyan, 2021
Dvin	3	Armenia	Excavation	Badalyan, 2021
Gegharot	2	Armenia	Excavation	Chataigner & Gratuze, 2014
Jrahovit	3	Armenia	Excavation	Badalyan, 2021
Karnut 1	2	Armenia	Excavation	Badalyan & Avetisyan, 2007
Kohne Pasgah Tepesi	7	NW Iran	Excavation	Maziar & Glascock, 2017
Kohne Tepesi	7	NW Iran	Excavation	Maziar & Glascock, 2017
Kül Tepe 1	6	Nakhichevan	Excavation	Badalyan, 2021
Kul Tepe Jolfa	6	NW Iran	Excavation	Khademi Nadooshan et al., 2013
Kuli Tepe	7	NW Iran	Survey	Maziar & Glascock, 2017
Mokhrablur	3	Armenia	Excavation	Badalyan, 2021
Nadir Tepesi	7	NW Iran	Excavation	Abedi et al., in press
Ovçular Tepesi	5	Nakhichevan	Excavation	Maziar, 2021
Shengavit	3	Armenia	Excavation	Badalyan et al., 2004
Shirakavan	2	Armenia	Excavation	Badalyan & Avetisyan, 2007
Sos Höyük	1	Anatolia	Excavation	Brennan, 2000

Table 3.6 Sources collected in the obsidian database.

Source	Modern region	Supplied sites	Analytical method
Arteni	Armenia	Agarak	pXRF
		Gegharot	LA-ICP-MS
		Jrahovit	-
		Karnut 1	NAA
		Kültepe 1	-
		Mokhrablur	-
		Shirakavan	NAA
Atis	Armenia	Aygevan	-
		Dvin	-
Bayazet	Armenia	Karnut 1	NAA
Choraphor	Armenia	Kul Tepe Jolfa	XRF
Damlik	Armenia	Agarak	pXRF
		Gegharot	LA-ICP-MS
		Karnut 1	NAA
		Mokhrablur	-
Geghasar	Armenia	Agarak	pXRF
		Aygevan	-
		Dvin	-
		Jrahovit	-
		Kültepe 1	-
		Kul Tepe Jolfa	XRF
		Nadir Tepesi	-
		Ovçular Tepesi	-
Gügürbaba-Meydan	Anatolia	Dvin	-
		Kültepe 1	-
Gutansar	Armenia	Agarak	pXRF
		Aygevan	-
		Dvin	-
		Gegharot	LA-ICP-MS
		Jrahovit	-
		Kültepe 1	-
		Kul Tepe Jolfa	XRF
		Mokhrablur	-
		Shengavit	XRF
Hatis	Armenia	Agarak	pXRF
		Aygevan	-
		Dvin	-
		Jrahovit	-
		Mokhrablur	-
		Shengavit	XRF
Kamakar	Armenia	Agarak	pXRF
		Shirakavan	NAA
Kars	Anatolia	Shirakavan	FT
Pasinler	Anatolia	Sos Höyük	INAA
Syunik	Armenia	Kohne Pasgah Tepesi	XRF
		Kohne Tepesi	XRF
		Kuli Tepe	XRF

		Kul Tepe Jolfa	XRF
		Kültepe 1	-
		Nadir Tepesi	-
		Ovçular Tepesi	-
TCUNK 1	Unkown	Karnut 1	NAA
TCUNK 2	Unkown	Karnut 1	NAA
		Shirakavan	NAA
TCUNK 4	Unkown	Karnut 1	NAA
TCUNK 5	Unkown	Aygevan	-
		Karnut 1	NAA
		Mokhrablur	-
Tvatkar	Armenia	Agarak	pXRF

Many obsidian sources are located in the highlands stretching across the South Caucasus, most in Armenia. More than 20 sources, corresponding to 14 chemically distinct groups, have been identified. In addition to primary sources, obsidian can also be found in deposits of pebble beds, terraces, and alluvial fans downstream up to a dozen kilometers from their source (Batiuk et al., 2022, p. 292).

The collected data includes 18 obsidian sources or source groups (Table 3.6). The most common sources (Figure 3.25) in the dataset are Gutansar (n = 9), Geghasar (n = 8), Arteni (n = 7), and Syunik (n = 7). Bazayet, Chorapor, Kars, and Pasinler are the rarest sources recorded only once. Besides the three Anatolian sites, most sources are located in modern-day Armenia. Despite the knowledge of local Iranian sources (Orange et al., 2021a), they have not been identified at the selected settlements. No local obsidian sources from Nakhichevan are included in the data, but the area is very close to the Armenian obsidian outcrop of Syunik (Orange et al., 2021b, p. 926). The incidence matrix connecting the sites with the identified sources is attached in Appendix 6.

The heatmap in Figure 3.26 shows that Gutansar and Hatis, as well as Gutansar and Geghasar, co-occur six times. Gutansar and Arteni co-occur five times. Gutansar, Hatis, and Geghasar are neighboring outcrops, but Arteni is not close to Gutansar (Figure 3.27). The question arises why the communities procured obsidian from distant sources. An array of factors may influence obsidian procurement: Distance from the settlement, the quality and color of the obsidian, communication routes, and the social, cultural, and economic contexts all could have played a part in choosing obsidian sources (Orange et al., 2021b, pp. 928–929). The seasonal transhumant movements might also be a factor, as the Armenian obsidian outcrops are located at high altitudes, close to the summer pastures (Orange et al., 2021b, p. 928).

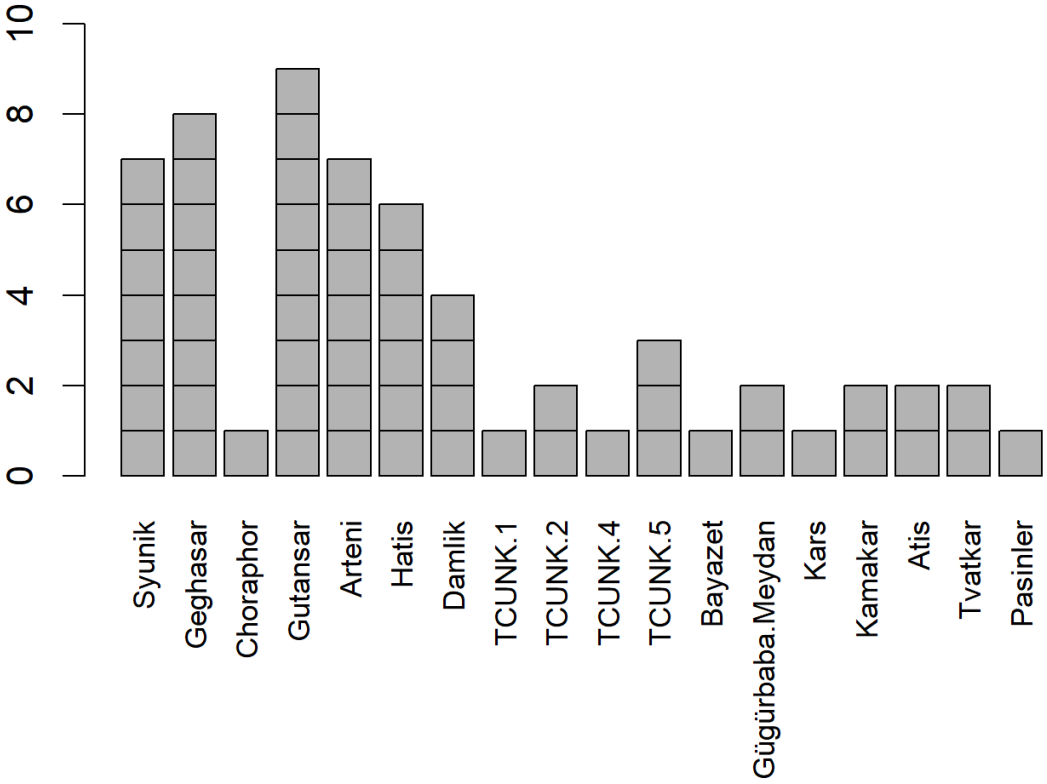

Figure 3.25 Bar plot of identified sources in the unfiltered obsidian dataset (Figure by N. Mez).

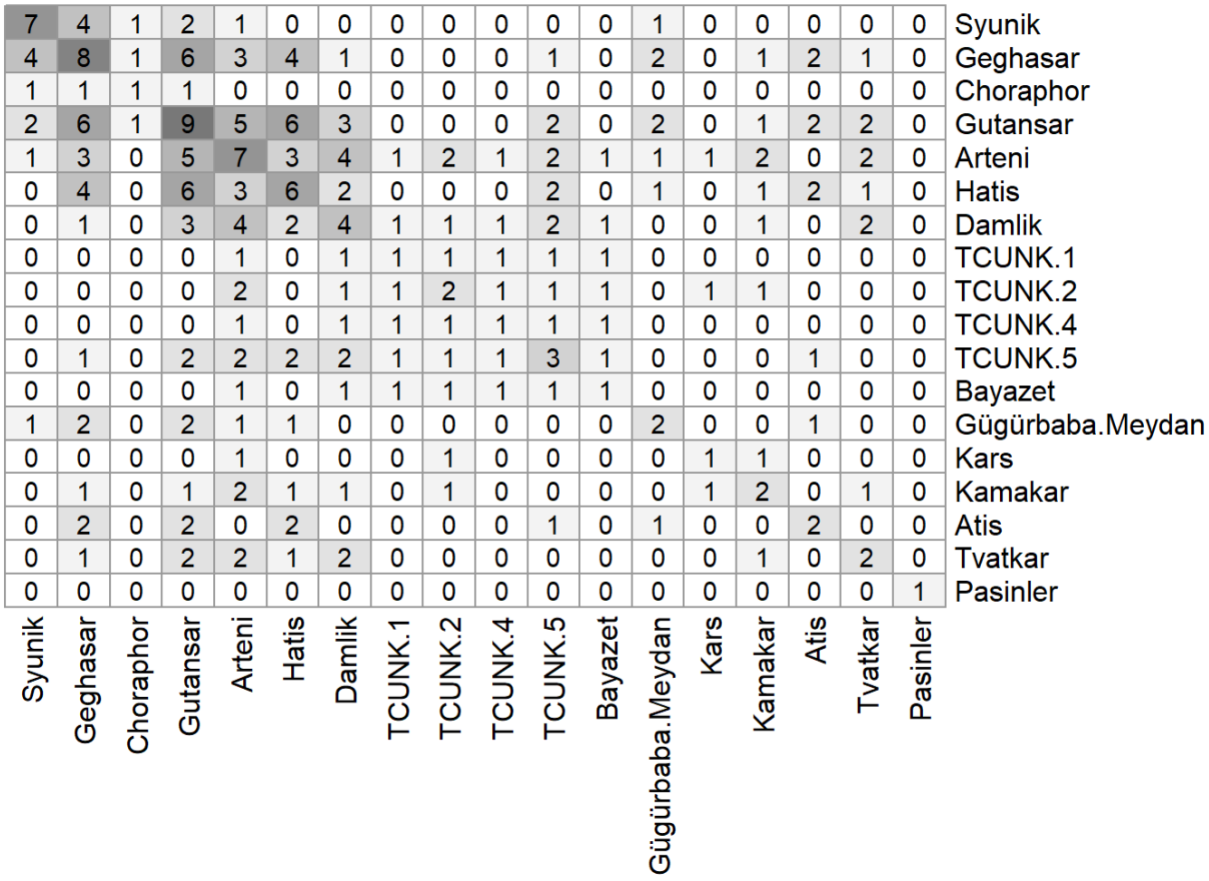

Figure 3.26 Heatmap displaying co-occurrences of obsidian sources (Figure by N. Mez).

Although the locations of many obsidian sources have been determined (Figure 3.27), some are not localized yet. Some non-localized sources were defined in their elemental composition and grouped into the six so-called Trans-Caucasian Unknown Groups (TCUNK) (Badalyan et al., 2004, p. 439). These TCUNK 1–6 sources are incorporated into the obsidian procurement network, as the differences between each other and the localized sources are apparent, despite the lack of geographic information. The TCUNK groups may not reflect procurement routes but can still inform about the similarity in obsidian source diversity among settlements. Furthermore, for some sites, the samples could not be attributed to a known source (Abedi et al., in press). All unknown sources were excluded, as they cannot be represented in the network because it is unclear how these unknowns correspond.

Moreover, the names used for the obsidian sources are inconsistent. Syunik refers to a group of sources containing the three sub-sources Sevkar, Satanakar, and Bazenk (Chataigner & Gratuze, 2014, p. 64). The sub-sources are known for some sites, like Kohne Tepesi and Kohne Pasgah Tepesi. However, to allow for comparison, the subgroups are only referred to as Syunik to make a comparison with a less precise provenance analysis possible.

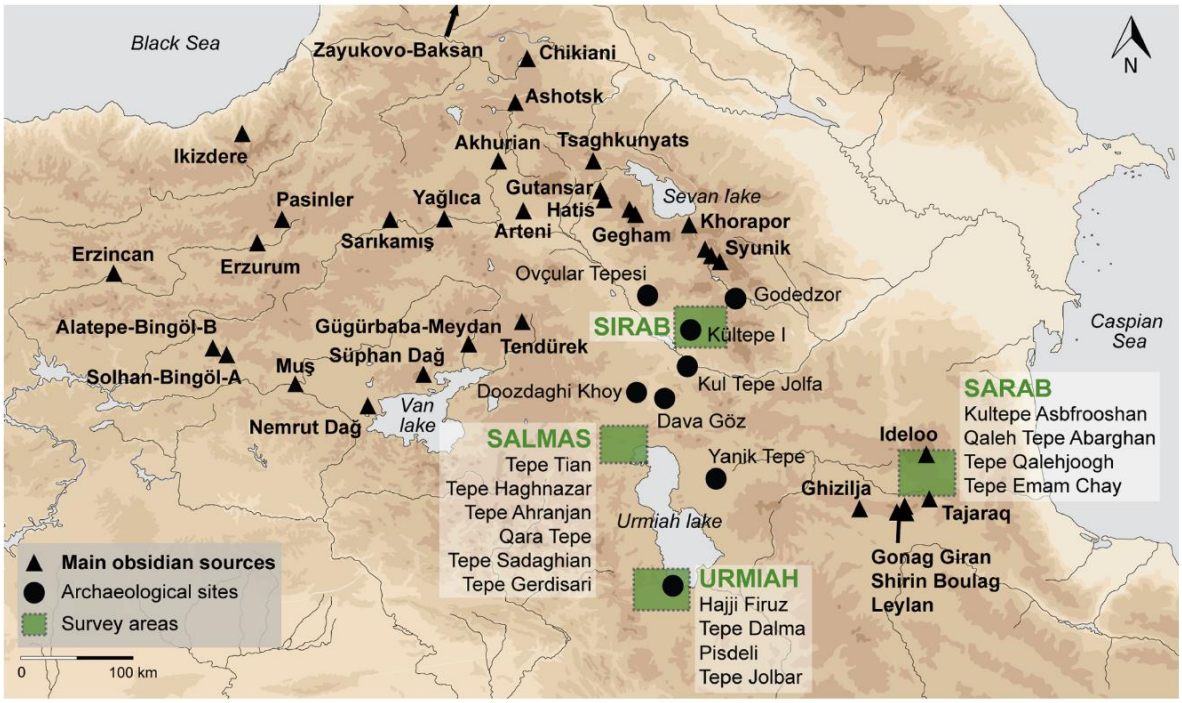

Figure 3.27 Obsidian sources exploited during prehistory (Orange et al., 2021b, Figure 1).

Like Syunik, Gegham is a compositional group including the sources Geghasar and Spitaksar (Khademi Nadooshan et al., 2013, p. 1963). Contrary to the Syunik sources, all used publications mention Geghasar explicitly. It can be referred to directly instead of through the Gegham group label. However,

the network now represents various detail levels that might obscure or overemphasize relevant obsidian procurement patterns. Furthermore, the obsidian from the sources featured in the network could have also been used outside of the study area, making the obsidian network incomplete by default, as it is limited to the Araxes River basin and adjacent regions.

Orange et al. (2021b) draw attention to the absence of precise terminology for the obsidian sources. One of these unclear names concerns the so-called “3a” source. This source probably corresponds to Gügürbaba-Meydan (Orange et al., 2021b, p. 927). I will follow this approach and save the provenance attributes referred to as 3a as Gügürbaba-Meydan in the network dataset. Moreover, they highlight the uneven availability of information on the different sources, which may have affected the identification of the sources, and the disparity in focus between regions and periods within the Caucasus (Orange et al., 2021b, p. 925).

The source names may lead to confusion, and the site names are also challenging because many sites have similar or multiple names, e.g., Kültepe 1/Kültepe Nakhichevan and Kul Tepe Jolfa/Kul Tepe Hadishar. The salt mine of Duzdağı in Nakhichevan shares the name with the northwest Iranian salt mine Doozdaghi in the Khoy Plain, which was also occupied during the Early Bronze Age and assigned to the Kura-Araxes period (Abedi et al., in press). Khoy Doozdaghi is not located in the geographic scope of the study area. Abedi et al. (in press) state that the obsidian source diversity at Khoy Doozdaghi is comparable to Duzdağı in Nakhichevan. However, the exact sources are not stated, and no published work is available. Therefore, Duzdağı cannot be included in the obsidian network.

Besides data gaps concerning entire sites, some of the source diversity is misrepresented by the obsidian network data. For Sos Höyük, four different primary sources of obsidian were recorded. However, none of these sources could be attributed to a known source. Only the obsidian procured from the secondary alluvial deposits near Pasinler is represented in the dataset (Brennan, 2000, p. 136).

Various techniques were used to attribute obsidian samples to known sources. X-ray fluorescence (XRF), also portable, provided the most provenance information in this dataset. Neutron activation analysis (NAA) and less frequently instrumental neutron activation analysis (INAA) are also used for provenance analysis. Analysts used inductively coupled plasma mass spectrometry (ICP-MS), laser ablation inductively coupled plasma mass spectrometry (LA-ICP-MS), and fission-track dating (FT) for a few of the collected samples. The analytical technique was added to Table 3.6 if explicitly stated for the site. According to Orange et al., a lack of standard reference materials and the many analytical techniques may inhibit meaningful comparisons between the assemblages (2021b, p. 925).

For some of Badalyan's provenance data, an array of analytical methods is listed (NAA, XRF, ICP-MS, and FT), but it was not stated what methods were used for which sites specifically (Badalyan, 2010, p. 27). The data for Ovçular Tepesi is taken from Maziar's (2021) article, where she states the information was obtained through personal communication and does not mention the analytical technique (p. 51). The information for Nadir Tepesi is from an article in preparation, where the method was not stated for this site specifically either (Abedi et al., in press). Besides the inconsistent terminology and disparate knowledge of sources, they point out different sampling strategies as another aspect of heterogeneity in obsidian provenance research (Orange et al., 2021b, p. 925).

3.4 Chapter Summary

This chapter described the materials used in this thesis. The sites were grouped into clusters in the first section based on their locations. Sites close to each other, usually located in the same or adjacent plains, were assigned the same cluster. This process created seven location-based clusters that will be used to incorporate spatial aspects in the network analysis. The following sections detailed the ceramics and obsidian data. Both datasets are binarized presence/absence matrices containing processed data collected from published and unpublished research. Several issues emerged from the data collection: source heterogeneity regarding research aims, sampling, and publication language; differences in research intensity, unpublished or unusable data; and a lack of fixed nomenclature.

The pottery network is based on 34 sites as nodes and 20 decorative features, including nine techniques and 11 motifs, as edges. The obsidian network is based on 17 sites as nodes and 18 obsidian sources as the second node type in the bimodal and as edges in the unimodal analysis. Because not all sites with published pottery were investigated for obsidian provenance, the settlements included in the obsidian network are a subset of the pottery sites. Based on this detailed knowledge of the materials and their related issues, the methodological choices made for this data can be explained in the following chapter.

4. Methods

4.1 Jaccard Similarity Coefficient

The methodology presented in this chapter creates similarity networks based on pottery and obsidian finds to build on Maziar's (2021) study of the same region. The open-source program R is the only specialized software needed. R scripts are included in the appendices. Detailed comments and a clean code layout are intended to facilitate reproducibility. Because the dataset had to be changed considerably to apply SNA, Maziar's findings are not tested as hypotheses. Her results are used as points to contrast the exploratory SNA with (Chapter 6.3).

The analysis focuses exclusively on the decoration techniques and motifs of the ceramics. However, as many sites share multiple pottery décor features, the network was too highly connected to observe possibly relevant local structures (Figure 4.1). It is necessary to simplify the graph by identifying the most relevant edges (Nocaj et al., 2015, p. 596). Global thresholding is a method used to subset weighted networks, which involves cutting off all edges below a particular value (Neal, 2022, p. 4).

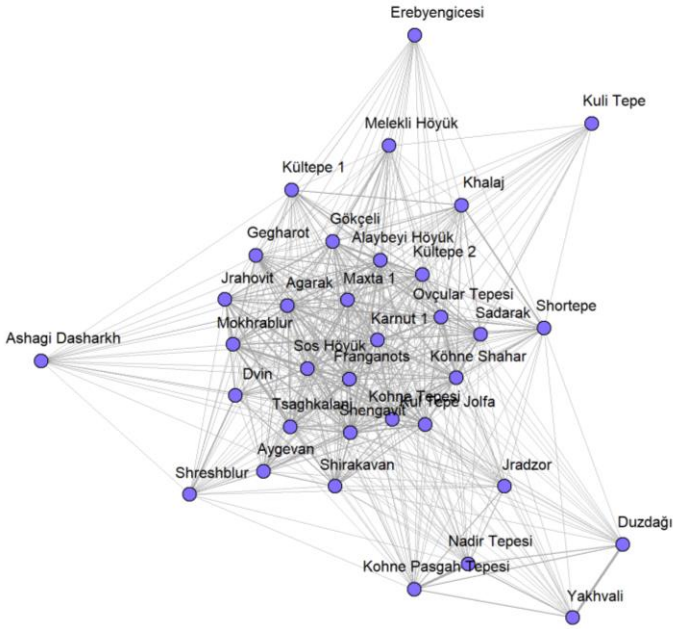

Figure 4.1 Pottery similarity network without threshold (Figure by N. Mez).

Therefore, the incidence matrices for pottery and obsidian data were subjected to similarity analysis by computing the Jaccard coefficient before creating the networks. The following step treated only connections above a certain Jaccard threshold as an edge. The threshold determination is discussed

in Chapter 4.2. For the Jaccard similarity coefficient, zero means no similarity and one identicalness, but how the values in between are interpreted varies by scientific context. Loosely inspired by a study comparing ceramic assemblages based on Jaccard indices, I propose to roughly interpret the values above 0.7 as high similarity, around 0.4 as moderate similarity (meaning neither different nor similar), and below 0.2 as low similarity (Sharp, 2016, p. 467).

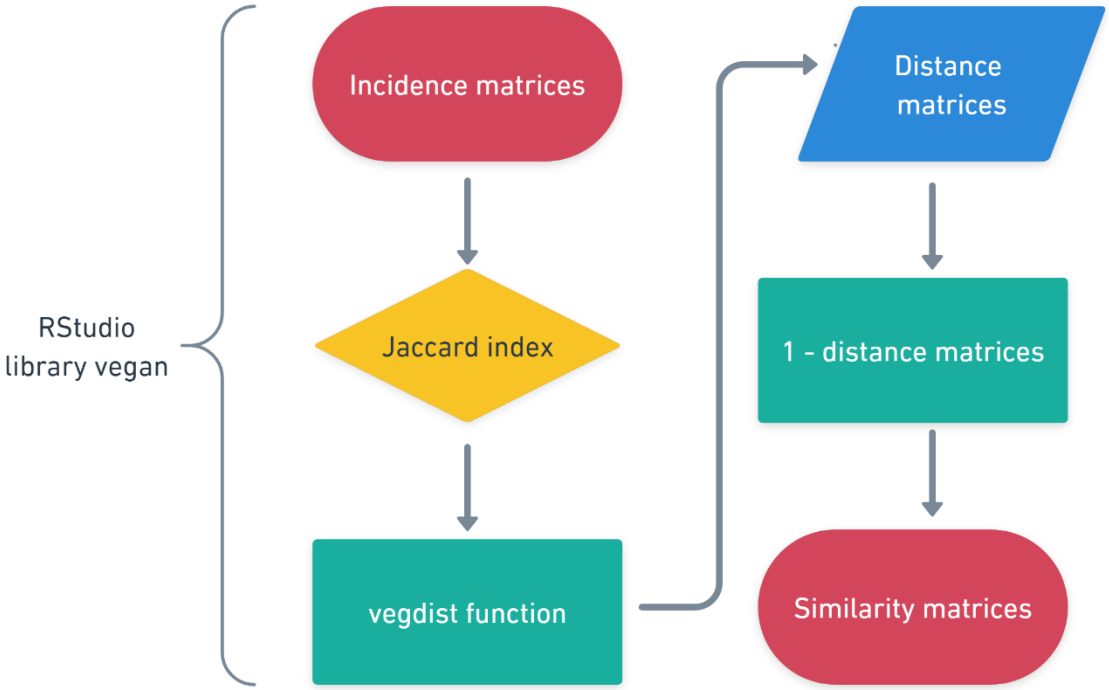

Figure 4.2 Jaccard similarity workflow diagram (Figure by N. Mez).

The first step in creating material culture similarity networks is determining the similarity. Both datasets were collected as incidence matrices in separate spreadsheets. The rows are the sites, and the columns are the decorative features or obsidian sources. These spreadsheets had to be converted into CSV format and imported into RStudio for further processing (Figure 4.2). The library "vegan" (Oksanen et al., 2022), an R package for community ecology, supplies the necessary function. Before processing the matrices, two bar plots were plotted, each showing the frequency of all decorative features (Figure 3.23) and obsidian sources (Figure 3.25) in the datasets. Next, two heatmaps displaying the frequencies of co-occurrences of pottery decorations (Figure 3.24) and obsidian sources (Figure 3.26) were created. The incidence matrices were processed using the function *vegdist* to calculate the Jaccard distance. *Vegdist* can calculate the distance (and therefore the similarity) between all possible site pairs using different similarity measures. *Vegdist* creates adjacency matrices that hold the Jaccard distances between all possible site pairs. The distance matrices were subtracted from one to

get the similarity matrices. These similarity matrices are the foundation for the unimodal similarity networks and their comparison. Last, histograms were created for the two similarity matrices to highlight the distribution of Jaccard indices in the pottery and obsidian datasets (Figures 5.1 and 5.2). The medians were added to each histogram to provide an estimate of the central value for each similarity matrix. The data is skewed toward lower values, not following a normal distribution. Therefore, the median was chosen instead of the mean.

4.2 Unimodal Social Network Analysis

The network methodology in this study consists of exploratory SNA. Östborn and Gerding (2014) describe exploratory SNA as experimenting with the networks and assessing the patterns they return. This approach requires interactive software that enables the quick plotting and measuring of graphs (Östborn & Gerding, 2014, p. 83). RStudio provides such an environment and is a suitable tool.

The two similarity networks are weighted, unimodal, and undirected. Since the similarity in pottery decoration features does not have a direction, we do not know how the objects/information/people traveled, and an undirected network representation was chosen. The obsidian data is directed, but an undirected similarity network ensures comparability to the pottery data. The edges connecting the nodes are the similarity indices between any pair of sites in the pottery and obsidian datasets, as based on the previous calculation of the Jaccard coefficient. The similarity index determines the edge weight. The higher the similarity, the stronger the particular edge weight.

The Jaccard similarity only reduces the number of edges if a threshold is defined. Thresholding is necessary as the networks, especially the pottery décor network (Figure 4.1), are too densely connected to interpret the graph visually or investigate the structure through community detection algorithms. Deciding on a minimum Jaccard similarity for any analysis depends on the field and case study (Perkins & Langston, 2009). Unfortunately, there is no archaeological indication for choosing a threshold for this case study, leading to the implementation of arbitrary thresholds. Three different thresholds were implemented to highlight the influence of these choices on the network structure.

To determine the lower threshold, the highest Jaccard minimum was chosen that did not disconnect the network or add new isolates. Other archaeologists followed the same procedure (Weidele et al., 2016, p. 109). The highest threshold that allows the ceramics network to remain connected is 0.19. Riris and Oliver (2019, p. 9) also employed a low Jaccard threshold; they used 0.1 as the minimum

similarity in their SNA. The 0.19 value was used as the lower threshold in all graphs generated to ensure comparability. For the obsidian network, this value does not create additional isolates either. However, as Sos Höyük does not share its only obsidian source with any other site, this isolate is always in the unimodal version of the obsidian network.

Subsets of differing sizes confirmed this lower threshold. Multiple subsets of the 0.19 pottery and obsidian networks were created to understand how this threshold holds up against removing random nodes and, therefore, edge loss. Each time, the first three results were selected. For the pottery network, all but 10 (Figure 4.3), 15 (Figure 4.4), 20 (Figure 4.5), and 25 (Figure 4.6) random nodes were deleted. Only the 25-node subset remains without isolates in all examples. Each other subset contained at least one isolate in one of the three runs. For the obsidian network, all but 5 (Figure 4.7), 10 (Figure 4.8), and 15 (Figure 4.9) random nodes were deleted. In this case, the subsets with 10 and 15 nodes do not feature isolates aside from Sos Höyük.

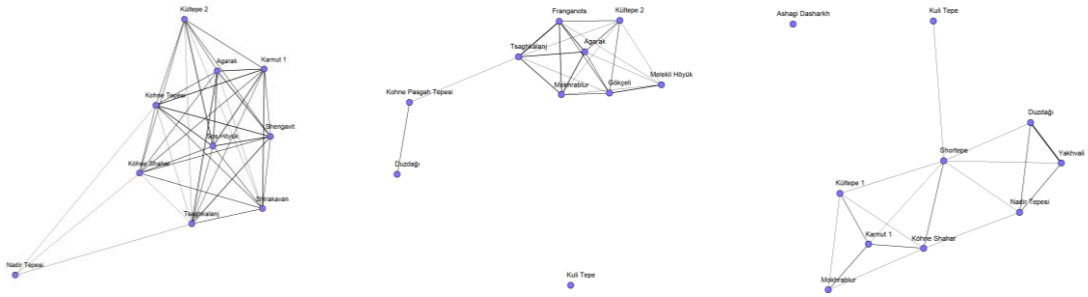

Figure 4.3 Three subsets of the pottery network featuring 10 random nodes (Figure by N. Mez).

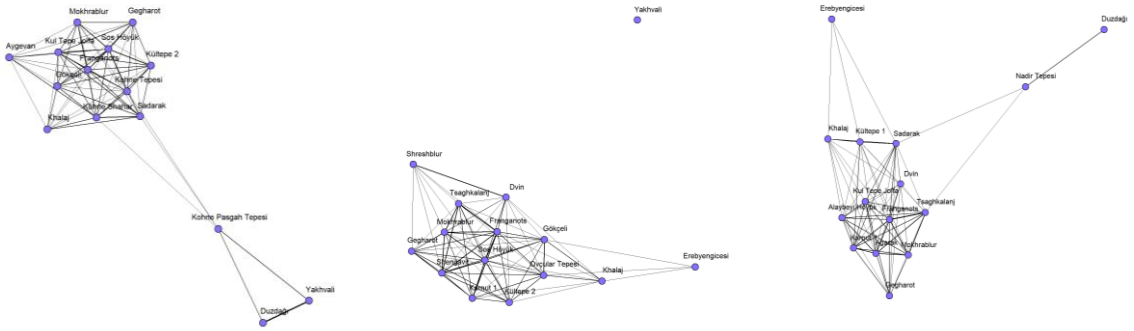

Figure 4.4 Three subsets of the pottery network featuring 15 random nodes (Figure by N. Mez).

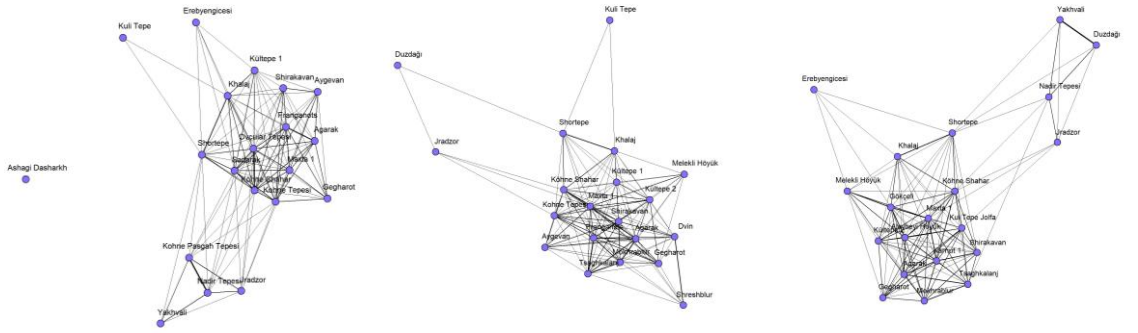

Figure 4.5 Three subsets of the pottery network featuring 20 random nodes (Figure by N. Mez).

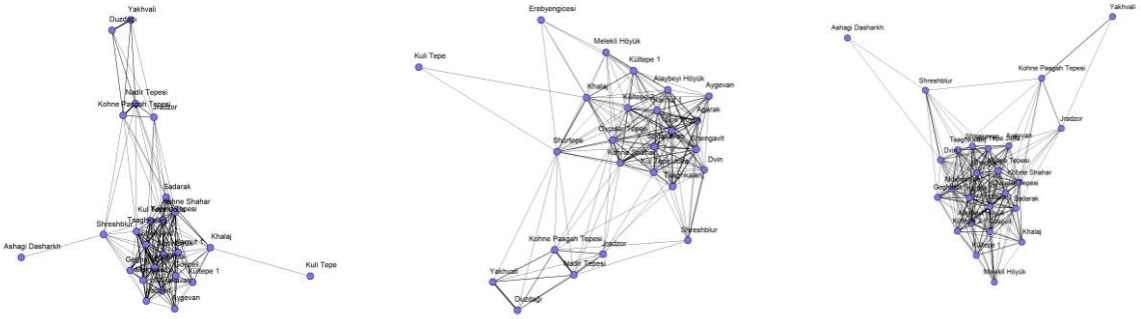

Figure 4.6 Three subsets of the pottery network featuring 25 random nodes (Figure by N. Mez).

Figure 4.7 Three subsets of the obsidian network featuring five random nodes (Figure by N. Mez).

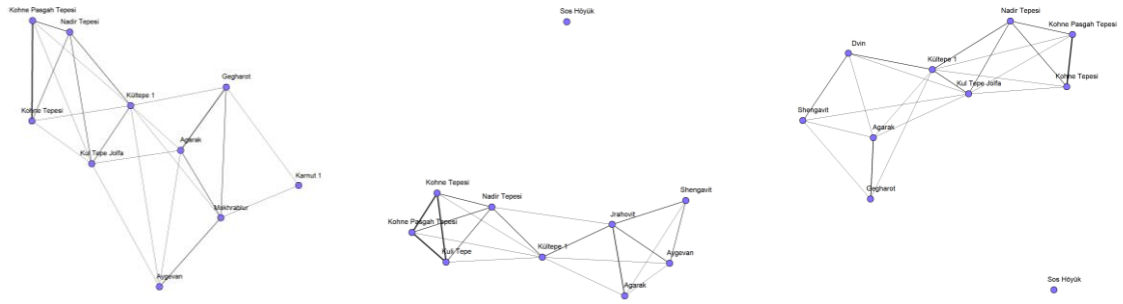

Figure 4.8 Three subsets of the obsidian network featuring 10 random nodes (Figure by N. Mez).

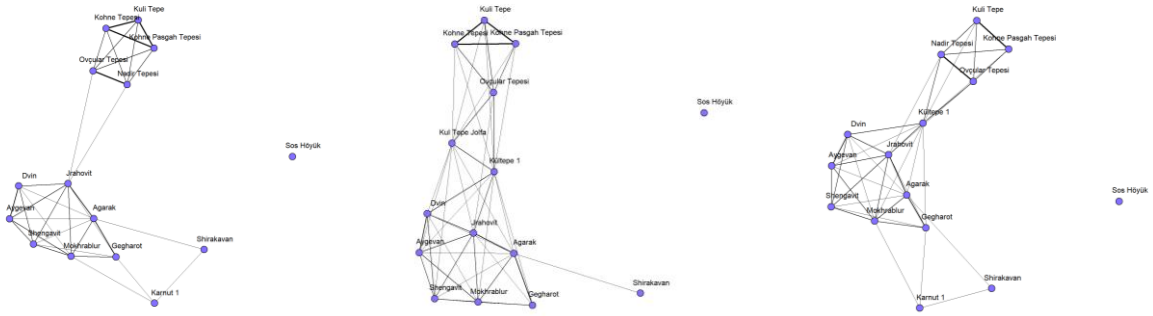

Figure 4.9 Three subsets of the obsidian network featuring 15 random nodes (Figure by N. Mez).

A second threshold with minimum Jaccard indices of 0.5 was added to investigate moderate similarities. The connections in these 0.5 graphs would reflect similarity practically without including somewhat dissimilar connections or thresholding out considerable similarities. A third threshold is set to 0.7 to include only high similarity values, thus revealing only the strongest inter-site connections. Applying three thresholds across the range of possible Jaccard indices allows us to observe their effects on the network structures and metrics.

Depending on the degree of thresholding, the graphs can still feature a complex structure caused by nodes clustering into dense groups. Community detection methods, in this case, the Leiden algorithm, are employed to investigate this structure, which was unknown prior to the analysis (Traag et al., 2019, p. 1). The Leiden algorithm groups nodes into subsets to maximize the network's modularity. Modularity measures the extent to which nodes within the same subset are more densely connected than they are to the remaining nodes in the other subsets. The modularity score can range from -0.5 to one. Therefore, a higher modularity value indicates more intense connections within the subsets than between them in the network (McNulty, 2022, Section 7.13.).

The Leiden algorithm works by iteratively optimizing the quality of the community partition (Figure 4.10). In the first step, each node is assigned to its own community. Then, the nodes are aggregated into communities to create a coarser network. Next, the algorithm optimizes the modularity by

moving nodes between communities to improve the modularity score. The community partition is refined by optimizing the balance between modularity and the number of communities. This refinement helps to ensure that the final community partition is not too fine- or coarse-grained. Finally, the algorithm repeats these steps until the community partition stabilizes or a stopping criterion is met (McNulty, 2022, Section 7.13.). The Leiden algorithm differs from the Louvain algorithm, on which it is based, by the additional refinement step to optimize modularity (Traag et al., 2019, p. 4). An independent study also confirmed that the Leiden algorithm could attain better-connected communities than the Louvain algorithm (Anuar et al., 2021, p. 4).

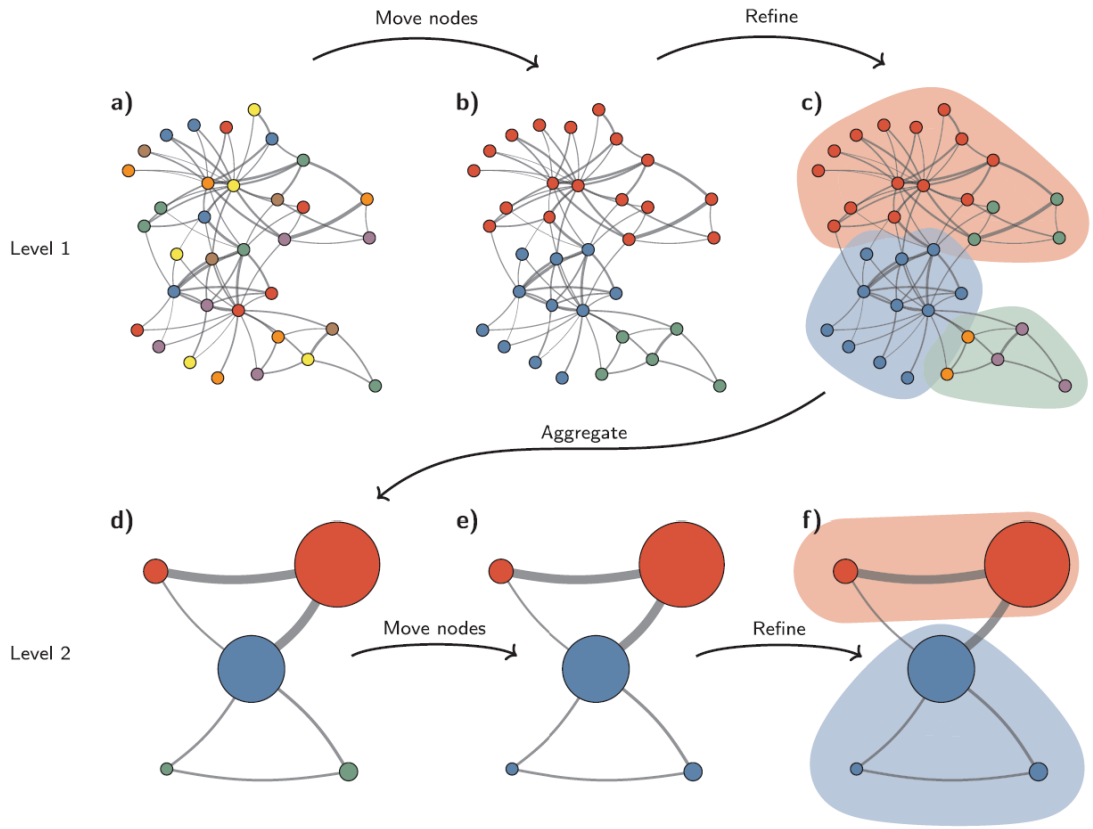

Figure 4.10 Steps in the Leiden algorithm (Traag et al., 2019, Figure 3).

The Leiden algorithm detects communities but does not address the reasons behind this structure (McNulty, 2022, Section 7.13.). In our case study, these Leiden communities tell us which nodes are clustered by the highest similarities in ceramic décor or obsidian source choice. The Leiden groups can be compared to the location-based clusters defined in Chapter 2.1 to see if the sites sharing similarities are located close to each other. Leiden groups mixed from multiple, distant site clusters may indicate large-scale migration or long-distance trade, whereas Leiden communities from the same or close

local clusters might hint at an exchange or seasonal transhumance between neighboring communities. Thus, comparing Leiden groups derived from the similarity network structure to the geographic site clusters informs about possible influences on material culture similarities.

This study is not the first to compare similarity communities based on modularity to geographic factors. Ladefoged et al. (2019) similarly researched Māori obsidian procurement in New Zealand. They compared communities based on shared obsidian sources, produced by the Louvain algorithm, to least-cost paths between the sites (Ladefoged et al., 2019, p. 8).

The "igraph" package (Csárdi & Nepusz, 2006) is the core tool for SNA chosen in this study. Therefore, the "igraph" manual pages were the primary resource consulted during the coding process. Ognyanova's (2016) tutorial for SNA using "igraph" was also very beneficial. Furthermore, contributions on StackOverflow and GitHub aided with customization and problem-solving. The scripts were run multiple times to implement the different thresholds, each time commenting out the lines of code not desired for this specific run.

The unimodal similarity networks were created in R Studio, and the corresponding R scripts "01_pottery_similarity.R" (Appendix 7) and "02_obsidian_similarity.R" (Appendix 8) are attached in the appendix. These scripts contain each the calculation of the Jaccard similarity (Figure 4.2) and the subsequent network creation and visualization (Figure 4.11). Additionally to the library "vegan", the package "igraph" (Csárdi & Nepusz, 2006) was used for the network analysis, and "RColorBrewer" (Neuwirth, 2022) to create color palettes and assign them to different values.

After the Jaccard adjacency matrices were created, the network analysis was conducted. The steps taken for both networks are identical. The matrices were turned into unimodal network objects through the function *graph_from_adjacency_matrix*. Within this function, it was specified that the networks are weighted. Next, the graphs were made undirected by collapsing all edges with the *as.undirected* function. Because the similarity matrices contain all possible pairs – including the sites with themselves – the nodes have edges with themselves, called loops. These loops were removed for both graphs using the *simplify* function. The edge weight, determined by the Jaccard similarity between nodes, was visualized in the plot as the edge width. A node attribute named "Location" was added to assign the sites to their geographic clusters, as shown in Table 3.1. Different node colors were assigned all possible values for "Location" with the *brewer.pal* function in the "RColorBrewer" palette. After this, the network objects were plotted using the *plot* function in the "igraph" package. Specifications for node labels and node and arrow sizes were made within the *plot* function.

The Fruchterman-Rheingold layout algorithm, one of the most commonly used for graphs, was chosen (Fruchterman & Reingold, 1991). The algorithm is a simulation that involves repelling nodes connected by springs instead of edges. Spring connections keep nodes close to each other, while repulsion helps open the graph. For each algorithm run, the layout can vary due to the random initial configuration (Weidele et al., 2016, p. 109). After this step, the visualization was completed, and the analysis was performed.

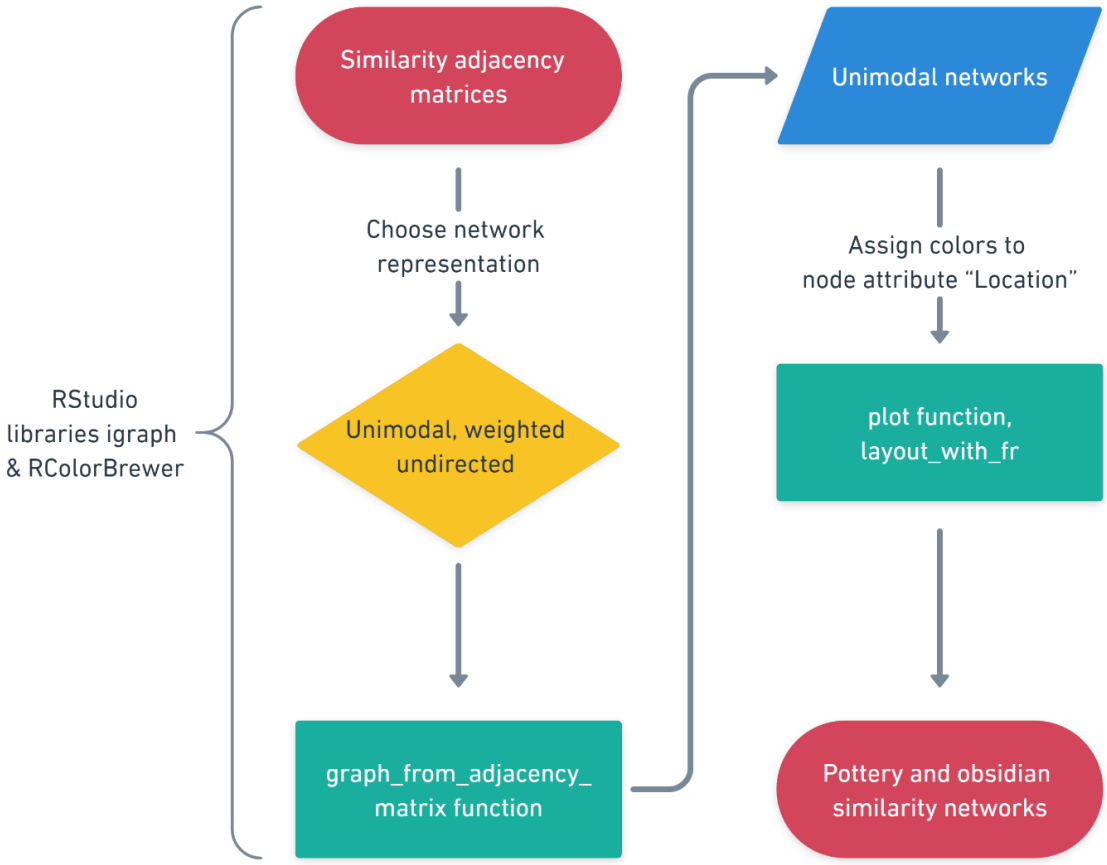

Figure 4.11 Similarity networks workflow diagram (Figure by N. Mez).

The network analysis started with calculating network-level metrics using various "igraph" functions. First, the numbers of nodes, edges, and isolates were queried. Next, the d*ensity*, *diameter*, *transitivity, centralization*, and *degree* functions were employed. These values give an impression of the network size and connectivity. The network density indicates how interconnected the nodes are. In a network, density is calculated by dividing the number of edges by the total number of edges possible. The density can range from zero to one. A complete graph would possess all possible edges and have a density of one. Graphs with lower density are called sparse graphs (McNulty, 2022, Section 5.14.).

Besides network density, other measures, in particular the diameter, are also highly reflective of the overall closeness of the network (McNulty, 2022, Section 5.14.). In a network, the diameter represents the distance between any two nodes by calculating the shortest path between each pair of nodes and selecting the longest. In disconnected networks, the diameter is the longest shortest path for the largest connected component. The diameter indicates how close the nodes in the network are to each other (McNulty, 2022, Section 5.14.) and gives an impression of the network size. The lower the diameter, the closer the nodes are to each other.

Transitivity, also known as the clustering coefficient, measures the average likelihood that two nodes connected to a third are themselves connected (Collar et al., 2015, p. 19) and ranges between zero and one (McNulty, 2022, Section 8.1). High transitivity implies that the nodes cluster together densely. Network transitivity is closely related to the social science concept of transitivity, which captures the idea that "a friend of a friend is a friend" (Collar et al., 2015, p. 19). Isolates were treated as nodes with a local transitivity of zero, as specified within the function in the script.

The tendency of nodes with the same properties to share edges is homophily (Collar et al., 2015, p. 22). The homophily of a network can be investigated through the assortativity coefficient. The assortativity can be based on a categorical property as a node attribute, or a numeric property, such as the degree centrality. The coefficient ranges from minus one to one. Assortative networks have an assortativity coefficient close to one, and the prospect of nodes with the same property being connected is high. A disassortative network has an assortativity coefficient close to minus one and a low probability of nodes sharing the same property being connected. The network has neutral assortativity if the coefficient is close to zero (McNulty, 2022, Section 8.1).

The centralization measure expresses how strongly a graph is organized around one or more focal points. This indicator is calculated by adding the centrality scores of all nodes in the network together (Valeriola, 2021, p. 89). There are different types of centralization, each based on a different concept of centrality. The centrality measure chosen in this study is the degree centrality. The number of edges determines a node's degree centrality (Valeriola, 2021, p. 88). Therefore, the degree centralization shows to what extent the graph is organized around nodes with many edges. The centralization scores are normalized in these R scripts for a more straightforward interpretation and better comparison among the graphs. As a result, the centralization score can range between zero and one.

In addition to the centralization, the underlying degree centralities for the individual nodes are also provided in the normalized form to allow for better cross-network comparisons. These measurements were also performed for a variation of the ceramics dataset, including the different wares as edges.

The purpose was to check whether the inclusion of the ware groups tentatively formed in Chapter 3.2 meaningfully affects the network structure or can be seen as noise to be excluded for clarity.

The next step in the analysis was community detection using the Leiden algorithm. "Igraph" provides the *cluster_leiden* function. In these scripts, it was set to optimize modularity without initial community memberships. The networks were plotted again with the Leiden communities marked by a color overlay and node colors corresponding to the location-based clusters introduced in Chapter 3.1. The black edges show connections within the same Leiden community, and the edges in red bridge the communities. This visualization shows the Leiden communities mapped onto the network structure and allows for comparisons between the communities derived from modularity and the areas the sites are located in. No community detection was performed for the runs with the 0.7 Jaccard thresholds, as the graphs were highly fragmented. These networks were plotted again, showing the area clusters as node colors to observe how the remaining connections relate to the locations.

4.3 Bimodal Social Network Analysis

The third network is an unweighted, bimodal, and directed network based on the shared use of obsidian sources. The first node type is the sites, and the second is the obsidian sources. The edges represent a provenanced sample discovered at a site. Contrary to the obsidian similarity network, the provenance network is unweighted as the sources are listed as presence/absence data. The network can be directed since it is clear that the obsidian must have been brought from the source to the site, directly or indirectly via other localities.

The bimodal obsidian network was created in RStudio (Figure 4.12), and the corresponding script "03_obsidian_bimodal.R" was attached in Appendix 9. First, the "igraph" library was loaded for network creation and plotting. Then, the two CSV files containing the links and nodes were imported. The dataset comprising the links was saved as a matrix. Subsequently, the obsidian incidence matrix was turned into a network object through the function *graph_from_incidence_matrix*. Within this function, the direction of the network was specified. Next, the two node types were assigned different colors and shapes, making the sites and sources visually distinct. After this, the network object was plotted using the "igraph" *plot* function. Specifications for node labels, as well as node and arrow sizes, were made. As with the unimodal networks, the Fruchterman-Rheingold layout was chosen. Last, the numbers of nodes, edges, and isolates were queried.

This bimodal network is a powerful visualization of supply relations. However, to increase the comparability with the pottery network, measurements are only calculated for the unimodal similarity network based on the obsidian data (Chapter 4.2). This approach is sensible because the investigation of the sites and their similarity in resource use is in question, not the relation among the sources. Furthermore, this brief exploration of the bimodal version illustrates how a dataset can be represented in multiple network variations.

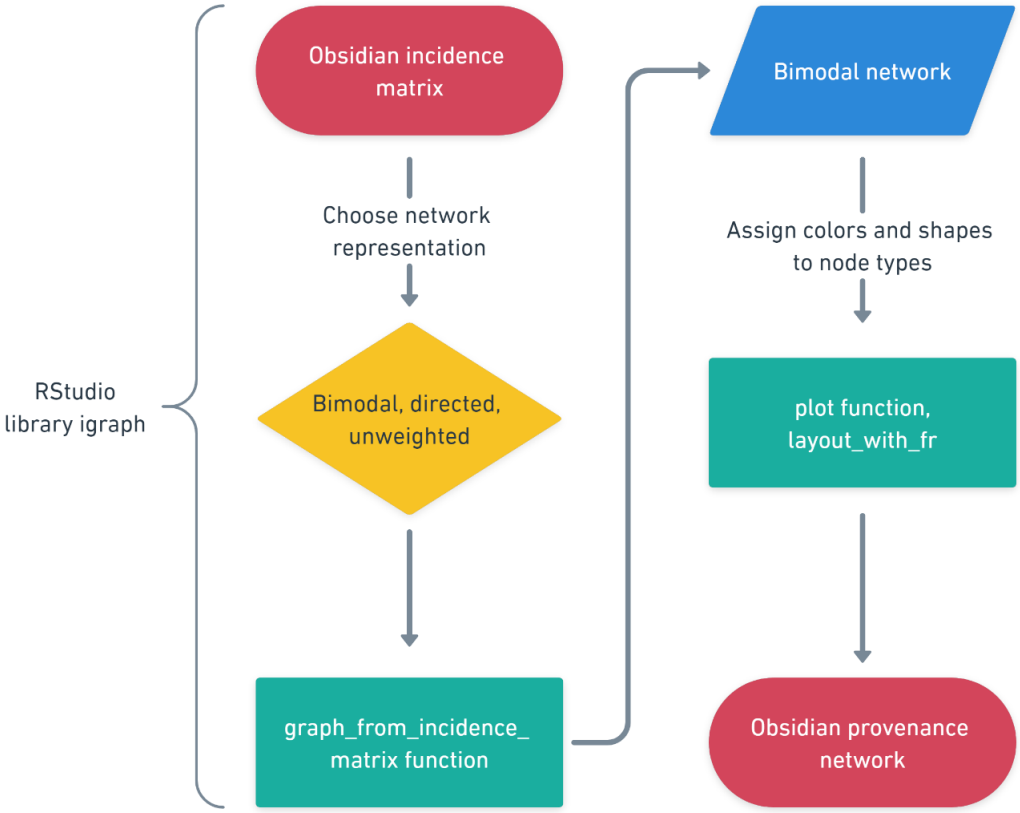

Figure 4.12 Bimodal network workflow diagram (Figure by N. Mez).

4.4 Graph Comparison

Often in archaeological SNA, networks containing the same nodes representing subsequent periods are compared diachronically (Hart & Engelbrecht, 2012). Comparing two synchronous networks based on different material culture types is uncommon (Mills et al., 2013). However, in other fields of

network research, approaches comparing graphs with the same nodes but different types of edges are more usual (McNulty, 2022), providing inspiration on how to accomplish the comparison.

The networks must be compared to investigate if and how the similarities in ceramics use, and obsidian procurement amongst the sites differ. Thus, the obsidian similarity network was compared to a subset of the pottery similarity network. The corresponding R script "04_graph_comparison.R" is attached in Appendix 10. First, the required libraries were loaded: "igraph" for network analysis, "vegan" for Jaccard similarity, and "RColorBrewer" for color control in the network plot. The subsequent data import concerned the CSV files for the obsidian nodes, obsidian similarity, pottery nodes, and edges.

The subset was created by removing all the sites not included in the obsidian data using the *subset* and *order* functions to modify the pottery nodes and edges datasets. The resulting dataset was saved as a matrix. This subset of the incidence matrix was then processed like the complete pottery dataset in Chapters 4.1 and 4.2: First, the Jaccard similarities were calculated, and second, the similarity network was created and analyzed.

The pottery subset was compared to the unimodal obsidian network in multiple ways (Figure 4.13). First, the two graphs were checked for isomorphism. When two graphs with different sets of nodes are structurally identical, they are isomorphic (McNulty, 2022, Section 8.3). Isomorphism was checked using the graph isomorphism function included in the "igraph" package. The result is TRUE when the graphs entered are isomorphic and FALSE when they are not.

Graph isomorphism checks if the edges are identical, but examining the similarity between two networks with the same nodes and different edges is also relevant in network comparison (McNulty, 2022, Section 8.3). A function calculating the Jaccard similarity of the edge sets was employed to determine the similarity in network structure. The function was taken from a network analysis handbook (McNulty, 2022, Section 8.3).

After the graphs have been compared, it is interesting to find the sites that share ceramic decorations and obsidian sources to some extent. The first step was binarizing the data: All values above zero were set to one in the obsidian and pottery Jaccard similarity matrices. Second, the two matrices were added together to a third matrix. In this new matrix, all values below two were removed to ensure that only entries remained where the connection between this site pair was present in at least one of the two original matrices. All values of precisely two are set to one to finish the binarization. Last, the adjacency matrix was exported as a CSV file.

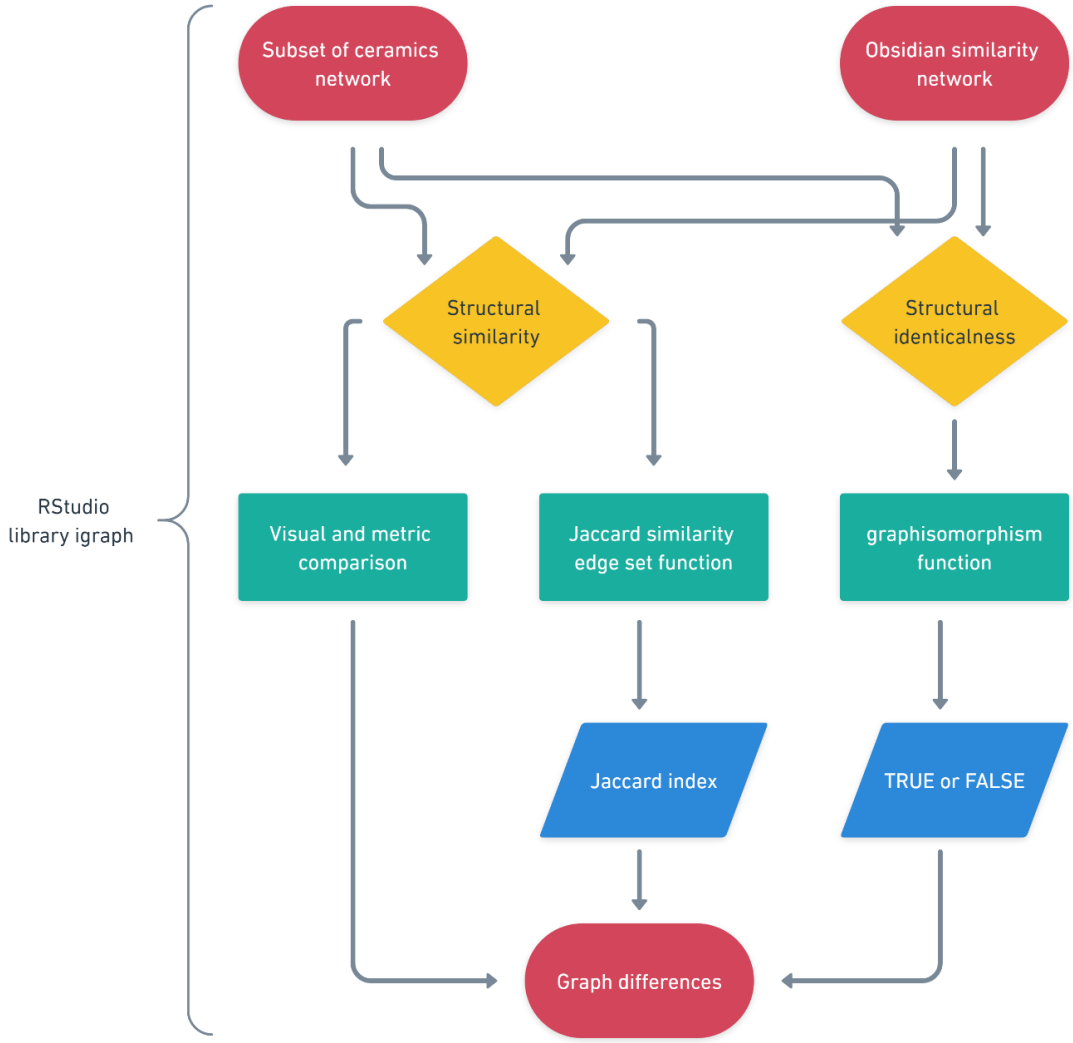

Figure 4.13 Graph comparison workflow diagram (Figure by N. Mez).

4.5 Network Backbone Extraction

A methodological limitation of the chosen approach is the loss of edges due to thresholding. Cutting off edges below a certain threshold was chosen as an efficient means of de-cluttering the networks and making their structure more comprehensible. However, a thresholding approach may exclude important weak ties, especially for networks with long-tailed distributions or characteristic edge weights in different network parts (Neal, 2022, p. 4). This issue is even more severe for arbitrarily chosen thresholds not derived from the archaeological context, as in the present study.

An alternative to thresholding is the extraction of network backbones that only contain the most critical edges. For extracting the backbone of weighted unimodal networks, a popular method is a disparity filter that only preserves edges if their observed weight is statistically significantly stronger than expected in a null model, in which the weight is distributed evenly among all the node's edges (Neal, 2022, p. 4). The backbones are not used as the basis for further analysis but as a means to find the statistically significant edges, since the previous methodological steps do not address this aspect.

The backbones for the complete pottery and obsidian graphs were created with the "backbone" package (Neal, 2022). The code segments implementing the backbone extraction were added to the last section of the R scripts for the pottery and obsidian similarity networks. Statistical backbones for the non-thresholded adjacency matrices were extracted using the *disparity* function (Neal, 2022, p. 5). For each edge, this function calculates a *p* value. These *p* values represent the probability of a higher weight on the same edge in a random network. The remaining edges will have *p* values smaller than the specified α value (Neal, 2022, p. 17).

In this case, the α value is set to 0.05. A preserved edge is thus one whose weight is greater than its corresponding edge's weight in at least 95 % of null model networks (Neal, 2022, p. 5). Scientists across different fields use $p = .05$ as a cut-off point, with lower values indicating statistical significance (Andrade, 2019, p. 210). Small sample sizes can contribute to high *p* values (Nahm, 2017, p. 242), which puts such data at risk of losing many edges. However, increasing the α value to a custom threshold until "sufficient" edges prevail is just as arbitrary as determining the global threshold in Chapter 4.2. Even if edges are excluded from the statistical backbone, they can be scientifically relevant as "statistical significance is not equal to scientific significance" (Nahm, 2017, p. 242) because *P* values only indicate the compatibility of the data with a statistical model (Nahm, 2017, p. 241). The statistical (in)significance should be acknowledged but not used to strip the insignificant edges from their capacity for archaeological interpretation.

4.6 Chapter Summary

This chapter explained the methods chosen for the present study. The Jaccard index gauged the inter-site similarities that form the basis for the unimodal SNA. Three different thresholds drew attention to the influence of varying minimum similarities on the networks' structures. The similarities in pottery décor and obsidian source choice were studied through unimodal network analysis. The nodes represent the sites, and the Jaccard similarities between each possible site pair make out the edges. Bimodal

network analysis of the obsidian data, using the sites and sources as two types of nodes, provided more insight into the procurement systems connected to obsidian provenance.

The differences in similarity patterns between the pottery and obsidian networks were investigated through multiple steps. First, a subset of the pottery network, containing only sites included in the obsidian dataset, was created. Next, the graphs were checked for identicalness, the extent of the differences was calculated using the Jaccard index, and the subset was compared to the unimodal obsidian networks though visualizations and metrics. Last, the network backbones for the complete pottery and obsidian graphs were extracted to determine the statistically significant connections. Now that the methodological choices have been described and the workflow has been outlined, the corresponding results can be presented in the following chapter.

5 Results

5.1 Jaccard Indices

The incidence matrices show the broad spectrum of attributes considered: decorations and motifs for the pottery and sources for the obsidian network. The first incidence matrix shows which sites share ceramic decorations (Appendix 5), and the second matrix shows which sites share obsidian sources (Appendix 6). The Jaccard similarities between all possible site pairs for both datasets were calculated based on these two incidence matrices. The resulting adjacency matrices with the Jaccard similarities for the pottery and obsidian datasets are attached in Appendices 11 and 12.

Histograms, including the median Jaccard indices, were created to comprehend the distribution of similarity scores in the two datasets. These histograms reveal a generally low similarity among the sites regarding their pottery decorations and obsidian sources. For the sites in the pottery dataset, the median of the Jaccard similarities is 0.25 (Figure 5.1), and for the obsidian sites, it is 0.14 (Figure 5.2). The bulk of Jaccard indices in both datasets is below 0.5, and only a few sites show high similarity values. Because the matrices feature all possible site pairs, even with themselves, they include self-similarities. Thus, in the pottery histogram, 34 entries, and in the obsidian histogram, 17 entries for 1.0 can be neglected. The results are rounded to two decimals here and in the following sections.

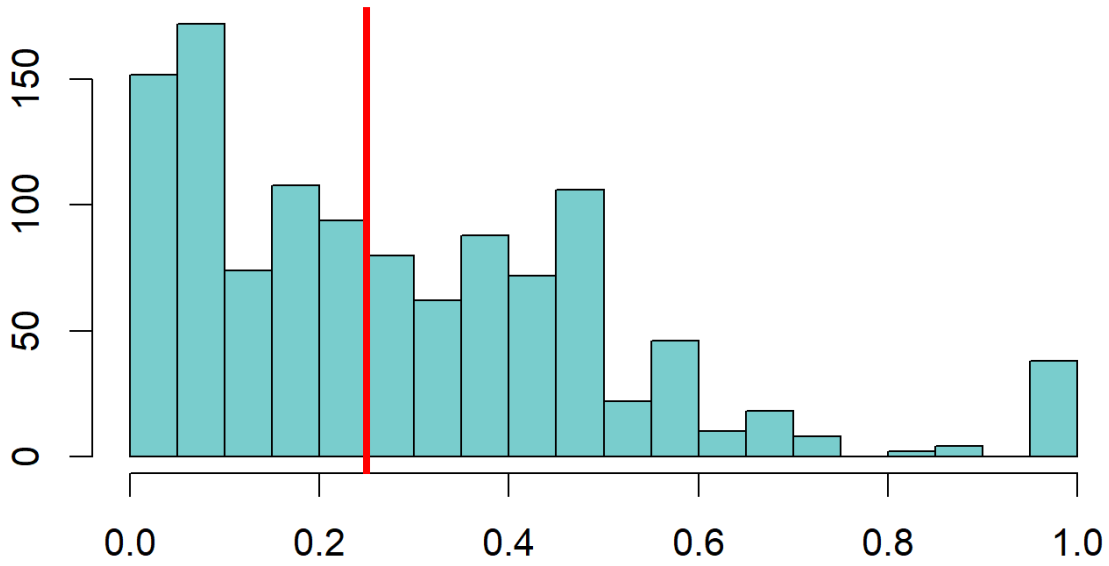

Figure 5.1 Histogram of Jaccard indices in the pottery data, median as red line (Figure by N. Mez).

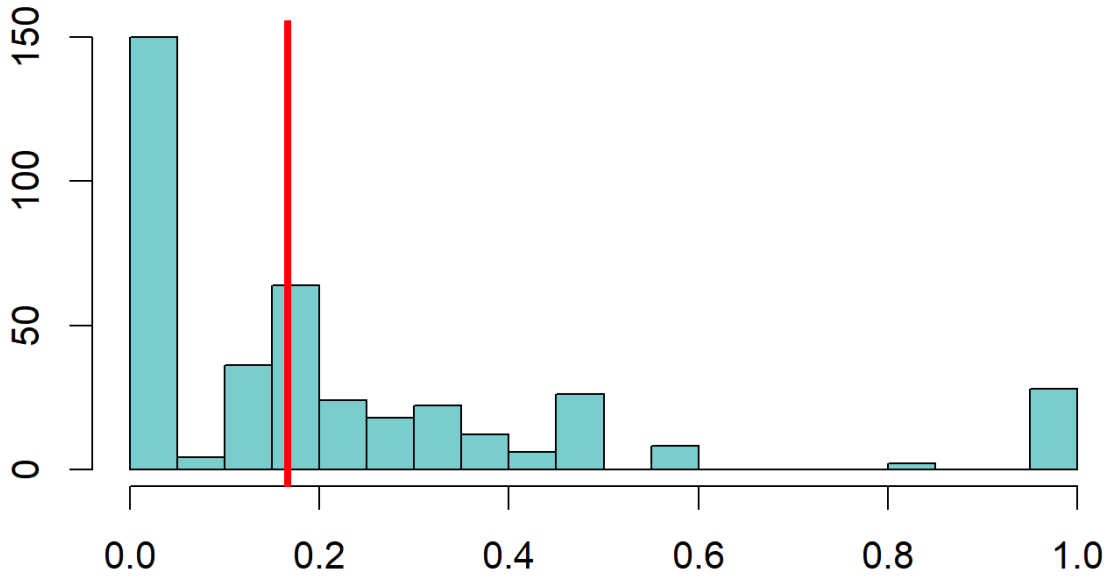

Figure 5.2 Histogram of Jaccard indices in the obsidian data, median as red line (Figure by N. Mez).

5.2 Unimodal Pottery Similarity Network

Figure 5.3 provides the first impression of the ceramics network. The pottery similarity network with Jaccard indices above 0.19 shows a large, densely connected subgraph in the center of the network. Few individual nodes are distantly connected to the subgraph. There is another less tightly interconnected group, which is also attached to the larger subgraph. There are no isolated nodes due to the choice of threshold. The second plot of the pottery similarity network with the 0.19 threshold shows the detected Leiden communities with the site locations as node colors (Figure 5.4). The dense subgraph has been split into two communities, and the smaller group is assigned to a third community. The community memberships are listed in Table 5.1. The community memberships are compared to the location-based site clusters (Table 3.1). Community 1 contains sites from Clusters 1, 2, 3, 5, 6, and 7. Community 2 features sites in Clusters 2, 4, 6, and 7. The sites in Community 3 are located in Cluster 3, 4, 5, 6, and 7.

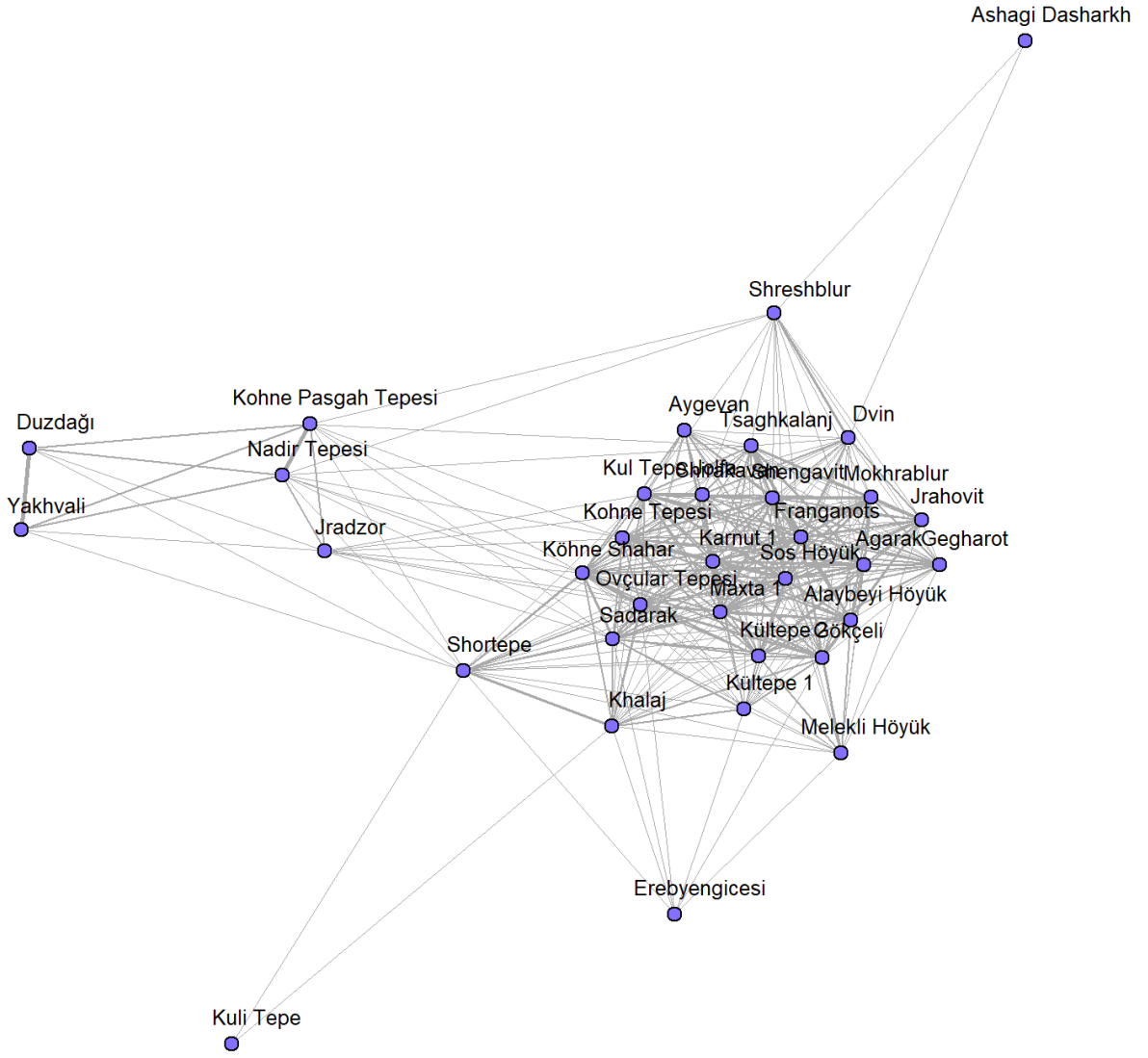

Figure 5.3 Ceramics similarity network with 0.19 threshold (Figure by N. Mez).

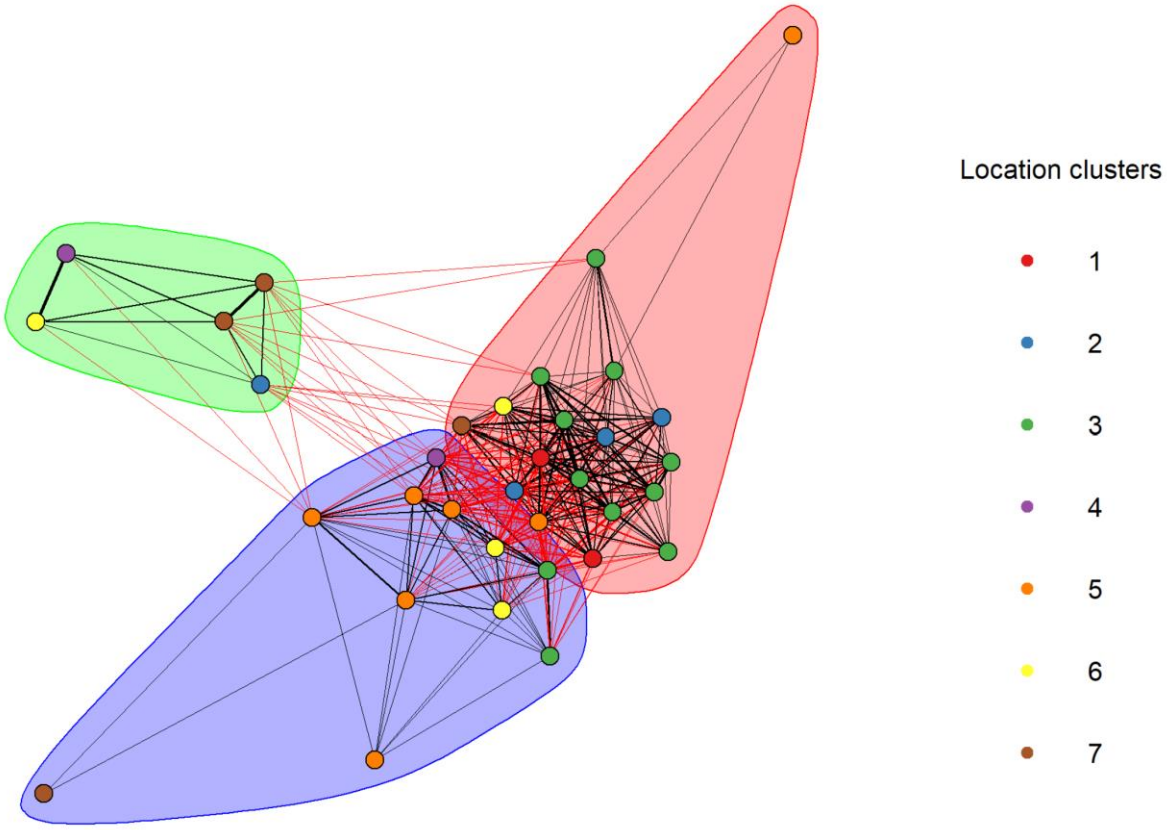

Figure 5.4 Leiden groups and locations in the 0.19 ceramics network (Figure by N. Mez).

Table 5.1 Leiden communities in the ceramics network (0.19 threshold).

Leiden communities	1	2	3
Sites	Agarak	Duzdağı	Erebyengicesi
	Alaybeyi Höyük	Jradzor	Gökceli
	Ashagi Dasharkh	Kohne Pasgah Tepesi	Khalaj
	Aygevan	Nadir Tepesi	Köhne Shahar
	Dvin	Yakhvali	Kuli Tepe
	Franganots		Kültepe 1
	Gegharot		Kültepe 2
	Jrahovit		Melekli Höyük
	Karnut 1		Ovçular Tepesi
	Kohne Tepesi		Sadarak
	Kul Tepe Jolfa		Shortepe
	Maxta 1		
	Mokhrablur		
	Shengavit		
	Shirakavan		
	Shreshblur		
	Sos Höyük		
	Tsaghkalanj		

When comparing the metrics for the pottery networks without and with the wares included, it becomes clear that the wares do not strongly influence the network structure (Table 5.2). Because more features were included in the analysis, the wares network has more edges and a higher density than the graph excluding wares. The transitivity, nominal assortativity, and degree centralization vary only by 0.01, 0.03, and 0.02. These insights justify the exclusion of the wares.

Table 5.2 Metrics for the ceramic network with and without wares.

Dataset	Pottery including wares	Pottery excluding wares
Threshold	0.19	0.19
No. of nodes	34	34
No. of edges	408	330
No. of isolates	0	0
Density	0.73	0.59
Diameter	1.29	1.83
Transitivity	0.82	0.83
Assortativity (nominal)	-0.03	0.00
Centralization (degree)	0.24	0.26

Figure 5.5 shows the pottery network with Jaccard indices above 0.5. A large, densely connected subgraph dominates the network structure. A second smaller group of five nodes is disconnected from the main subgraph. Besides these two subgraphs, one dyad and four isolates are present. The second plot of the 0.5 graph shows the detected Leiden communities and the site locations as node colors (Figure 5.6). The dense subgraph has been split into three communities, and the smaller group and dyad are assigned their own communities. Due to their lack of connections, the isolates are assigned their own communities. The Leiden community memberships are listed in Table 5.3. The communities with multiple sites are compared to the location-based clusters (Table 3.1). Community 1 contains only sites from Clusters 3. Sites from Clusters 1, 2, 3, 5, 6, and 7 are featured in Community 2. The sites in Community 4 are located in Clusters 2, 4, 6, and 7. Community 5 only features sites from Cluster 3. The settlements in Community 7 are located in Clusters 3, 4, and 5.

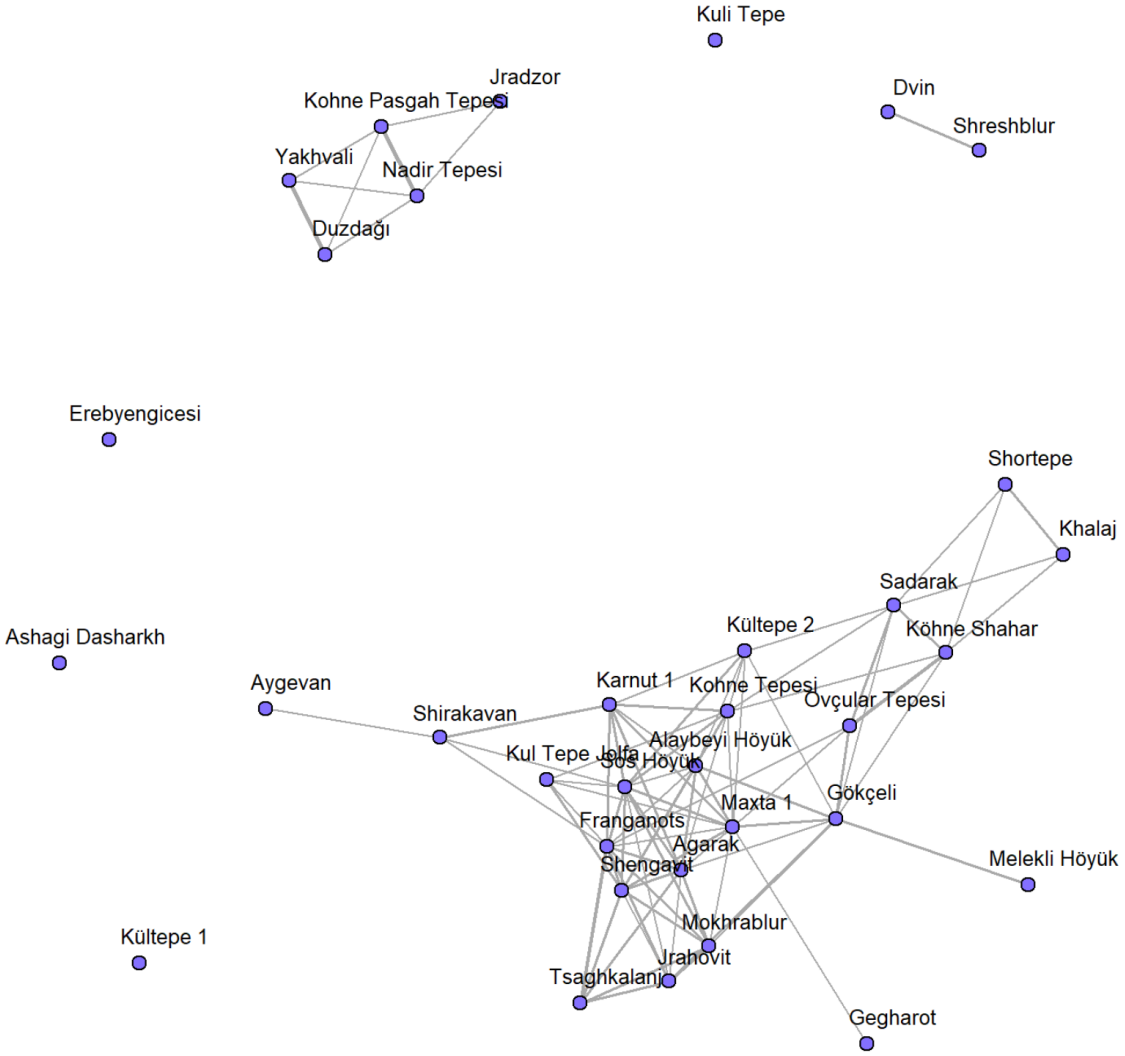

Figure 5.5 Ceramics similarity network with 0.5 threshold (Figure by N. Mez).

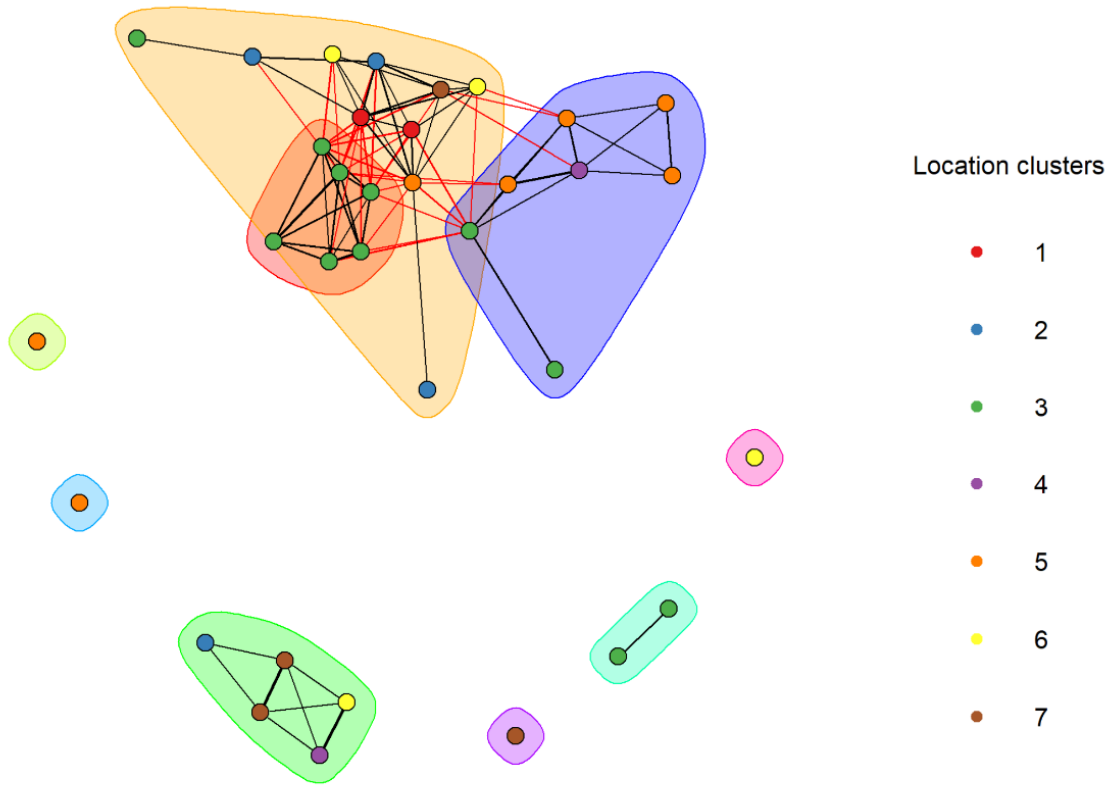

Figure 5.6 Leiden groups and locations in the 0.5 ceramics network (Figure by N. Mez).

Table 5.3 Leiden communities in the ceramics network (0.5 threshold).

Leiden communities	Sites
1	Agarak, Franganots, Jrahovit, Mokhrablur, Shengavit, Tsaghkalanj
2	Alaybeyi Höyük, Aygevan, Gegharot, Karnut 1, Kohne Tepesi, Kul Tepe Jolfa, Kültepe 2, Maxta 1, Shirakavan, Sos Höyük
3	Ashagi Dasharkh
4	Duzdağı, Jradzor, Kohne Pasgah Tepesi, Nadir Tepesi, Yakhvali
5	Dvin, Shreshblur
6	Erebyengicesi
7	Gökçeli, Khalaj, Köhne Shahar, Melekli Höyük, Ovçular Tepesi, Sadarak, Shortepe
8	Kuli Tepe
9	Kültepe 1

After applying the higher 0.7 threshold for the similarity indices, the pottery network shows a strikingly different appearance (Figure 5.7). The network is very disconnected, with the largest subgraph comprising six nodes. Besides this subgraph, there are only one triad and two dyads. The remaining nodes are all isolates. Figure 5.8 shows the locations assigned to the nodes in the network. The largest component, the triad, and one dyad are mixed. The two remaining dyads belong to the same location clusters.

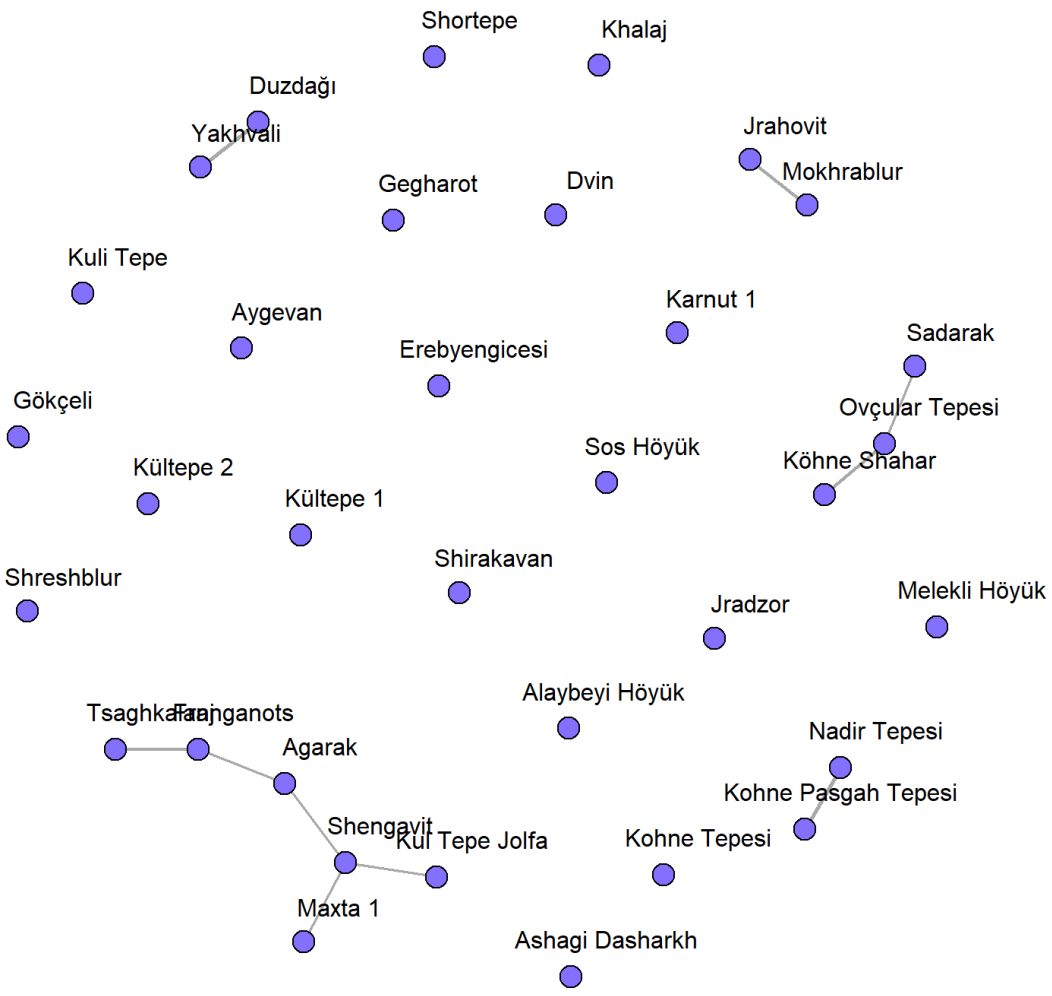

Figure 5.7 Ceramics similarity network with 0.7 threshold (Figure by N. Mez).

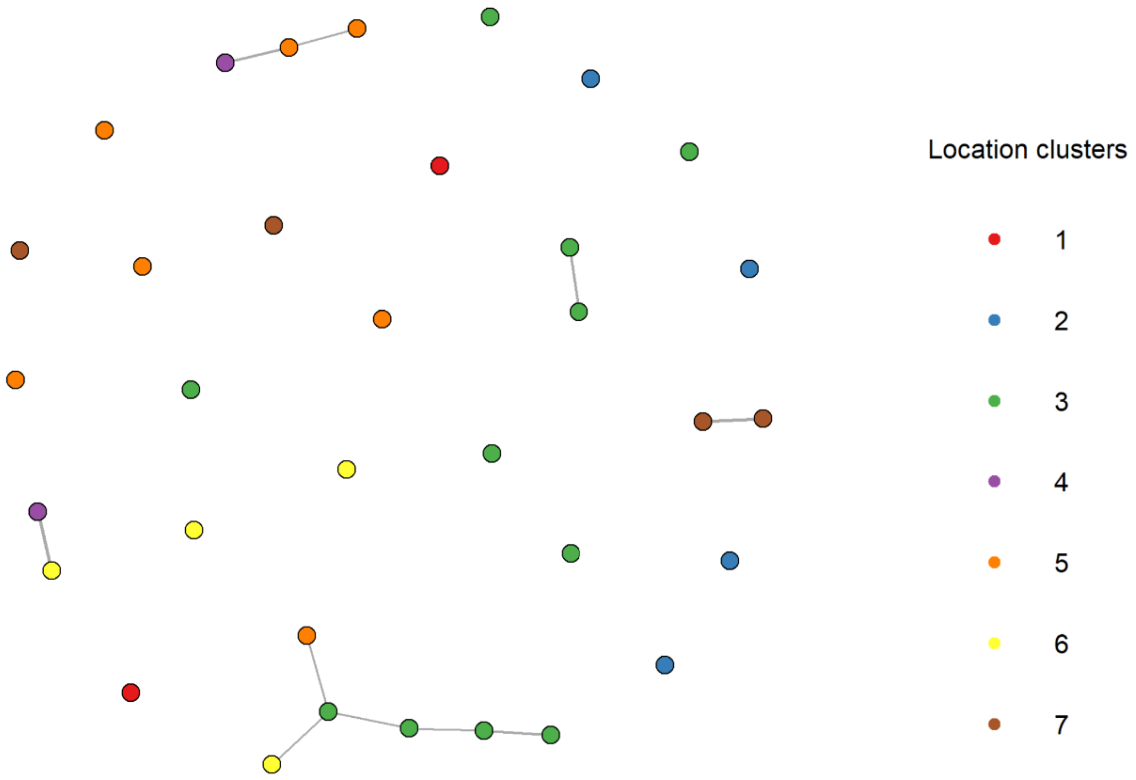

Figure 5.8 Locations in the 0.7 ceramics network (Figure by N. Mez).

Table 5.4 contains the network metrics for the 0.19, 0.5, and 0.7 pottery similarity networks. Because the lower threshold was selected to keep the pottery network connected, the 0.19 graph has no isolates, while the 0.5 graph has four and the 0.7 graph has 19. As did the density, the number of edges decreased by applying the higher thresholds. The small diameter and high transitivity in the 0.19 network show that it is well-connected. With the higher thresholds, the diameter increased due to the graph becoming more disconnected. The very low negative nominal assortativity in the 0.19 graph points at barely an influence of the assigned locations on homophily. In the 0.5 network, the assortativity is low but positive. The 0.7 network's higher positive assortativity implies a more significant influence of location on homophily. The degree centralizations for the 0.19 and 0.5 networks are relatively low, and Table 5.4 provides the degree centralities for the nodes in these two graphs. The 0.7 graph is even less centralized, with a meager degree centralization.

Table 5.4 Metrics for the ceramics networks.

Dataset	Pottery		
Threshold	0.19	0.5	0.7
No. of nodes	34	34	34
No. of edges	330	87	10
No. of isolates	0	4	19
Density	0.59	0.16	0.02
Diameter	1.83	5.37	5.96
Transitivity	0.83	0.57	0
Assortativity (nominal)	0.00	0.13	0.41
Centralization (degree)	0.26	0.24	0.07

Table 5.5 Normalized degree centralities in the ceramics networks.

Site	0.19	0.5	Site	0.19	0.5
Agarak	0.73	0.03	Kul Tepe Jolfa	0.73	0.15
Alaybeyi Höyük	0.73	0.24	Kuli Tepe	0.06	0.00
Ashagi Dasharkh	0.06	0.00	Kültepe 1	0.67	0.00
Aygevan	0.61	0.03	Kültepe 2	0.70	0.21
Duzdağı	0.15	0.09	Maxta 1	0.76	0.39
Dvin	0.73	0.03	Melekli Höyük	0.55	0.03
Erebyengicesi	0.21	0.00	Mokhrablur	0.70	0.24
Franganots	0.76	0.36	Nadir Tepesi	0.33	0.12
Gegharot	0.67	0.03	Ovçular Tepesi	0.85	0.15
Gökçeli	0.76	0.30	Sadarak	0.82	0.21
Jradzor	0.33	0.06	Shengavit	0.70	0.30
Jrahovit	0.70	0.21	Shirakavan	0.73	0.12
Karnut 1	0.70	0.24	Shortepe	0.67	0.09
Khalaj	0.64	0.09	Shreshblur	0.42	0.03
Kohne Pasgah Tepesi	0.33	0.12	Sos Höyük	0.76	0.36
Köhne Shahar	0.82	0.18	Tsaghkalanj	0.73	0.15
Kohne Tepesi	0.79	0.27	Yakhvali	0.15	0.09

5.3 Unimodal Obsidian Similarity Network

Figure 5.9 shows the structure of the obsidian network with minimum Jaccard values above 0.19. The network contains three groups of fully interconnected nodes with the appearance of pentagrams. Two pentagrams share two of their nodes and are connected to the third directly through multiple edges. There is one isolate. The second plot of the 0.19 similarity network (Figure 5.10) shows the detected Leiden communities and site locations (Table 3.1) as node colors. Two of the pentagrams are assigned their own communities with a few attached nodes, separating the third pentagram. The isolate is

placed in its own community. Table 5.6 lists the Leiden community memberships. Community 1 comprises sites from Clusters 2, 3, and 6. The sites in Community 2 belong to Clusters 5, 6, and 7. Community 3 contains only the isolate from Cluster 1.

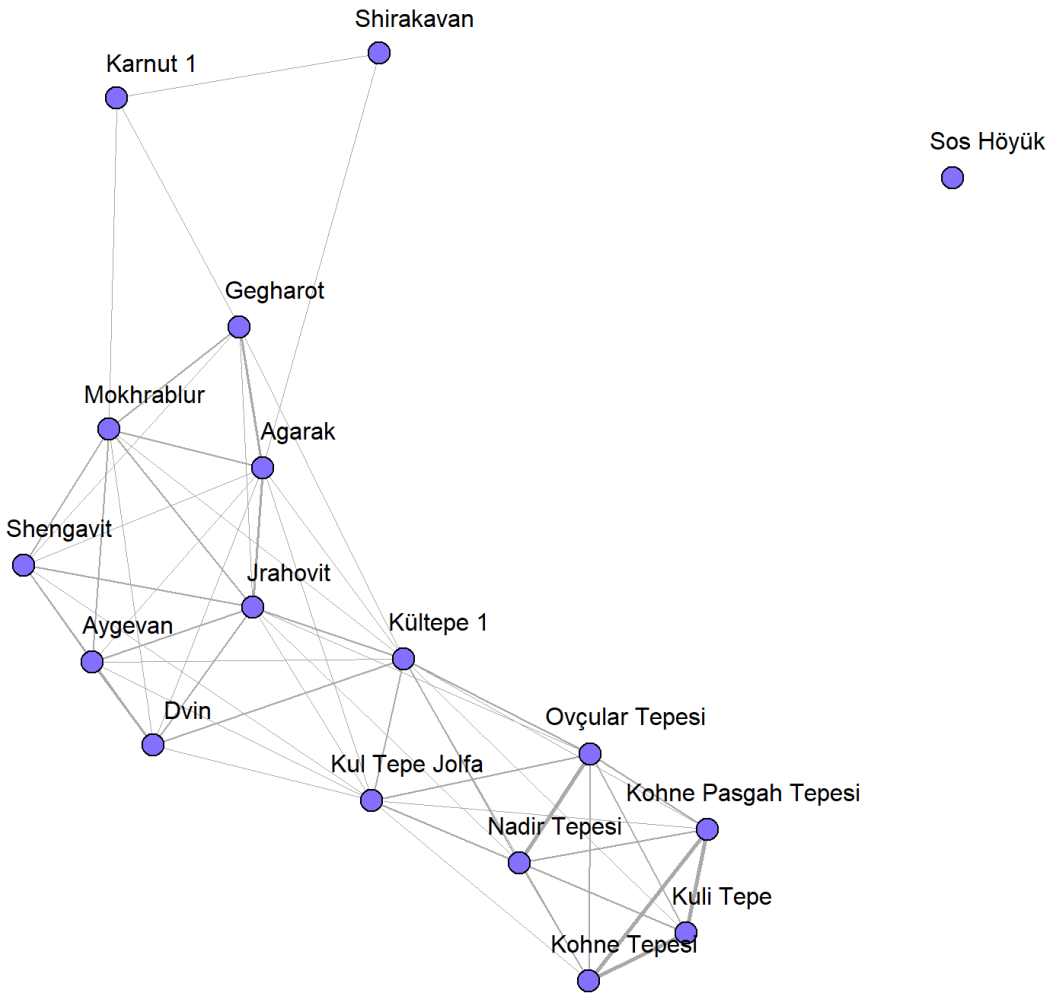

Figure 5.9 Obsidian similarity network with 0.19 threshold (Figure by N. Mez).

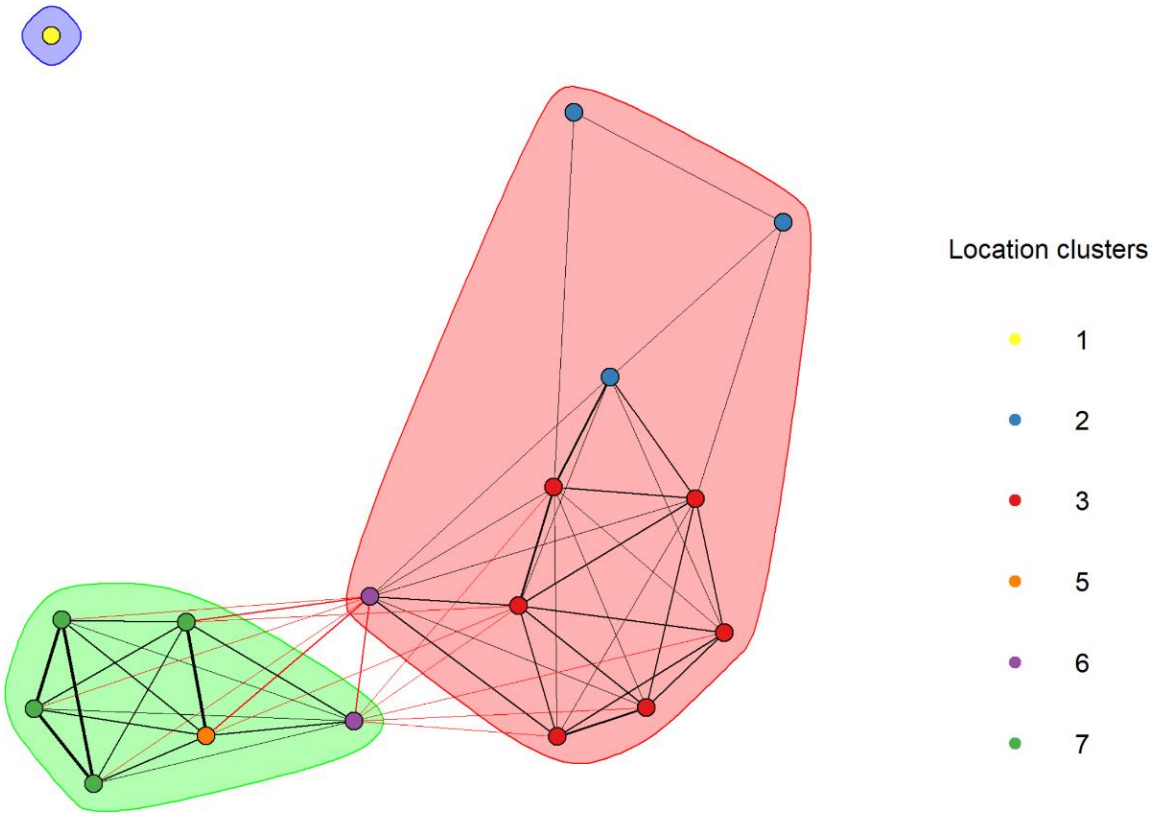

Figure 5.10 Leiden groups and locations in the 0.19 obsidian network (Figure by N. Mez).

Table 5.6 Leiden communities in the obsidian network (0.19 threshold).

Leiden communities	1	2	3
Sites	Agarak	Kohne Pasgah Tepesi	Sos Höyük
	Aygevan	Kohne Tepesi	
	Dvin	Kul Tepe Jolfa	
	Gegharot	Kuli Tepe	
	Jrahovit	Nadir Tepesi	
	Karnut 1	Ovçular Tepesi	
	Kültepe 1		
	Mokhrablur		
	Shengavit		
	Shirakavan		

Figure 5.11 shows the obsidian network with a similarity threshold of 0.5. The network contains one subgraph of fully interconnected nodes. This subgraph is linked to another group of connected nodes. The three remaining nodes are isolates. The second plot of the 0.5 obsidian network (Fig 5.12) features

the detected Leiden communities, and the site locations are highlighted as node colors. The largest connected component is divided into two groups, and the isolates are put into their own communities. The Leiden community memberships are listed in Table 5.7. Except for the isolated nodes, the communities are compared to the location-based site clusters (Table 3.1). Community 1 contains sites from Clusters 2, 3, and 6. The settlements in Community 3 are from Clusters 5, 6, and 7.

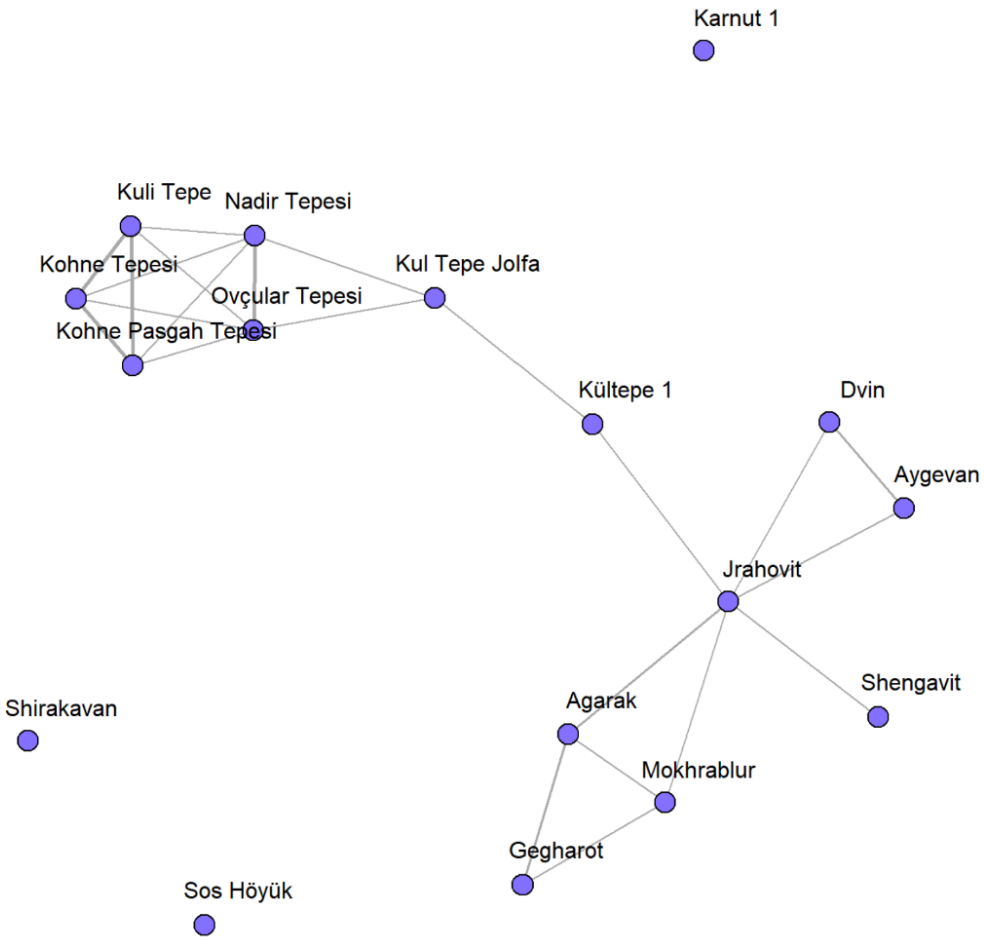

Figure 5.11 Obsidian similarity network with 0.5 threshold (Figure by N. Mez).

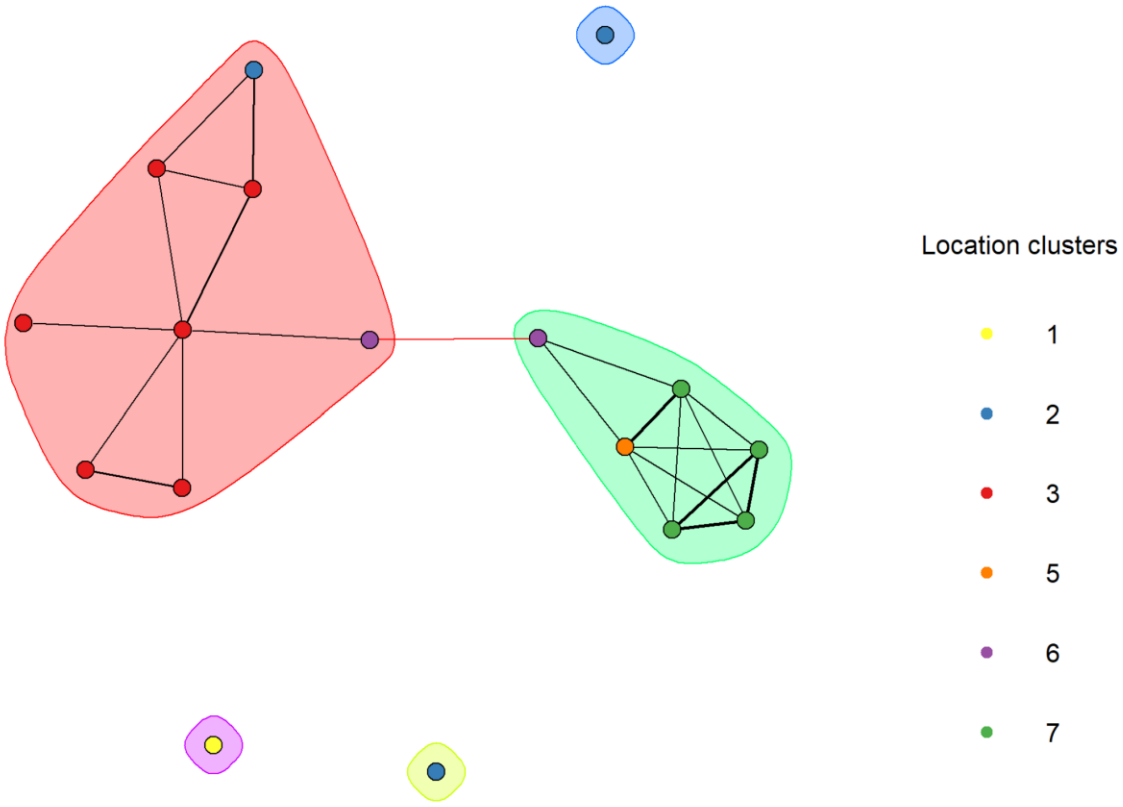

Figure 5.12 Leiden groups and locations in the 0.5 obsidian network (Figure by N. Mez).

Table 5.7 Leiden communities in the obsidian network (0.5 threshold).

Leiden communities	Sites
1	Agarak, Aygevan, Dvin, Gegharot, Jrahovit, Kültepe 1, Mokhrablur, Shengavit
2	Karnut 1
3	Kohne Pasgah Tepesi, Kohne Tepesi, Kul Tepe Jolfa, Kuli Tepe, Nadir Tepesi, Ovçular Tepesi
4	Shirakavan
5	Sos Höyük

Like the pottery graph, the obsidian similarity network changes drastically when the threshold is set to 0.7. Figure 5.13 shows that only one triad and one dyad remain. The rest of the nodes are disconnected from each other. The second plot in Figure 5.14 shows that the sites in the triad are located in the same area cluster, while the settlements in the dyad are not.

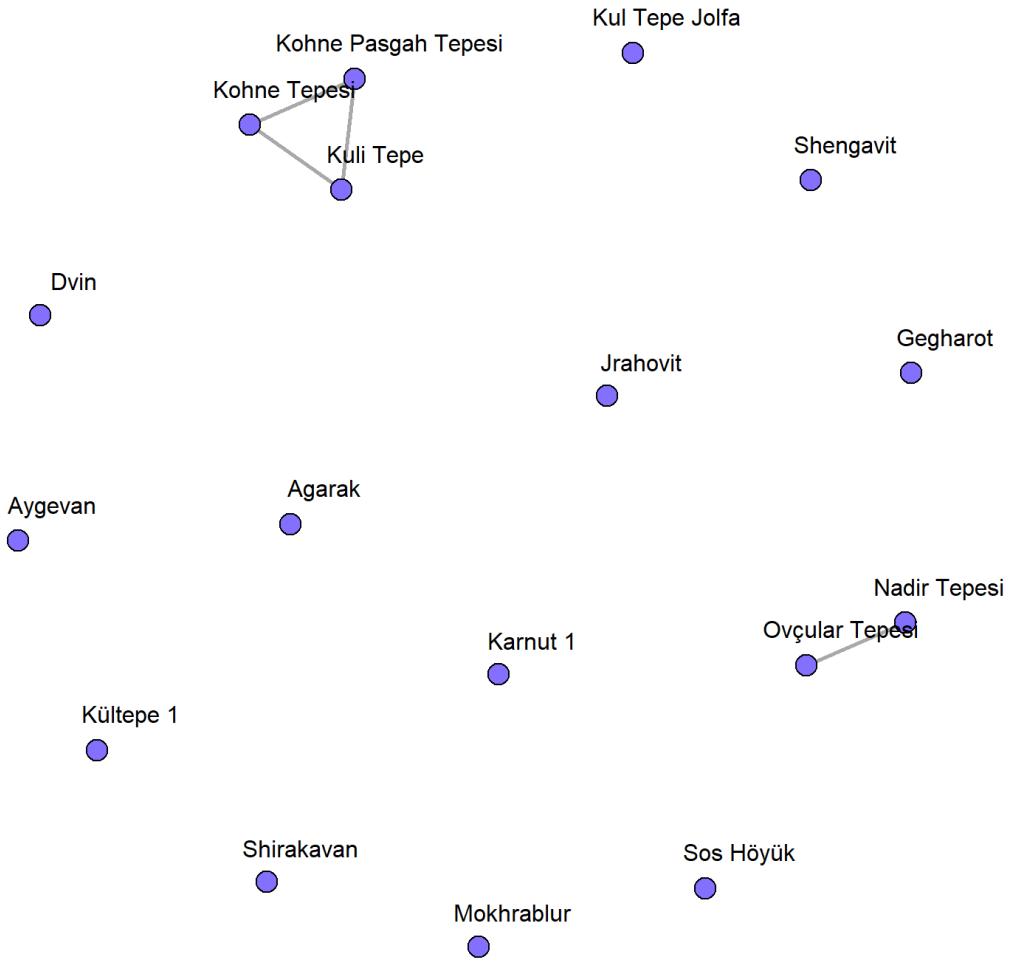

Figure 5.13 Obsidian similarity network with 0.7 threshold (Figure by N. Mez).

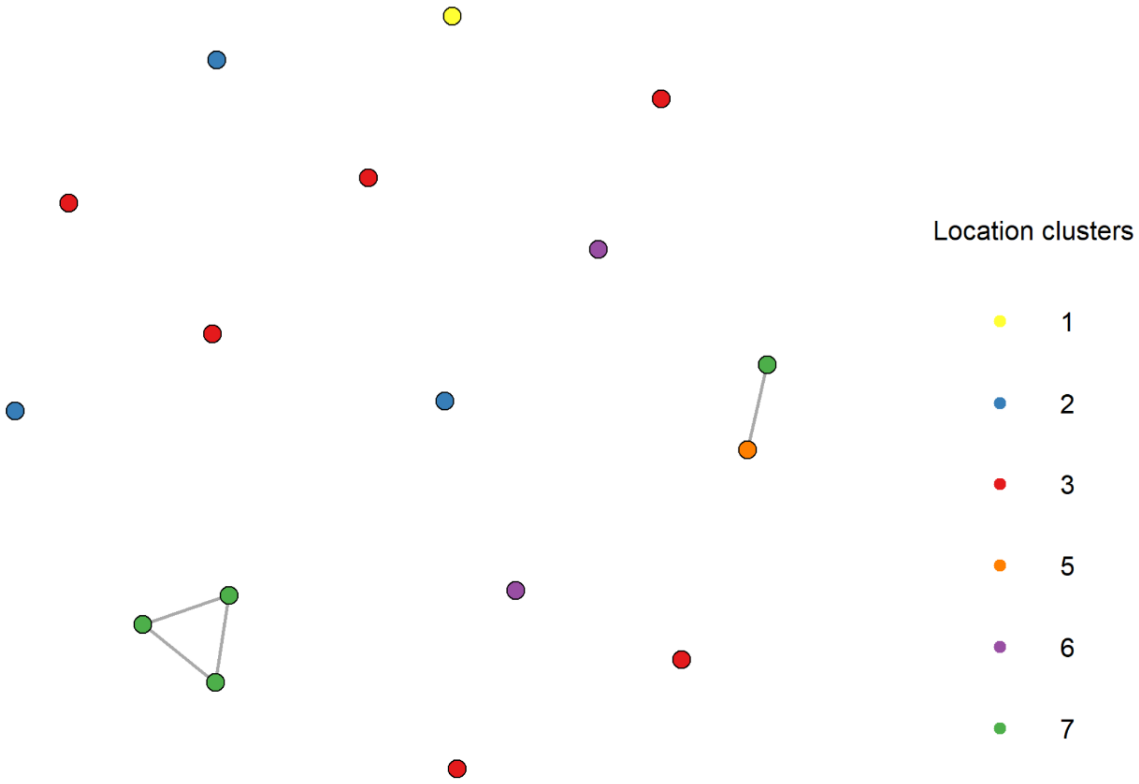

Figure 5.14 Locations in the 0.7 obsidian network (Figure by N. Mez).

Table 5.8 contains the network metrics for the 0.19, 0.5, and 0.7 obsidian similarity networks. The 0.19 network has one isolate, the 0.5 graph has three, and the 0.7 graph has 12. The high density and transitivity values reflect the strong connectivity in the 0.19 graph. The higher thresholds decreased the number of edges and the density. With the higher thresholds, the diameter increased due to the network becoming more disconnected. All three graphs have a relatively low degree centralization, gradually decreasing for the higher thresholds. The degree centralities for the nodes in the 0.19 and 0.5 obsidian networks are provided in Table 5.12. The 0.19 network has a low positive assortativity regarding the sites' locations, meaning nodes in the same location-based clusters are more likely to be connected. For the 0.5 graph, this value is twice as high, reflecting a stronger tendency for homophily concerning the assigned locations. The 0.7 graph shows a low negative assortativity, meaning nodes in the same location cluster are less likely to be connected.

Table 5.8 Metrics for the obsidian networks.

Dataset	Obsidian		
Threshold	0.19	0.5	0.7
No. of nodes	17	17	17
No. of edges	57	23	4
No. of isolates	1	3	12
Density	0.42	0.17	0.03
Diameter	1.89	6	2
Transitivity	0.71	0.64	1
Assortativity	0.20	0.44	-0.14
Centralization (degree)	0.33	0.21	0.10

5.4 Bimodal Obsidian Provenance Network

The bimodal obsidian network in Figure 5.15 shows which obsidian sources supply which sites. The graph has 35 nodes, 60 edges, and no isolates. The network structure features different procurement patterns. Some sources only supply one site, others two or more. The site-source pair Sos Höyük – Pasinler is the only dyad disconnected from the rest of the sites and sources.

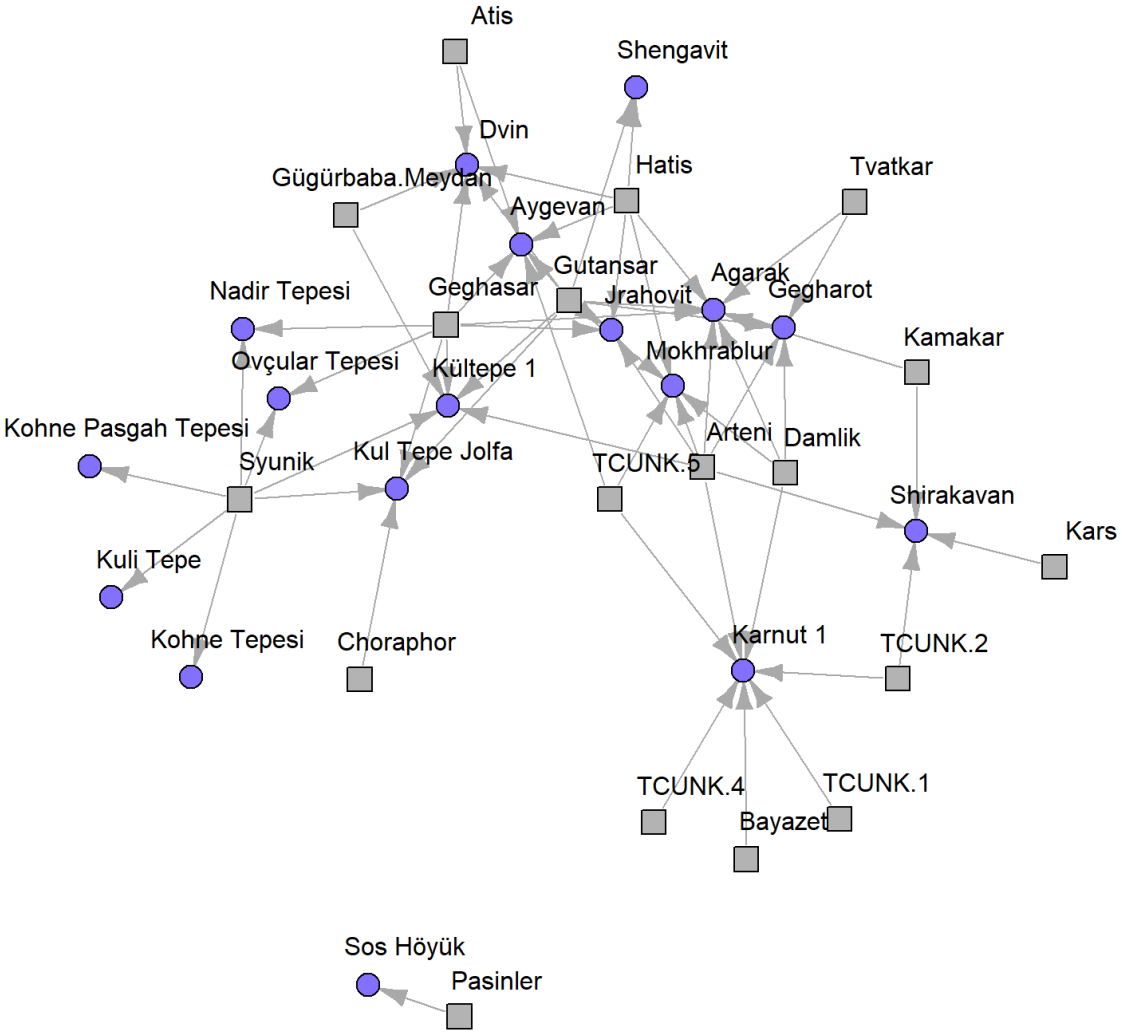

Figure 5.15 Bimodal obsidian provenance network (Figure by N. Mez).

5.5 Graph Differences

The differences between the obsidian and the pottery subset graphs were assessed through isomorphism, the Jaccard index between the two edge sets, and visual and metric comparisons between the network structures. The test for isomorphism between the pottery subset and the unimodal obsidian graph gives FALSE as an output, determining that the graphs are not structurally identical. The Jaccard index for the edge sets is 0.34. The combined presence/absence matrix showing which sites share both ceramic decorations and obsidian sources to some extent is attached in Appendix 14.

The pottery subset includes only sites also featured in the obsidian network. The similarity network of this subset is displayed in Figure 5.16. The adjacency matrix with Jaccard similarities for the subset is attached in Appendix 13. The threshold of 0.19 isolated one node. Almost all other nodes are part of a tightly interconnected subgraph. Both nodes in the only distant dyad are connected to the subgraph through multiple edges. As visible in Figure 5.17, the Leiden community detection split the dense subgraph into two communities. The dyad is assigned to a third community, and the isolate to a fourth. Table 5.9 lists the Leiden communities and the nodes assigned to them. Community 1 contains sites from Clusters 2 and 3. The settlements in Community 2 are located in Clusters 2, 3, 6, and 7. In Community 3, the sites are from Cluster 7. Community 4 features the isolated site from Cluster 7.

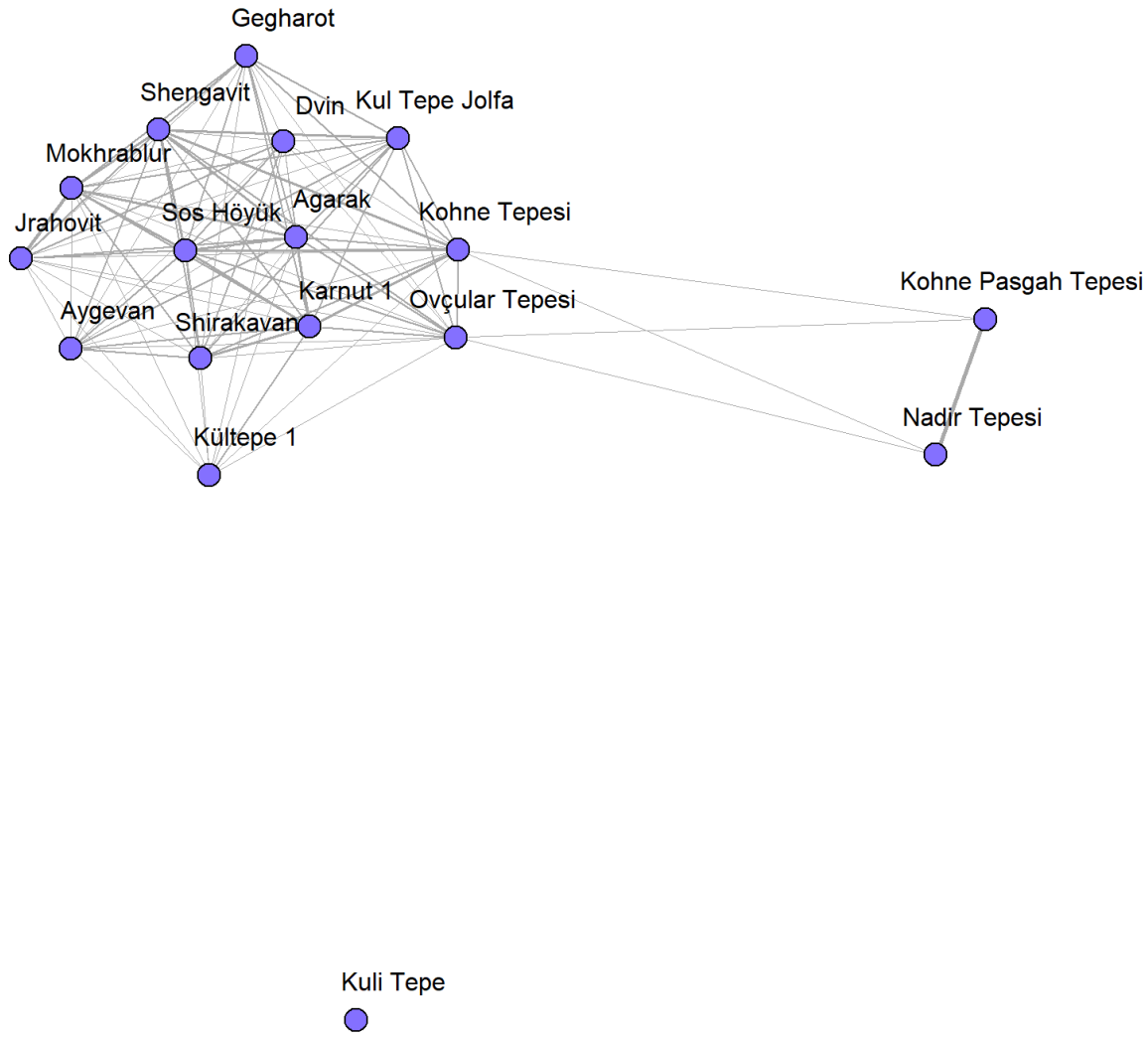

Figure 5.16 Subset of ceramics network with 0.19 threshold (Figure by N. Mez).

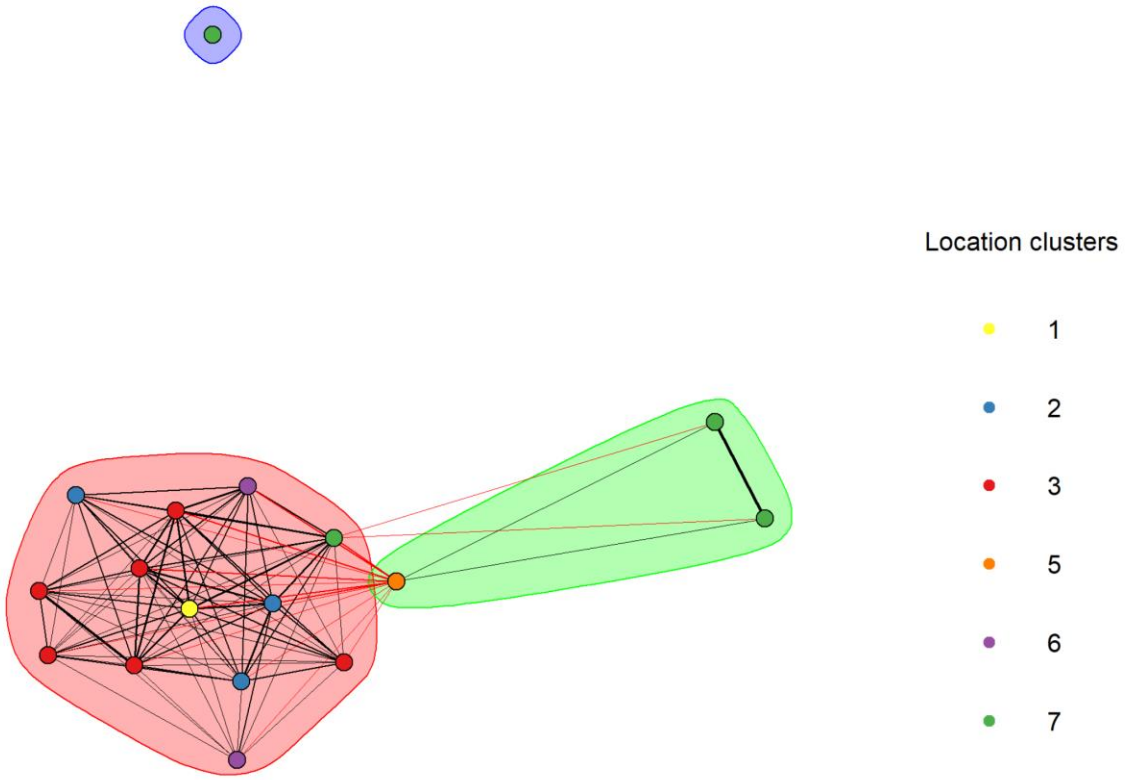

Figure 5.17 Leiden groups and locations in the 0.19 ceramics subset network (Figure by N. Mez).

Table 5.9 Leiden communities in the pottery subset network (0.19 threshold).

Leiden communities	1	2	3	4
Sites	Agarak Dvin Gegharot Jrahovit Kul Tepe Jolfa Mokhrablur Shengavit Sos Höyük	Aygevan Karnut 1 Kohne Tepesi Kültepe 1 Ovçular Tepesi Shirakavan	Kohne Pasgah Tepesi Nadir Tepesi	Kuli Tepe

Figure 5.18 depicts the pottery subset with a 0.5 threshold. The largest connected component features 10 nodes. Otherwise, only one dyad and five isolates are part of the network structure. Figure 5.19 shows how the Leiden community detection split the large subgraph into three communities. The dyad and isolates are assigned to their own communities. The Leiden community memberships are listed in Table 5.10. Except for the isolates, the assigned communities are compared to the location clusters (Table 3.1). Community 1 contains only sites from Cluster 3. The settlements in Community 2 are from Clusters 2 and 3. Community 5 only comprises sites in Cluster 7. The sites in Community 6 belong to Cluster 1, 3, 6, and 7.

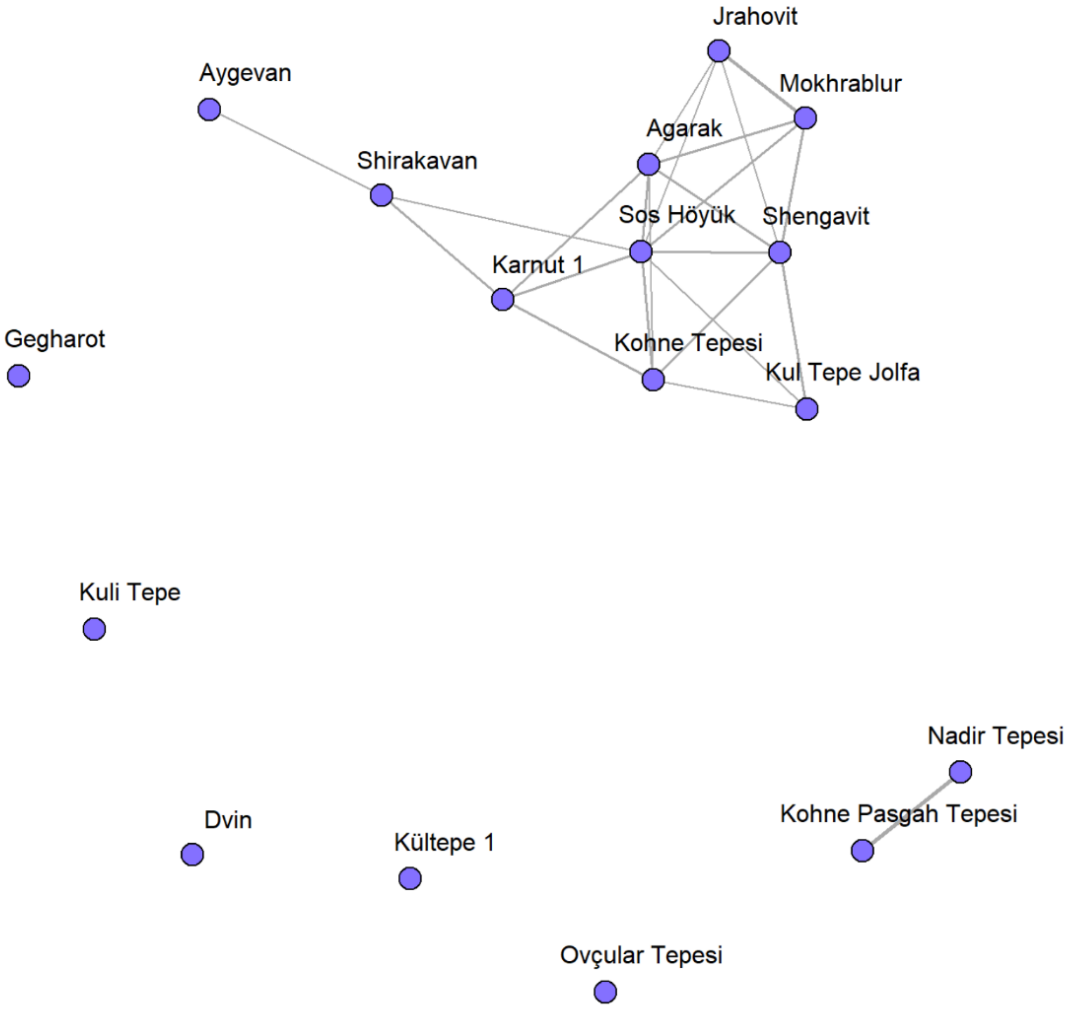

Figure 5.18 Subset of ceramics network with 0.5 threshold (Figure by N. Mez).

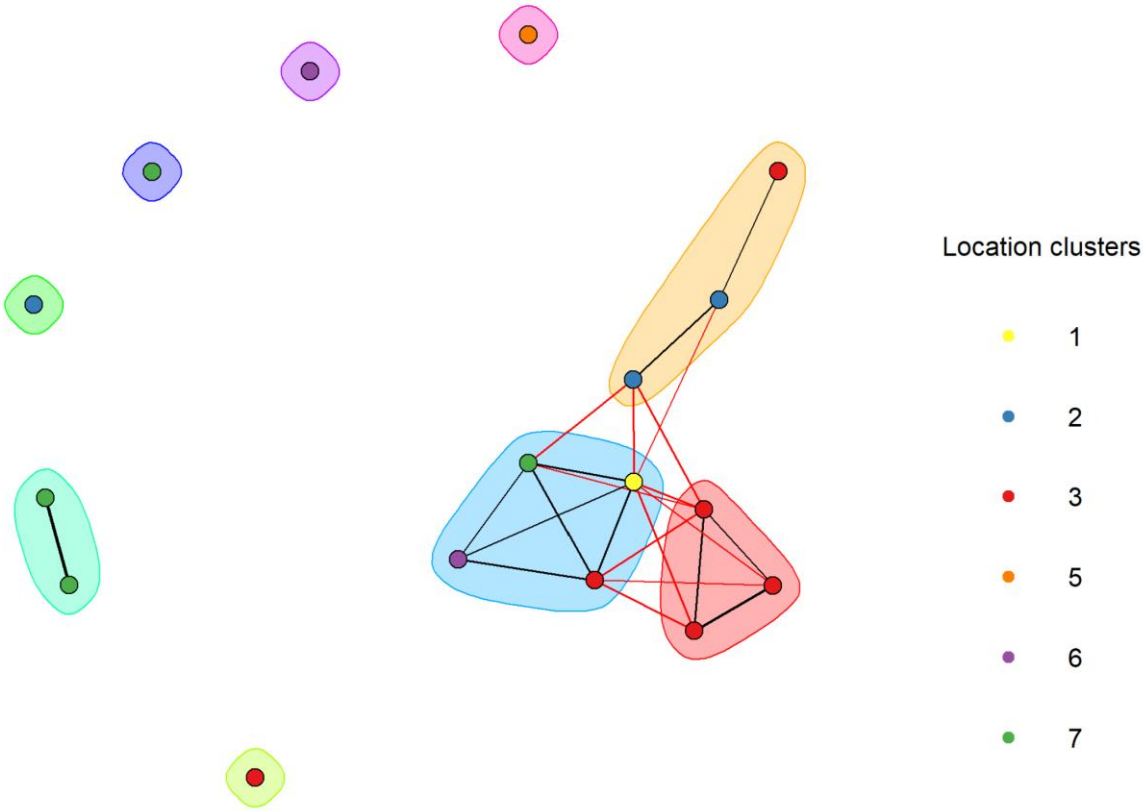

Figure 5.19 Leiden groups and locations in the 0.5 ceramics subset network (Figure by N. Mez).

Table 5.10 Leiden communities in the pottery subset network (0.5 threshold).

Leiden communities	Sites
1	Agarak, Jrahovit, Mokhrablur
2	Aygevan, Karnut 1, Shirakavan
3	Dvin
4	Gegharot
5	Kohne Pasgah Tepesi, Nadir Tepesi
6	Kohne Tepesi, Kul Tepe Jolfa, Shengavit, Sos Höyük
7	Kuli Tepe
8	Kültepe 1
9	Ovçular Tepesi

Table 5.11 contains the network metrics for the pottery subset and obsidian graphs with the 0.19 threshold. Both networks have one isolate. While having the same number of nodes, the pottery subset has more edges than the obsidian network, resulting in a higher density. The pottery subset also has a smaller diameter and higher transitivity than the obsidian network. These metrics indicate a more closely connected network for the pottery than the obsidian data. Nonetheless, the pottery subset shows a lower degree centralization, so the higher connectivity does not appear to correlate with a higher degree centralization. The degree centralities for the nodes in the pottery subset and the obsidian networks for the 0.19 and 0.5 thresholds are listed in Table 5.12. The nominal assortativity in the pottery subset is very close to zero, indicating no homophily regarding the location.

Next, the pottery subset and obsidian networks are compared using a 0.5 threshold (Table 5.11). The obsidian network has three isolates, and the pottery subset has five. Both networks have the same number of edges and, therefore, the same density. The transitivity values vary by 0.01, but the pottery subset's diameter is smaller than the obsidian's. As for the 0.19 threshold, the 0.5 pottery subset shows a slightly lower degree centralization than the obsidian network. Unlike the assortative 0.5 obsidian graph, the nominal assortativity in the pottery subset is very close to zero, indicating no homophily regarding the sites' locations.

Table 5.11 Metrics for the obsidian and pottery subset networks.

Dataset	Obsidian	Pottery subset	Obsidian	Pottery subset
Threshold	0.19	0.19	0.5	0.5
No. of nodes	17	17	17	17
No. of edges	57	93	23	23
No. of isolates	1	1	3	5
Density	0.42	0.68	0.17	0.17
Diameter	1.89	1.38	6	3.38
Transitivity	0.71	0.93	0.64	0.65
Assortativity (nominal)	0.20	-0.03	0.44	0.08
Centralization (degree)	0.33	0.25	0.21	0.33

Table 5.12 Normalized degree centralities in the obsidian and pottery subset networks.

	Obsidian		Pottery subset	
Sites	0.19	0.5	0.19	0.5
Agarak	0.56	0.19	0.81	0.38
Aygevan	0.44	0.13	0.81	0.06
Dvin	0.44	0.13	0.81	0.00
Gegharot	0.38	0.13	0.75	0.00
Jrahovit	0.63	0.38	0.81	0.25
Karnut 1	0.19	0.00	0.81	0.25

Kohne Pasgah Tepesi	0.38	0.25	0.19	0.06
Kohne Tepesi	0.38	0.25	0.94	0.31
Kul Tepe Jolfa	0.69	0.19	0.75	0.19
Kuli Tepe	0.38	0.25	0.00	0.00
Kültepe 1	0.75	0.13	0.63	0.00
Mokhrablur	0.50	0.19	0.81	0.25
Nadir Tepesi	0.44	0.31	0.19	0.06
Ovçular Tepesi	0.44	0.31	0.94	0.00
Shengavit	0.44	0.06	0.75	0.38
Shirakavan	0.13	0.00	0.81	0.19
Sos Höyük	0.00	0.00	0.81	0.50

The pottery network does not differ much from its subset regarding the metrics (Tables 5.4 and 5.11). The transitivity, nominal assortativity, and degree centralization vary by 0.1, 0.03, and 0.01 for the 0.19 threshold. For the 0.5 threshold, the transitivity, nominal assortativity, and degree centralization vary by 0.08, 0.05, and 0.12. Thus, it can be noted that the subset of the pottery graph highlights the robustness of these network metrics in the case of node loss. Furthermore, the general network layout featuring one large subgraph and a few less connected or isolated nodes is also retained.

5.6 Statistical Backbones

The backbones of the non-thresholded similarity matrices only contain edges statistically significantly stronger than expected in a null model. For the pottery network, Figure 5.20 shows that only the dyads Nadir Tepesi – Kohne Pasgah Tepesi and Duzdağı – Yakhvali are connected by statistically significant Jaccard indices. For the obsidian network, Figure 5.21 shows no statistically significant connections.

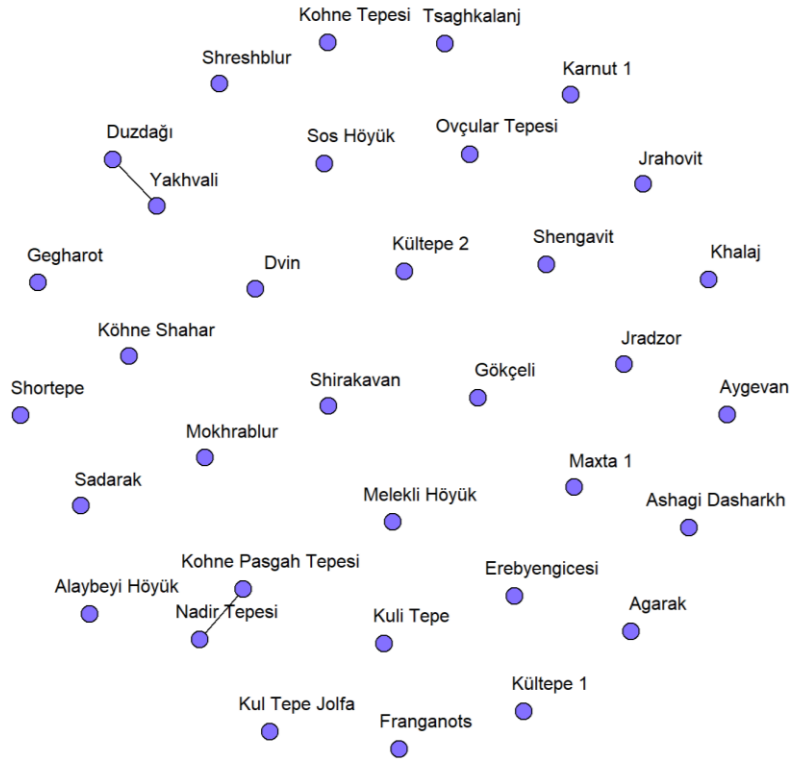

Figure 5.20 Backbone of the pottery network with α = 0.05 (Figure by N. Mez).

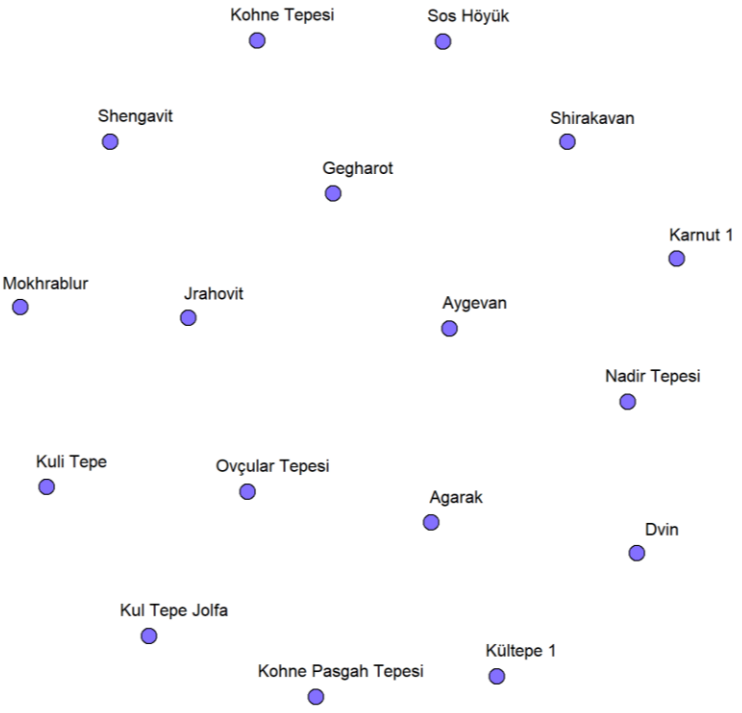

Figure 5.21 Backbone of the obsidian network with α = 0.05 (Figure by N. Mez).

5.7 Chapter Summary

This chapter presented the results that the methods generated. The Jaccard indices for the pottery and obsidian data were plotted in histograms, revealing the majority of site pairs as dissimilar. The unimodal pottery similarity network was plotted, measured, and subjected to Leiden community detection for three different thresholds: 0.19, 0.5, and 0.7. This process was repeated for the unimodal obsidian similarity network. Next, a bimodal provenance network for the obsidian data was plotted.

The investigation of graph differences revealed that the pottery subset and obsidian graphs are structurally different and share roughly a third of their connections. The subset of the pottery network was thresholded, plotted, measured, and subjected to Leiden community detection in the same manner as the other unimodal networks. Last, the statistical backbones of the non-thresholded, complete pottery, and obsidian datasets revealed that only two connections are statistically significant for the pottery and none for the obsidian graph. In the subsequent chapter, these results are discussed concerning geographical aspects, other Kura-Araxes, and SNA research. Furthermore, shortcomings of the networks related to the underlying data and methods are considered.

6 Discussion

6.1 Location and Geographical Proximity

In this chapter, the results presented in the previous sections are discussed. These observations are related to the findings of Maziar (2021), other research concerning the Kura-Araxes phenomenon, and articles about similarity networks from various archaeological contexts. Geographical proximities and locations are addressed before assessing the output in this research context. Ultimately, this study is reviewed in light of its limitations and biases.

First, the Leiden communities in the networks are contrasted with the location-based site clusters defined in Chapter 3.1 (Table 3.1) to determine the influence of location on the networks. The three Leiden communities in the 0.19 pottery network (Table 5.1) are all mixed of four or five location clusters. For the 0.19 subset of the ceramics data (Table 5.9), Community 1 consists of Clusters 2 and 3, and the sites in Community 4 are from the same cluster. Nonetheless, Community 2 contains settlements from four different site clusters.

The 0.5 pottery network has nine Leiden communities, four assigned to isolates (Table 5.3). Communities 3, 4, and 7 feature sites from multiple site clusters. The sites in Communities 1 and 4 are from the same clusters each. The 0.5 subset (Table 5.10) has 10 Leiden communities. Five belong to isolates. Community 6 is made up of four different site clusters. Nevertheless, Community 2 only comprises sites from Cluster 2 and 3. Communities 1 and 5 only contain sites from the same clusters each.

The 0.19 obsidian network features three Leiden communities, one assigned to an isolate (Table 5.6). The sites in Community 1 belong to Cluster 2, 3, and 6. Community 2 features settlements in Clusters 5, 6, and 7. The higher 0.5 threshold for the obsidian network leads to five Leiden communities, three assigned to isolates (Table 5.7). Communities 1 and 2 have the same makeup as in the 0.19 network.

In several instances, the Leiden communities are mixed from multiple non-neighboring area clusters for the 0.19 pottery networks. In these cases, the location does not seem to strongly influence the internal network structure revealed by the Leiden community detection algorithm. Location seems to substantially influence the pottery networks with 0.5 thresholds, as they feature more Leiden communities comprising only one site cluster.

The locations of the Leiden communities in the obsidian network give a different impression. Clusters 2 and 3 are located north and south of Aragats Mountain (Figure 3.1) and appear together in Leiden communities in the obsidian networks. In the obsidian graphs, Community 2 contains sites in Clusters

5, 6, and 7 that are all located next to each other along the Araxes River in the eastern part of the study area. The mix of location clusters in the Leiden communities in the 0.19 and 0.5 obsidian networks is stable. These factors suggest a more substantial location influence on the similarities in obsidian source choice than on pottery décor. Because obsidian procurement is tied to a specific source location, it might be more susceptible to travel constraints than pottery decorations.

The geographical proximity between sites can factor into material culture similarity (Maziar, 2021, p. 51). This proximity is reflected in the location clusters but can also be viewed through distances. The distance matrix for all sites, calculated with the Haversine formula (Isern et al., 2014, p. 451) and the site coordinates, is attached in Appendix 15. The distances vary dramatically in the vast study area. The most distant sites are Alaybeyi Höyük and Nadir Tepesi, and the closest are Kohne Tepesi and Kohne Pasgah Tepesi (Table 6.1). For these examples, the far distance between Alaybeyi Höyük and Nadir Tepesi might have influenced the low Jaccard index. Alaybeyi and Sos Höyük are roughly twice as similar in their pottery decoration as Kohne Pasgah and Kohne Tepesi, despite the Anatolian sites being farther apart. This example suggests that the distance might have played less of a role.

Table 6.1 Distances and similarities for selected sites in the pottery dataset.

Site pair	Distance	Pottery similarity index
Alaybeyi Höyük – Nadir Tepesi	547.56 km	0.08
Alaybeyi Höyk – Sos Höyük	41.34 km	0.53
Kohne Tepesi – Kohne Pasgah Tepesi	270 m	0.2

In the obsidian network (Table 6.2), the farthest site pair by distance is Shirakavan and Nadir Tepesi. These sites share no obsidian sources. The site closest to Nadir Tepesi is Kohne Tepesi. Ovçular Tepesi is further from Nadir Tepesi but uses the same obsidian sources. These few data points indicate the same trend as the pottery similarities. Sites far away are unlikely to have high similarity scores. However, whether the site is a close neighbor or further away does not clearly correspond to the similarities for the selected examples.

Table 6.2 Distances and similarities for selected sites in the obsidian dataset.

Site pair	Distance	Obsidian similarity index
Shirakavan – Nadir Tepesi	339.21 km	0
Ovçular Tepesi – Nadir Tepesi	200.68 km	1
Kohne Tepesi – Nadir Tepesi	57.04 km	0.5

As addressed in Chapter 3.1, sheer proximity alone does not accurately reflect the cost of travel in the past. Because site clusters are based on proximity, they are located within the same or adjacent plains. For some cases, like Cluster 7, the plains are not directly adjacent, but the Araxes Valley might have served as a corridor for mobility. In other cases, like Cluster 4, the sites are separated by hilly terrain. The accessibility of sites is also influenced by knowledge, seasonality, and topography. Seasonality and topography are integrated into Fabian's cumulative cost path map for the South Caucasus (Figure 6.1). It displays potential pedestrian travel routes based on the least-cost paths. Although she seeks to investigate the Parthian-Roman period (Fabian, 2018, p. 26), the underlying landscape and elevations are presumably comparable to the Early Bronze Age.

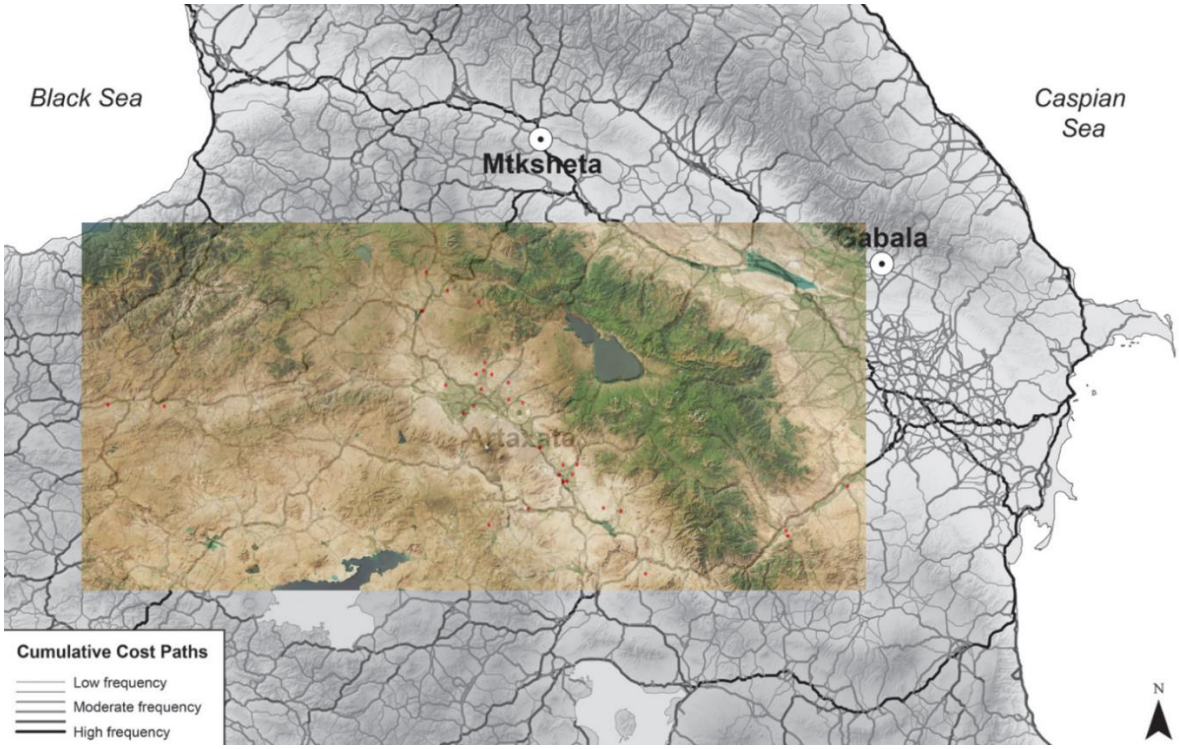

Figure 6.1 Cumulative cost path map (Fabian, 2018, Figure 4 modified by N. Mez)

This map reflects travel during seasons when the mountain passes were crossable (Fabian, 2018, p. 29). In this model, east-west riverine corridors along the Kura and Araxes are the most conducive spaces for movement. Furthermore, the Ararat Plain is a focal point of movement at the nexus of both north-south and east-west routes. Various north-south routes are displayed because of the absence of any excellent choices. The "frequencies" represent how accessible a path is relative to the other available options in the model (Fabian, 2018, pp. 29–30).

Combined with the site map in Appendix 1, Fabian's investigations display how the studied settlements are located along or near high-frequency cumulative cost paths (Figure 6.1). The largest site

accumulation, Cluster 3, is located in the Ararat Plain, and most settlements are found along the Araxes Valley. Such relatively accessible routes might have facilitated the interaction between more or less close sites, potentially enhancing the similarity in pottery decorations and obsidian source choices among sites in different regions or vicinities. Therefore, this ease of movement along the river basin could explain the similarities between less close sites highlighted in Tables 6.1 and 6.2.

6.2 Patterns and Trends in the Similarity Networks

Before comparing the present findings to Maziar's, the similarities among sites based on pottery decoration and shared obsidian sources are assessed. The distinctive features of the pottery and obsidian similarity networks and differences in network structures among the sites present in both networks are identified. First, the network level patterns and trends are discussed for the pottery, obsidian, and pottery subset networks through their respective plots and measurements. Next, the degree centralities highlight peculiarities on the node level. All of these observations are interpreted archaeologically regarding homogeneity and regionalism. The previous chapter addressed the community level by comparing the Leiden communities to the location-based clusters.

The visual examination provides an entry point into the network-level interpretation. The large, dense subgraph of the pottery networks with minimum Jaccard indices of 0.19 and 0.5 (Figures 5.3 and 5.5) could represent a regional group connected through economic or social relations. As the subgraph in both networks consists of sites from all location-based clusters (Figures 5.4 and 5.6), it does not appear to be a regional group. The ceramics are primarily crafted from local clays (Chapter 2.1), making the trade with pottery – or the goods stored within – and recent population movement unlikely explanations for the commonalities in décor.

Geographic periphery in the study area does not appear to be the main cause for decentral network positions. The nodes positioned at some distance from the central subgraph could represent peripheral groups caused by geographic isolation. Some peripheral nodes, namely Kohne Pasgah Tepesi, Kuli Tepe, Nadir Tepesi, and Jradzor are located on the research area's fringes. Although Kohne Tepesi is also located there, the site is part of the large network cluster. In addition, despite their geographically central locations, Ashagi Dashrakh, Duzdağı, and Yakhvali are also located outside the dense subgraph.

Certain groups or individuals may have migrated from the central locations to establish settlements in the periphery of the study area, resulting in their inclusion in the network despite their geographical location. Alternatively, these physically peripheral nodes might represent trade or interaction hubs that attracted communities from various locations, leading to their central network position. Such hubs were not detected in the ceramics or obsidian networks but could be tied to other material culture types or aspects of the subsistence economy.

Social or cultural reasons such as conflict or cultic practices could have also contributed to isolated network positions, although they cannot be inferred from the pottery or obsidian data alone. Pottery decorations or obsidian procurement are only one facet of life in these villages. Isolation in pottery décor or obsidian source use does not have to imply general isolation from the other sites in the study area. This aspect is highlighted by the different degree centralities between the sites in the pottery subset and the obsidian graphs (Table 5.12).

The structure of the obsidian similarity network with minimum Jaccard indices of 0.19 is characterized by three dense node groups (Figure 5.9). The overlap and shared connections between the groups suggest that there might be an intersection between the archaeological communities exploiting the different obsidian sources. However, only one of these groups persists in the 0.5 graph (Figure 5.11). This small site group is also absent in the 0.19 and 0.5 pottery graphs (Figures 5.3 and 5.5).

The isolated position of Sos Höyük in the obsidian networks suggests infrequent interaction with the other archaeological communities included in the dataset. This isolation is contradicted by the high degree centrality of Sos Höyük in the 0.19 pottery network subset (0.81), showing multiple stylistic similarities with other sites. In this case, migration might serve as an explanation: People could have migrated to Sos Höyük, bringing their decorative traditions with them. Residing there, they might have been too far from the Caucasian sources or the other sites to exchange obsidian with them. However, the two Anatolian obsidian sources used by Caucasian sites in the study area, Gügürbaba-Meydan and Kars, were not identified in the assemblage at Sos Höyük.

Increasing the minimum similarity for the networks further disrupts their structural integrity. The extremely disconnected graphs for the 0.7 threshold stress the inhomogeneity in pottery décor (Figure 5.7) and obsidian source choice (Figure 5.13) among the site assemblages. In the pottery network, the sites in the only larger subgraph are located in three different location clusters, making a regionally shared ceramic tradition unlikely. Because parallel terms for the same decorations or motifs were

grouped into feature categories (Chapter 3.2), this high dissimilarity is not necessarily caused by inconsistent terminology.

Several metrics allow more profound insights into the network-level structures in conjunction with the visual examination. In the 0.19 pottery network (Table 5.4), the high density, diameter, and transitivity hint at a shared decorative tradition, possibly caused by a regional network. The 0.5 threshold decreases the previously high density to a low value and lowers the transitivity significantly. The diameter in the 0.5 version is nearly as high as in the 0.7 graph. Because of these changes, the interpretation as a well-connected regional network appears debatable. Additionally, most connections are based on low similarities (Figure 5.1), and the large subgraph disappears in the 0.7 graph (Figure 5.7).

For the 0.7 pottery network, the high number of isolates, low transitivity, and low degree centrality indicate an inhomogeneous and fragmented cultural landscape regarding pottery decoration. Adherence to traditions and signaling of group identity (de Groot, 2019, p. 603) may explain these dissimilarities. Whether these decoration preferences were spread through migration, diffusion, or other processes is not discernible from the current network perspective.

In the 0.7 obsidian graph (Figure 5.13), the high transitivity is caused by the only triad being the largest connected component and does not imply interconnectedness on the network level. The network shows a low negative assortativity, resulting from the many isolates in various location clusters. Without the visual inspection (Figure 5.14), it could be assumed that the location has no effect, despite the sites in the only triad being in the same location cluster.

The pottery network's backbone (Figure 5.20) reveals that only the dyads Nadir Tepesi – Kohne Pasgah Tepesi, and Duzdağı – Yakhvali are statistically more significant than expected. Both pairs are located in different but neighboring location clusters, only 57.28 km and 56.18 km apart. Geographical proximity might have affected the statistical significance in these cases, but not enough edges are retained in the backbone to assess this securely. No statistically significant connections are preserved in the backbone of the obsidian network (Figure 5.21).

The network differences for sites in both datasets are investigated by comparing the obsidian similarity network to a subset of the pottery network. The two graphs are not isomorphic, meaning their structure differs. The intensity of these differences is reflected by the Jaccard index for the edge sets (0.34). This low similarity suggests that some preferences behind the choice of pottery decorations

and obsidian sources vary. This distinctness might be explained by ceramic consumption and obsidian procurement highlighting different aspects of prehistoric societies: Ceramics are products of manufactured technology, while obsidian provenance shows the choice in resource use. Nonetheless, roughly a third of the edges are shared, indicating some overlap in underlying preferences or influence of one network over the other.

Compared to the 0.19 obsidian network, the pottery subset with the same threshold has a higher density, smaller diameter, and higher transitivity. These differences suggest that the pottery subset network is more interconnected than the obsidian network, as shown in the plot (Figure 5.16). The more robust interconnection might indicate that ceramic decorations were assimilated more frequently than the obsidian source choice. As for the obsidian and complete pottery networks, the degree centralization for the 0.19 pottery subset is relatively low (0.25).

The 0.5 obsidian and pottery subset graphs have the same density and nearly the same transitivity, but the pottery subset has a smaller diameter. The degree centralization for the pottery subset increases slightly with the higher threshold, while the value for the obsidian data decreases marginally. These low degree centralizations could imply that the pottery was created and the obsidian was procured by many communities, not only from elites or specialized groups at specific sites. The low degree centralization also reflects the relatively even distribution of pottery similarities. Furthermore, the low degree centralization implies no dominant obsidian source in the study area, whether exploited directly or via a trade hub. Therefore, among the previously investigated settlements, none dominates the networks by connecting the sites as a hub.

As for the complete dataset, the nominal assortativity for the 0.19 and 0.5 pottery subsets is close to zero, suggesting no discernible influence of the location on the site connections. The nominal assortativity is very low positive in the 0.19 and medium positive in the 0.5 obsidian graph, suggesting a substantial preference for high-similarity connections within the same location clusters. As a raw material, obsidian is highly dependent on its specific geographic source, necessitating direct access to these locations for procurement. In contrast, pottery decoration networks may be more flexible regarding material acquisition, as potters can utilize various clay sources not limited to specific geographic areas. Consequently, the direct association between obsidian and its source location makes it more susceptible to the influence of geographical constraints, resulting in a more substantial impact on its use compared to the broader and less location-dependent pottery decoration networks. This argument could also explain the more frequent assimilation of décor commented on previously.

The site's degree centralities provide more information about tendencies on the node level. In the 0.19 pottery network, degree centrality does not correspond to a central location. Ovçular Tepesi has the highest degree centrality (0.85), and Sadarak and Köhne Shahar have the second highest (0.82). Ovçular Tepesi and Sadarak are located in a large site cluster at the nexus of the study area, but Köhne Shahar lies further from the river somewhat remotely. However, the large settlement possesses a fortification wall, an unusual feature for Kura-Araxes settlements (Sagona, 2018, p. 242). Fortifications imply that the inhabitants experienced (hostile) encounters if used for defensive purposes. Such contacts – possibly the non-violent ones – could have influenced the exchange of material culture and, by extension, pottery décor.

Ovçular Tepesi and Kohne Tepesi (0.94) have the highest degree centralities for the pottery subset, followed by seven Armenian sites and Sos Höyük (all 0.81). Ovçular Tepesi is centrally positioned in the research area, but Kohne Tepesi is not. Unlike the Armenian sites in the Ararat Plain, which are at the focal point of many least-cost paths (Figure 6.1), Sos Höyük is located remotely in the study area. In the 0.19 obsidian network, Kültepe 1 (0.75), Kul Tepe Jolfa (0.69), and Jrahovit (0.63) have the highest degree centralities. Kültepe 1 is close to other sites and might have had access to multiple trading partners. Kul Tepe Jolfa is 51.28 km from its nearest neighbor. However, this settlement is comparably large (Abedi & Omrani, 2015, p. 56), possibly indicating a sizeable population in need of obsidian tools.

The application of the 0.5 threshold results in a reduction of all degree centralities for the obsidian nodes. In most cases, the same values decrease equally. Conversely, the 0.5 pottery subset experiences a more pronounced decrease in centralities. Additionally, the same values undergo varying degrees of reduction, suggesting that the changes in centrality differ across the pottery subset. These findings indicate that the obsidian data exhibits more stability when subjected to higher thresholds.

Despite salt being a valued and distributed commodity, Duzdağı's low degree centrality does not reflect extensive connections through ceramic décors. According to Marro, the ceramic containers were most likely used for storage or food and drink consumption, not for salt mining activities. Therefore, the lack of decorations is probably not explained by the different purposes of the compared ceramics (Marro, 2021, Paragraph 11).

As for the complete pottery dataset, the high degree centralities in the obsidian and pottery subset networks do not reflect exceptionally central geographic locations. The degree centralities for the pottery subset and obsidian network confirm the structural differences highlighted on the network level

by the metrics and plots. However, Jrahovit is the only site among the highest values in both networks and is located amidst a group of Armenian settlements.

To summarize, the pottery decorations network is disconnected by the high similarity threshold, decentralized, and shows barely an influence of location. The obsidian source choice network is also disconnected by the high threshold and decentralized but shows a more substantial influence of the location on the edges. The sites in both networks have somewhat dissimilar connections, implying only limited influence of one network over the other and different underlying economic or cultural preferences.

6.3 Relation to Kura-Araxes Research

Regarding the pottery decoration network, Maziar (2021) concludes that the pottery style in the southern Araxes Basin shows no detectable connections with the Karnut-Shengavit or Shresh-Mokhrablur traditions in Armenia (p. 55). The results of the present study do not support this, as the sites are generally dissimilar, with few exceptionally high similarities. The 0.5 pottery network (Figure 5.5) features links between sites north and south of the Araxes. However, only three connections between sites north and south of the river persist in the 0.7 pottery network (Figure 5.7). When examining the similarity matrix (Appendix 11), similarities with northwestern Iran range between 0 – 0.25 to Shreshblur, 0 – 0.41 to Mokhrablur, 0.1 – 0.67 to Karnut 1, and 0.06 – 0.71 to Shengavit.

Table 6.3 Decorative techniques and motifs connecting sites north and south of the Araxes.

Techniques	Motifs
Nakhichevan lug	Horizontal line
Dimple	Cross-hatched lines
Groove	Parallel lines
Relief	Zigzag
Incision	

The features connecting the sites south and north of the Araxes in Iran and Armenia more than once are listed in Table 6.3. Maziar does not address the features “Horizontal line”, “Cross-hatched lines”, “Parallel lines” and “Zigzag”. Nakhichevan lugs are mentioned but not described as a connecting element (Maziar, 2021, p. 49). Together with the changes in site selection, this might explain the differences between Maziar’s and the present findings.

Maziar concludes that in the northwestern Iranian Araxes Basin and southern Armenian Syunik region, the obsidian sources reflect connections that are suggested though not directly expressed (Maziar, 2021, p. 55). The bimodal obsidian network (Figure 5.15) reveals Syunik as the sole supplier for Kohne Pasgah Tepesi, Kohne Tepesi, and Kuli Tepe; one of two suppliers for Nadir Tepesi and Ovçular Tepesi; and one of multiple for Kul Tepe Jolfa and Kültepe 1. Syunik does not supply Armenian sites in the dataset. In the 0.5 obsidian graph (Figure 5.11), Kül Tepe 1 and Ovçular Tepesi are the only sites north of the Araxes sharing obsidian sources with settlements south of the river. Only one edge in the 0.7 obsidian network (Figure 5.13) connects Ovçular Tepesi to Nadir Tepesi south of the Araxes River. The obsidian graphs created in this study align with Maziar's assessment. The results show connections between sites south of the Araxes and Syunik as a source area but low similarities between the settlement south and north of the river in their obsidian procurement.

Maziar (2021) states that the networks of obsidian procurement and pottery decoration differ (p. 55). This statement is confirmed as the obsidian and pottery subset networks are not isomorphic, and the Jaccard similarity of the edges is relatively low. Maziar claims the sites north and south of the Araxes show more explicit connections regarding their use of obsidian sources than ceramic decorations (Maziar, 2021, p. 55). The SNA results are ambiguous. The pottery subset network is more interconnected than the obsidian network, displayed by the higher density, smaller diameter, and lower transitivity. The higher density is caused by the pottery dataset containing more features than the obsidian data. Some sites feature up to 15 decoration techniques and motifs, whereas no site has more than seven identified obsidian sources assigned to it. These differences could have caused the complete pottery dataset to have a higher median Jaccard similarity than the obsidian data, indicating more homogeneity in pottery decorations. Nonetheless, a common obsidian source could be seen as a stronger connection than a shared pottery feature because a shared source indicates a physical connection to the same locality, directly or indirectly.

Maziar (2021) describes the Kura-Araxes economic system in the study area as localized (p. 54). The obsidian network shows a low positive assortativity for the 0.19 graph and a medium positive assortativity for the 0.5 graph. The influence of the assigned locations on the 0.19 pottery networks is close to zero and very low positive for the 0.5 graph. Therefore, only the obsidian networks indicate a significant influence of the location as a factor for the sites being connected. Besides the nominal assortativity for the location, the Leiden communities can also indicate geographic localization, as examined

in Chapter 6.1. These compositions show that the obsidian networks hint at higher geographic localization than the pottery networks.

To summarize, this study did not confirm the lack of detectable connections for the pottery decorations, as low similarities were present. The low similarities confirmed the weak connections in the obsidian source choice. These results also confirmed the differences in the networks. The description of the networks as geographically localized was only partially confirmed for the obsidian network and not confirmed for the pottery network.

The bimodal obsidian provenance network demonstrated that three different procurement models occur. Some sites procure their obsidian from a single source, others show dual-source usage, while the majority rely on multiple sources (four, five, or seven). This multisource model, featuring between three and seven sources, is attested for the Early Bronze Age sites in the Tsaghkahovit, Shirak, and Ararat plains. Usually, one source is dominant, supplying between 50 and 80 % of the obsidian (Badalyan, 2021, p. 432). However, the present network analysis cannot inform about this aspect. Batiuk et al. (2022) state that obsidian was moved locally and distantly and that settlements do not appear to exert exclusive control over specific obsidian sources (p. 292). This assessment aligns with the low centrality values in the obsidian networks.

Although several sources occur more frequently in our dataset, none dominates the procurement network. This distribution aligns with Maziar and Glascock's (2017) observation that the network features multiple equivalent connected centers (p. 34). The network analysis does not investigate the centralization on the intra-site level, but an apparent centralization on the inter-site level is absent. The economic system of obsidian exchange was not under centralized control by specific elites or actors, emphasizing the role of the household and local production (Maziar & Glascock, 2017, p. 36).

Other research on stylistic connections between pottery assemblages indicates similar patterns to Maziar's observation. Batiuk et al. (2022) observe that the area in the Eastern part of the Araxes, mainly northwestern Iran in our database, shows few connections in pottery style to the Kura-Araxes heartland during the period KA II. The surface treatment and, in some instances, the vessel shapes are comparable, but the ceramics often have dimples and grooves instead of incised designs (Batiuk et al., 2022, p. 307). Additionally, black and grey burnished wares appear more frequently among the Iranian assemblages than the Red-Black Burnished Wares prevalent elsewhere. Palumbi and Chataigner (2014) interpret this as an adaptation according to local technologies and preferences (p. 255). Eastern Anatolia, including Sos Höyük, displays stylistic connections to the Armenian pottery traditions during the KA II. However, the pointed bases and solid tab handles are seen as local developments (Sagona, 2018, p. 261). These local variations could reflect the ability of communities to adapt and modify their

pottery styles to suit their specific environmental, social, or cultural contexts. Migration – from the emigrants' or immigrants' perspective – might have exposed populations to new materials, technologies, or artistic influences, prompting them to incorporate these elements into their pottery traditions.

In Armenia during phase KA II, ceramics' decorative and morphological repertoires were fragmented and regionalized. Kura-Araxes communities' alleged cultural and social unity is challenged by the diversity of Kura-Araxes material culture, including these regional ceramic trends (Palumbi & Chataigner, 2014, pp. 253–254). Işıklı (2019) emphasizes that regionalism is crucial in the Kura-Araxes cultural horizon, considering it the primary feature. He believes this regionalism to be a natural consequence resulting from the vast geographical extent of the culture (Işıklı, 2019, p. 143). As indicated by the mix of location clusters in the Leiden communities, this fragmentation in decoration practices affects all regions, not only Armenia, while regionalism is less apparent. Overall, the inhomogeneity in the datasets and low centralization scores in the networks correspond to the scarce information about the society and economy during the Kura-Araxes period, pointing to "segmented village societies rather than a proto-state regional formation" (Marro, 2021, Paragraph 35).

After placing the results into the context of Maziar's conclusions, the applicability of SNA to her research has to be reviewed. One significant research design change was necessary for adapting Maziar's case study to this framework. The temporal scope was narrowed down to the later Kura-Araxes period only. Comparing the entire Kura-Araxes to the Neolithic and Chalcolithic periods in the same area (Maziar, 2021, p. 46) would have added an interesting diachronic perspective. Nevertheless, this approach would have been too extensive as this study already addresses two material culture spheres and experiments with different levels of similarity and subsetting.

Changes in data selection were necessary to apply SNA to the case study. As mentioned previously, some sites Maziar (2021) included in her discussion are not sufficiently published for SNA and, therefore, could not be included to create meaningful networks (p. 51). So, additional sites in the Araxes Valley had to be researched. The geographic scope was broadened in size but not in terrain, as all new sites are still located in the Araxes Basin and adjacent areas. Maziar (2021) acknowledges a dearth of information and describes her findings as speculations needing verification with more data (p. 55). Although there is still a lack of information, adding more sites north and south of the Araxes allowed for reevaluating the findings in the 2021 article.

Another hurdle in applying social network analysis to Maziar's case study was that it does not compare the same sites for obsidian and pottery. Maziar (2021) compares Syunik north of the Araxes and northwestern Iran south of the Araxes (p. 43). However, there are no sites from Syunik with sufficiently published pottery or obsidian analyses, so the comparison relies only on Armenian sites further north

near the Araxes (Maziar, 2021, p. 48). Additionally, Maziar does not define or use a similarity measure, making these methodological choices another requirement for SNA application.

6.4 Considerations from Archaeological Similarity Networks Research

Because the data used to create archaeological networks varies drastically between case studies, and there is currently no SNA research on the Kura-Araxes, one has to be cautious when comparing their archaeological interpretations. Nonetheless, comparing the considerations other researchers factored into their interpretations is worthwhile since some of the same challenges were faced.

First, some general remarks about the explanatory potential of similarity networks are considered, as these lines of thought help put the results into perspective. Östborn and Gerding (2014) state that false positives or negatives (edges that were or were not present in the past) cannot be excluded confidently. Consequently, interpretations should never rely on a single edge only (Östborn & Gerding, 2014, p. 83), which I have followed in my assessments.

Similarity networks can be interpreted as reflecting the relationships underlying them, but such interpretations must hold up when the similarity criterion is varied within reasonable limits (Östborn & Gerding, 2014, p. 83). In this study, thresholds up to 0.19 do not disrupt the similarity patterns significantly, but higher thresholds disintegrate the networks. The 0.7 threshold nearly eradicates all relationships, suggesting that the networks are too unstable for far-reaching interpretations. A more practical choice seems to be the 0.5 threshold, as it removes roughly half of the edges for the obsidian data and almost a third for the pottery data while still displaying interpretable connectivity patterns.

Golitko and Feinman (2015) follow the same framework as this study. In their publication on Pre-Hispanic Mesoamerican obsidian, the similarity coefficients based on shared features reflect the intensity of possible past contact (Golitko & Feinman, 2015, p. 215). The edge strength, therefore, only hints at the likeliness of a tie being present and relevant in the past (Golitko & Feinman, 2015, p. 216). I do not claim that the existing edges are a solid representation of the past. Changes in the underlying datasets due to new research have the potential to shift the network structures, especially for the sites with currently few edges.

Additionally, Golitko and Feinman (2015) stress that social networks are not a reconstruction of geographical trade networks (p. 215). In this thesis, neither the obsidian nor the pottery networks

represent trade routes or the like. The similarities reflect closeness in material culture. Nonetheless, this closeness is undoubtedly influenced by geographic factors.

Aside from these general factors, the question arises, what networks of shared obsidian can tell us about past economies. Golitko and Feinman (2015) focus on hierarchy and integration in their research. An integrated network features a high density, small diameter, short path length, and an even distribution of ties. Hierarchical networks have high centralization indices on the network level, while non-hierarchical networks are the opposite (Golitko & Feinman, 2015, pp. 214–215). Golitko and Feinman (2015) stress that this type of hierarchy does only inform about the distribution of obsidian, not the production thereof or quantities transported through the nodes (p. 215).

According to this line of interpretation, the created obsidian networks are non-hierarchical, as they have a low degree centralization. For the 0.19 obsidian network, the density is medium-high and the diameter relatively short, partially falling into Golitko and Feinman's (2015) description of an integrated network. The 0.5 obsidian network has a low density and large diameter, showing the disintegration by application of a higher threshold. Though, SNA based on obsidian sources only reflects the endpoint of distribution, not the distributive system through which the obsidian reached the sites (Golitko & Feinman, 2015, p. 214). Therefore, the obsidian network in this study cannot provide insight into the mode of production and exchange.

In most studies, only one type of material culture represents the contact between sites. Ceramics are often chosen, although other material culture groups may reveal different trends (Wehner, 2019, p. 101), as demonstrated by the significant differences between the ceramic subset and obsidian networks. This result strengthens the approach of including different material groups in similarity networks of sites and challenges the practice of discussing ceramic networks as reflective of entire sites regarding material culture similarity.

Mills et al. (2013) examined similarities in ceramic assemblages and obsidian procurement in the Late Precontact Southwest USA using SNA. It should be noted that only five obsidian sources were studied (Mills et al., 2013, p. 14). For the obsidian networks, in earlier periods, the sites mostly procured their obsidian from easily accessible outcrops. In later periods, however, there are more sites with an overrepresentation of distant sources and an underrepresentation of close sources (Mills et al., 2013, p. 15). These findings highlight that closeness in social networks is affected by multiple factors, not only spatial proximity (Mills et al., 2013, p. 8).

Mills et al. (2013) observe that the sites with the same overrepresented obsidian sources are more similar in ceramic decoration (compared to the average similarity between their studied sites). They

conclude that the social networks indicated by pottery similarity also affected obsidian procurement (Mills et al., 2013, p. 15). In this thesis research, the low Jaccard similarity of the edge sets in the pottery subset and obsidian similarity network implies some influence. Which network affected which, and the type of influence remains unknown.

No historic social units are known to compare the network clusters for the Kura-Araxes, making the comparison so reliant on location. Other case studies addressing networks of pottery décor (Hart & Engelbrecht, 2012, p. 338) and obsidian procurement (Ladefoged et al., 2019, p. 22) attested a possible interplay between historically known social units and communities detected in the networks, for which proximity did not explain material culture similarity.

6.5 Biases and Limitations

The present study is affected by various biases and limitations. Although most of them cannot be mitigated, they must at least be acknowledged. Certain limitations regarding the data were addressed in Chapters 3.2 and 3.3. These limitations include source heterogeneity, language barriers, data incompleteness, and inconsistent terminology for pottery decorations and obsidian sources. Although not free of issues, handling the obsidian data was less problematic than the pottery data and might be more suitable for SNA in this specific scenario, as the terminology for the obsidian was more unifiable than the ceramics. Therefore, it is essential to have the obsidian network to compare the possibly flawed ceramics network to.

Temporality is a critical issue concerning data and methodology. Data broadly attributed to the later Kura-Araxes periods was included in the database. However, for some ceramic and obsidian contexts, radiocarbon dates are unavailable. Associating materials from diachronic processes into a single time unit is called “time-averaging” (Daems et al., 2023, p. 2). Therefore, the graphs might show patterns that never existed because the finds were not contemporaneous. The generated networks are snapshots of possible past connections grouped into a single timeframe of ca. 500 years (2900 to 2400 BCE). The influence of time-averaging on networks is significant but variable, depending on the underlying data. Thus, no universal solution exists (Daems et al., 2023, p. 30). More precise dates would produce narrower time slices, but issues concerning time-averaging could still affect the networks.

Some of the methodological limitations of SNA were touched upon in Chapters 2.2 and 4.5. These shortcomings include the subjectivity of similarity (precisely the categories and resulting assemblage

diversity the measurements are based on), possible irrelevance of connections, ignorance of geographical considerations, exclusion of nodes and edges due to the spatial scope, temporal changes, weak links, misinterpretation of absences and loss of relevant edges due to thresholding.

First, the generated networks are representations of archaeological research, not of the past. Also, these research networks only included publications that were accessible and usable. Furthermore, Golitko and Feinman (2015) stress the issue of equifinality by explaining how two very different systems of obsidian distribution would result in identical networks. Assuming there is no preference for a specific source, with either a redistributive or a down-the-line system, the relative source frequencies are approximately the same for all sites. In both cases, a similarity matrix will reveal a network with about equal strengths of connections between nodes (Golitko & Feinman, 2015, p. 216).

Besides these biases, which are in some ways inherent to SNA in archaeology, there are others explicitly created by the research design. The geographic limits are necessary, but the choices made in this study probably exclude relevant sites and sources, resulting in partial and incomplete network representations. The scope issue also relates to selecting features as the basis of edges. Despite the ceramic wares not resulting in relevant differences, focusing only on decorative features might elude other meaningful differences and commonalities between pottery assemblages.

Another limitation connected to the chosen methodology is binarization. In some cases, binarization was necessary for the quantities of obsidian or pottery finds due to data limitations. However, the binarization of the pottery and obsidian similarity indices for the combination matrix (Appendix 14), highlighting which sites share pottery decorations and obsidian sources, obscures the different intensities of similarities in these two systems between the sites. Instead of binarizing the similarity scores before combining the matrices, this combination of the two networks might have been better solved as a duplex network (a network with two types of edges connecting the nodes), retaining the similarity scores as edge weights for each edge type.

Further issues stem from the central role of similarity in the approach followed. The assumption that similarity adequately represents community interactions might not be the case for the studied sites during the Early Bronze Age. Additionally, focusing on similarity might obscure other patterns for the obsidian network. However, for the ceramic network, the similarity was the only aspect investigable with the selected framework. Also, the assemblage diversity plays into similarity scores and, therefore, the network structure.

This problem of assemblage diversity is connected to the Jaccard similarity coefficient. According to de Groot (2019), the Jaccard coefficient cannot handle varying attribute diversities between sets. The

probability of connecting with another site is higher for assemblages with diverse decorative features/obsidian sources. This tendency may skew the resulting networks (de Groot, 2019, p. 603) as it leads to an overestimation of the similarity between sets with a high attribute diversity and an underestimation between sets low in attribute diversity (de Groot, 2019, p. 604). This general tendency is not verified in Riris and Oliver's (2019) study of rock art motifs using the Jaccard coefficient. They make the contrary observation that rock art diversity at a site is an ineffective predictor of how many connections it has to other site assemblages (Riris & Oliver, 2019, p. 9).

Finally, some biases and limitations are caused by the choice of network metrics. The nominal assortativity based on the location could misrepresent the homophily amongst the nodes, as the location-based clusters might not always adequately represent travel cost (Chapter 6.1). The Leiden community detection is based on modularity, with a resolution limit (Fortunato & Barthélemy, 2007). Consequently, smaller modules may not be resolvable due to this resolution limit. The possibility that modules of virtually any size are clusters of modules cannot be ruled out, since modularity optimization may miss significant network substructures (Fortunato & Barthélemy, 2007, p. 41). The low number of groups for the 0.19 threshold, three for the pottery network, four for the subset of the pottery network, and three for the obsidian network, might be influenced by this resolution limit.

6.6 Chapter Summary

This chapter deliberated the interpretation of the results. First, the Leiden communities, derived from the networks through a community detection algorithm, were compared to the location-based site clusters. This comparison revealed that location has a discernible influence on the obsidian networks but barely on the pottery networks. Geographical proximity was also compared to the similarity indices on a random basis, showing a tendency for very far away sites being dissimilar. Next, patterns and trends in the similarity networks were described and debated.

From this discussion, the findings are related to Kura-Araxes' research. The outcomes were partially aligned with Maziar's results and generally conformed to other research on the same topics. Some considerations from archaeological publications on similarity networks framed the output of this study. Last, the biases and limitations arising from the data and methodology were addressed. Some limitations can be used as stepping stones for future research, especially the ones related to the scope of the research design and data choices. These perspectives are addressed in the subsequent concluding remarks.

7 Conclusions

This study reinvestigated Kura-Araxes sites along the Araxes River Basin using a quantitative approach through material culture similarity networks. The similarities in pottery decoration and shared obsidian sources were selected to indicate past community interactions. SNA was applied to a case study that had already been researched, highlighting this procedure's advantages and disadvantages. A methodological hurdle to overcome was using data from various publications to create networks.

How similar are the sites regarding pottery décor and obsidian source use, and what do these similarities imply about regional homogeneity and possibly migration? The histograms and medians of the Jaccard similarities and the higher threshold unimodal networks reveal that the sites are generally dissimilar in their use of pottery decorations and choice of obsidian sources. This dissimilarity hints at cultural and economic inhomogeneity in the study area. The lack of regional standardization in pottery decorations could hint at a decentralized nature of the Kura-Araxes cultural horizon, in which the communities express themselves differently. Various obsidian sources could indicate differing access to and preferences for raw materials. The low similarities in themselves would not necessarily be solid indicators for migration. However, since location and proximity do not appear to determine the similarities in pottery decorations and only partially for obsidian source choice, large-scale migration could explain commonalities between more distant communities.

What are the characteristics of the pottery and obsidian similarity networks? Formal network metrics and visual representations exposed the characteristics of the pottery and obsidian similarity networks. Both networks are somewhat decentralized. Depending on the choice of threshold, the obsidian network shows a low to medium assortativity regarding location, while the pottery network shows none to low. This tendency is also reflected in the composition of the communities detected by the Leiden algorithm. The Leiden groups for the obsidian networks are more homogenous regarding the location-based clusters than for the pottery graphs. This difference might reflect issues related to raw material transport, as this only concerns obsidian procurement, not pottery decoration. Thus, an influence of location is only securely demonstrated for the obsidian procurement, not for pottery décors.

How do the network structures differ for the sites shared between the pottery and obsidian networks? The network structures of the sites present in the obsidian similarity network and the pottery subset differ, despite some commonalities, indicating different underlying preferences – their precise nature

remains elusive. The bimodal obsidian network displayed the multisource procurement model typical for the region and period.

To what limits can SNA be applied to regional archaeological studies, such as Maziar (2021), which were not intended for SNA? Besides reviewing and extending the data for Maziar's study, which she described as necessary, this research highlighted that when applying SNA to a case study, especially the data selection is subject to revisions, as more general comparisons require fewer specific data than network analysis. However, prior case studies' trajectory and research questions can provide a fruitful starting point for SNA. Furthermore, the data collection revealed that to properly investigate ceramic similarity networks for the Kura-Araxes, a unified and extensive supra-regional typology is needed to improve such meta-analyses. An alternative approach and idea for future research would be to compare a set of sites through networks of lithic technology and obsidian provenance. Such a comparison could show how the technologies at the sites differ and relate to the sources of raw materials.

Which research design and data selection changes were necessary to adapt Maziar's case study? The general framework regarding material culture selection and research questions addressing the interplay among communities north of the Araxes in Armenia and south of the Araxes in Iran were suitable for SNA. However, the data selection was only partially usable for SNA, resulting in significant changes in site selection. Besides the data selection, methodological choices had to be made, such as the choice of similarity measure and the integration of the two networks. Furthermore, although not a shortcoming of Maziar's (2021) research, the lack of a clear supra-regional typology for Kura-Araxes ceramics made applying SNA challenging. For the obsidian data, the state of research was more comprehensible and adaptable to SNA.

How do the results of the SNA relate to Maziar's findings? Maziar (2021) states that the pottery style shows no connection between the sites (p. 55). The results of the pottery networks diverge from Maziar's findings, as in some cases, higher similarities between sites in the southern part of the Araxes Basin exist. The obsidian similarity networks created in this study align with Maziar's (2021) assessment that the shared use of obsidian sources north and south of the Araxes hints at possible communication routes (p. 55). As in Maziar's findings, SNA revealed that the network structures for pottery decoration and obsidian procurement differ. Her observations that the network structures are localized (Maziar, 2021, p. 54) were partly debated, as only the obsidian networks demonstrate geographic

localization. All in all, the results partially confirm Maziar's findings despite data changes and methodological adaptations.

Several avenues for future research emerged throughout this study. Some of these ideas expand the study using the current data and results. It would be insightful to investigate the influence of individual features on the network. The most common (or rare) features could be deleted to assess their influence on the network structure, uncover potential biases, and identify irrelevant or critical features. Another option for methodological progression would be to include sensitivity analysis. In sensitivity analysis, the data or parameters are changed, and the variations in the results are recorded. Adding this procedure would allow determining the most influential pottery decorations and obsidian sources and assessing the networks' overall robustness (Kanters et al., 2021, p. 2). This knowledge of robustness also helps assess the effects of time-averaging in the networks (Daems et al., 2023, p. 29). A further idea would be to formally calculate the correlation coefficients between the proximity and similarity matrices. These calculations would allow a more precise assessment of the correlation similarity between pottery décor/obsidian source use and distance.

There are also several ideas for expanding the study through more data. A diachronic perspective was provided by Maziar (2021) in her comparison of the Neolithic and Late Chalcolithic periods at the Kura-Araxes sites in the study area. Accordingly, the next logical step would be to include pottery and obsidian assemblages from this timeframe in the study. In addition, recalibrated radiocarbon dates are available now that were not accessible to Maziar (Batiuk et al., 2022). Besides expanding the timeframe to the pre-Kura-Araxes periods, the subsequent period could also be included to examine the shifts at the end of the Kura-Araxes cultural horizon in this area.

Further, the geographic scope could be expanded. A reasonable geographic extension would be toward Lake Urmia. The lake and Araxes River are located in the larger region of northwestern Iran and are connected through several hypothetical routes, as shown by the cumulative cost path map (Fabian, 2018, Figure 4). Multiple well and less well-studied Kura-Araxes settlements are located around Lake Urmia. The new data from Lake Urmia can also be utilized as a sort of robustness test since introducing new nodes and edges into the networks challenges their structural stability.

Regarding the methodology, the present study could benefit from a mixed methods approach of GIS and SNA to better integrate physical and social space since a spatial expansion through diverse terrain defines the Kura-Araxes cultural horizon. Also, GIS would enable a more thorough investigation of the relationship between material culture similarity and geographical proximity, especially utilizing least-cost path methods.

Last, the SNA could be expanded by including more aspects of material culture, such as architectural elements, burial customs, or evidence connected to subsistence strategies from archaeozoological and archaeobotanical research. These networks could be constructed as general similarity networks incorporating all types of connections into an overall inter-site similarity score (Östborn & Gerding, 2014, p. 81). Alternatively, multiple different networks could be compared to each other and the existing pottery and obsidian provenance networks.

Despite commenting on a different issue, the often-quoted statement "all models are wrong, but some are useful" (Box, 1979, p. 202) encapsulates a vital aspect of this study. Considering the number of biases and limitations (Chapter 6.5), the networks are most certainly wrong in whatever way. The interpretative potential is also limited because only two connections in the pottery network and all connections in the obsidian network are statistically insignificant. Nevertheless, as the discussions in Chapters 6.2 and 6.3 demonstrated, the networks helped answer the research questions. As the array of avenues for future research shows, there are many possibilities to continue the SNA of Kura-Araxes sites. This study is intended as a demonstration and starting point. It is just a piece in the Kura-Araxes puzzle waiting to be connected to future SNA explorations.

Appendices

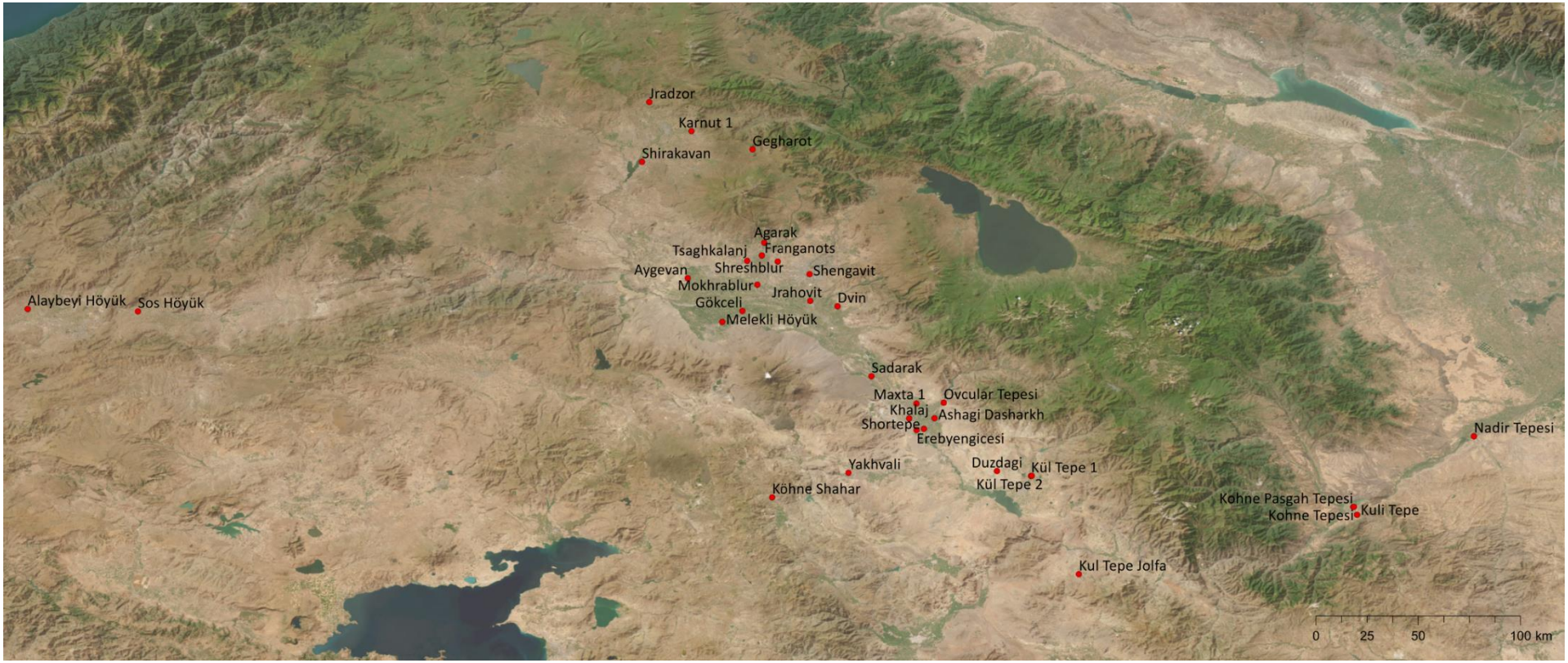

Appendix 1 Map of all investigated sites in the Araxes Basin

Long_WGS84	Lat_WGS84	Site_Name	Estimated
44,2766111	40,2953611	Agarak	
41,0372018	40,0038735	Alaybeyi Höyük	1
45,0271332	39,5242524	Ashagi Dasharkh	1
43,9401880	40,1393120	Aygevan	
45,3016570	39,2916981	Duzdağı	
44,6006680	40,0159780	Dvin	
44,9483190	39,4720447	Erebyengicesi	1
44,2659167	40,2390000	Franganots	
44,2252778	40,7056111	Gegharot	
44,1804180	39,9957940	Gökceli	
43,7712333	40,9137833	Jradzor	
44,4808370	40,0397480	Jrahovit	
43,9563333	40,7860000	Karnut 1	
44,9158845	39,5231386	Khalaj	1
46,8686060	39,1340600	Kohne Pasgah Tepesi	
44,3113890	39,1761110	Köhne Shahar	
46,8716600	39,1344970	Kohne Tepesi	
45,4519440	39,2702780	Kül Tepe 1	
45,4547220	39,2708330	Kül Tepe 2	
45,6619444	38,8386111	Kul Tepe Jolfa	
46,8852520	39,0992740	Kuli Tepe	
44,9477780	39,5883330	Maxta 1	
44,0918660	39,9474550	Melekli Höyük	
44,2460400	40,1107870	Mokhrablur	
47,3996160	39,4446150	Nadir Tepesi	
45,0678816	39,5921526	Ovçular Tepesi	
44,7500805	39,7082277	Sadarak	1
44,4778420	40,1571120	Shengavit	
43,7390000	40,6510556	Shirakavan	
44,9807434	39,4772570	Shortepe	1
44,3359060	40,2124950	Shreshblur	
41,5222877	39,9937275	Sos Höyük	
44,2016560	40,2155480	Tsaghkalanj	
44,6490000	39,2840000	Yakhvali	1

Appendix 2 Table of site coordinates.

Name	Red Black burnished	Black burnished	Monochrome burnished	Unburnished	Location
Agarak	1	1	0	0	3
Alaybeyi Höyük	1	0	0	0	1
Ashagi Dasharkh	0	1	0	1	5
Aygevan	1	0	0	0	3
Duzdağı	0	1	1	1	6
Dvin	1	0	0	0	3
Erebyengicesi	1	1	0	0	5
Franganots	1	1	0	1	3
Gegharot	1	1	0	0	2
Gökçeli	0	1	0	0	3
Jradzor	0	1	0	1	2
Jrahovit	1	1	0	0	3
Karnut 1	1	1	1	1	2
Khalaj	0	1	1	0	5
Kohne Pasgah Tepesi	0	1	1	1	7
Köhne Shahar	0	1	1	1	4
Kohne Tepesi	0	1	0	1	7
Kul Tepe Jolfa	0	1	0	1	6
Kuli Tepe	0	1	1	1	7
Kültepe 1	1	1	1	1	6
Kültepe 2	1	1	0	0	6
Maxta 1	1	1	1	1	5
Melekli Höyük	0	1	0	0	3
Mokhrablur	1	1	0	0	3
Nadir Tepesi	0	1	1	0	7
Ovçular Tepesi	1	1	1	1	5
Sadarak	1	1	1	1	5
Shengavit	1	1	0	0	3
Shirakavan	1	0	1	0	2
Shortepe	1	0	1	1	5
Shreshblur	1	1	0	0	3
Sos Höyük	1	1	1	0	1
Tsaghkalanj	0	1	0	0	3
Yakhvali	0	1	1	1	4

Appendix 3 Node sheet with wares for the pottery network.

Name	Source	Location
Agarak		3
Arteni	1	Armenia
Atis	1	Armenia
Aygevan		3
Bayazet	1	Armenia
Choraphor	1	Armenia
Damlik	1	Armenia
Dvin		3
Gegharot		2
Geghasar	1	Armenia
Gügürbaba-Meydan	1	Armenia
Gutansar	1	Armenia
Hatis	1	Armenia
Jrahovit		3
Kamakar	1	Armenia
Karnut 1		2
Kars	1	Anatolia
Kohne Pasgah Tepesi		7
Kohne Tepesi		7
Kul Tepe Jolfa		6
Kuli Tepe		7
Kültepe 1		6
Mokhrablur		3
Nadir Tepesi		7
Ovçular Tepesi		5
Pasinler	1	Anatolia
Shengavit		3
Shirakavan		2
Sos Höyük		1
Syunik	1	Armenia
TCUNK 1	1	Armenia
TCUNK 2	1	Armenia
TCUNK 4	1	Armenia
TCUNK 5	1	Armenia
Tvatkar	1	Armenia

Appendix 4 Node sheet for the obsidian network.

	Nakhichevan lug	Dimple	Groove	Application	Excision	Incision/ Scraped	Painted	Comb-scraping	Relief/ Embossing	Concentric circles	Ladder
Agarak	0	1	1	1	0	1	0	0	1	0	1
Alaybeyi Höyük	1	0	1	0	0	1	0	0	1	1	1
Ashagi Dasharkh	0	0	0	0	0	0	0	0	1	0	0
Aygevan	0	0	1	0	0	0	0	0	0	0	0
Duzdağı	1	0	0	0	0	0	0	0	0	0	0
Dvin	0	1	0	0	0	1	0	0	1	0	0
Erebyengicesi	0	0	0	0	0	0	1	0	0	0	0
Franganots	1	1	0	0	0	1	0	0	1	0	1
Gegharot	0	1	0	0	0	1	0	0	1	1	0
Gökçeli	0	1	1	0	0	1	1	0	1	1	1
Jradzor	1	1	1	0	0	0	0	0	0	0	0
Jrahovit	0	1	0	0	0	0	0	0	1	1	1
Karnut 1	1	0	0	1	0	1	0	0	1	0	0
Khalaj	0	0	0	0	0	1	1	0	0	0	0
Kohne Pasgah Tepesi	1	1	0	0	0	0	0	0	0	0	0
Köhne Shahar	1	1	1	0	0	1	1	0	0	0	0
Kohne Tepesi	1	1	0	1	0	1	0	0	1	0	0
Kul Tepe Jolfa	1	1	1	0	1	1	0	0	1	1	0
Kuli Tepe	0	0	0	0	0	1	0	1	0	0	0
Kültepe 1	0	0	0	1	0	0	1	0	1	0	0
Kültepe 2	1	1	0	1	0	1	1	0	1	1	0
Maxta 1	1	0	1	0	0	1	1	0	1	1	1
Melekli Höyük	0	0	1	0	0	1	1	0	0	1	1
Mokhrablur	0	1	0	0	0	0	0	0	1	1	1
Nadir Tepesi	1	1	0	0	0	0	0	0	0	0	0
Ovçular Tepesi	1	1	1	0	0	1	1	0	0	0	0

Sadarak	1	1	0	0	0	1	1	0	0	0	0
Shengavit	1	1	1	0	0	1	0	0	1	1	1
Shirakavan	1	0	0	0	0	0	0	0	1	0	0
Shortepe	1	0	0	0	0	1	1	0	0	0	0
Shreshblur	0	1	0	0	0	0	0	0	1	0	0
Sos Höyük	1	1	0	1	0	1	0	0	1	1	1
Tsaghkalanj	1	1	0	0	0	0	0	0	1	0	1
Yakhvali	1	0	0	0	0	0	0	0	0	0	0

	Spiral/ Loop	Horizontal line	Cross hatched lines	Parallel lines	Triangle	Hatched chevrons	Zigzag	Anchor	Geometric motif	Plant motif	Snake motif
Agarak	1	1	0	1	1	1	1	0	1	1	0
Alaybeyi Höyük	1	1	0	1	1	1	0	0	0	0	0
Ashagi Dasharkh	0	0	0	0	0	0	0	0	0	0	0
Aygevan	0	1	0	1	1	0	1	0	1	0	0
Duzdağı	0	0	0	0	0	0	0	0	0	0	0
Dvin	0	1	0	0	0	0	0	0	1	0	0
Erebyengicesi	1	0	0	0	0	0	0	0	0	0	0
Franganots	1	1	0	1	0	1	1	0	1	1	0
Gegharot	1	0	1	0	1	0	1	1	1	0	0
Gökçeli	1	1	0	1	0	0	0	0	0	0	0
Jradzor	0	0	1	0	0	0	0	0	0	0	0
Jrahovit	1	1	0	1	0	0	0	0	1	1	0
Karnut 1	1	1	0	1	1	0	1	0	1	0	0
Khalaj	0	1	0	1	0	0	0	0	0	0	0
Kohne Pasgah Tepesi	0	0	0	0	0	0	0	0	0	0	0
Köhne Shahar	0	1	0	1	0	0	1	0	0	0	0

Kohne Tepesi	0	1	1	1	1	0	1	0	0	0	0
Kul Tepe Jolfa	0	1	1	1	0	1	1	0	1	0	1
Kuli Tepe	0	0	0	0	0	0	0	0	0	0	0
Kültepe 1	1	1	0	1	0	0	0	0	0	0	0
Kültepe 2	1	1	0	1	1	0	0	1	0	0	1
Maxta 1	1	1	1	1	1	0	1	0	1	0	0
Melekli Höyük	1	0	0	0	0	0	0	0	0	0	0
Mokhrablur	1	1	0	1	0	0	1	0	1	1	0
Nadir Tepesi	0	0	0	0	0	0	0	0	0	0	0
Ovçular Tepesi	1	1	0	1	0	0	1	0	0	0	0
Sadarak	1	1	1	1	0	0	0	0	0	0	0
Shengavit	0	1	1	1	1	1	1	0	1	1	0
Shirakavan	0	1	0	1	0	0	1	0	1	0	0
Shortepe	0	0	0	1	0	0	0	0	0	0	0
Shreshblur	0	0	0	0	0	0	0	0	1	0	0
Sos Höyük	0	1	0	1	1	0	1	0	1	0	0
Tsaghkalanj	1	0	0	1	0	1	1	0	1	1	0
Yakhvali	0	0	0	0	0	0	0	0	0	0	0

Appendix 5 Incidence matrix of decorative pottery features for the network edges.

	Syunik	Geghasar	Choraphor	Gutansar	Arteni	Hatis	Damlik	TCUNK 1	TCUNK 2
Agarak	0	1	0	1	1	1	1	0	0
Aygevan	0	1	0	1	0	1	0	0	0
Dvin	0	1	0	1	0	1	0	0	0
Gegharot	0	0	0	1	1	0	1	0	0
Jrahovit	0	1	0	1	1	1	0	0	0
Karnut 1	0	0	0	0	1	0	1	1	1
Kohne Pasgah Tepesi	1	0	0	0	0	0	0	0	0
Kohne Tepesi	1	0	0	0	0	0	0	0	0
Kul Tepe Jolfa	1	1	1	1	0	0	0	0	0
Kuli Tepe	1	0	0	0	0	0	0	0	0
Kültepe 1	1	1	0	1	1	0	0	0	0
Mokhrablur	0	0	0	1	1	1	1	0	0
Nadir Tepesi	1	1	0	0	0	0	0	0	0
Ovçular Tepesi	1	1	0	0	0	0	0	0	0
Shengavit	0	0	0	1	0	1	0	0	0
Shirakavan	0	0	0	0	1	0	0	0	1
Sos Höyük	0	0	0	0	0	0	0	0	0

	TCUNK 4	TCUNK 5	Bayazet	Güğürbaba-Meydan	Kars	Kamakar	Atis	Tvatkar	Pasinler
Agarak	0	0	0	0	0	1	0	1	0
Aygevan	0	1	0	0	0	0	1	0	0
Dvin	0	0	0	1	0	0	1	0	0
Gegharot	0	0	0	0	0	0	0	1	0
Jrahovit	0	0	0	0	0	0	0	0	0
Karnut 1	1	1	1	0	0	0	0	0	0
Kohne Pasgah Tepesi	0	0	0	0	0	0	0	0	0
Kohne Tepesi	0	0	0	0	0	0	0	0	0
Kul Tepe Jolfa	0	0	0	0	0	0	0	0	0
Kuli Tepe	0	0	0	0	0	0	0	0	0
Kültepe 1	0	0	0	1	0	0	0	0	0
Mokhrablur	0	1	0	0	0	0	0	0	0
Nadir Tepesi	0	0	0	0	0	0	0	0	0
Ovçular Tepesi	0	0	0	0	0	0	0	0	0
Shengavit	0	0	0	0	0	0	0	0	0
Shirakavan	0	0	0	0	1	1	0	0	0
Sos Höyük	0	0	0	0	0	0	0	0	1

Appendix 6 Incidence matrix of obsidian sources for the network edges.

```
# Header ----------------------------------------------------------------

# Project name: Thesis - Pottery Similarity Network
# Contributor:  Natalie Mez
# Institution:  Leiden University - Faculty of Archaeology
# Contact:      natmez1@aol.com

# Code description ------------------------------------------------------

# This code calculates the Jaccard indices for the pottery matrix using the vegan
# package. A barplot, histogram, and heatmap provide information about the data.
# It also creates a similarity network for the pottery assemblages.
# The igraph package is used for network analysis and plotting the network.
# The code calculates network-level metrics such as the number of nodes,
# number of edges, density, diameter, clustering coefficient, and assortativity.
# Then, the similarity network is subjected to the Leiden community detection.
# Last, the statistically significant edges in the graph are determined through
# use of the backbone package.


# Load required libraries -----------------------------------------------
# igraph package for network analysis
library(igraph)

# vegan package for Jaccard similarity measure
library(vegan)

# RColorBrewer package for color control in the network plot
library(RColorBrewer)

# backbone package for extracting the statistically significant edges
library(backbone)

# pheatmap package to plot a heatmap including the underlying values
library(pheatmap)


# Data import and preparation -------------------------------------------
# import CSV files with nodes and edges for pottery dataset
nodes <- read.csv2("C:/Users/natme/Desktop/Thesis/Code/potteryNodes.csv",
                   header=T, as.is=T)
edges <- read.csv2("C:/Users/natme/Desktop/Thesis/Code/potteryEdges.csv",
                   header=T, row.names=1)

# convert edges dataset to incidence matrix
edges <- as.matrix(edges)


# Barplot of decorative feature frequencies -----------------------------
# create barplot of pottery edges matrix
par(mar = c(7, 2, 2, 2))
barplot(edges, las = 3, col = "coral2", cex.names = 0.8, ylim = c(0, 25))


# Co-occurrences of features --------------------------------------------
```

```
# transpose matrix
features <- t(edges)

# convert imported incidence to adjacency matrix
print.table(occurences <- tcrossprod(features))
occurences <- as.matrix(occurences)

# create heatmap of features co-occurrences
pheatmap(occurences, display_numbers = T, color = colorRampPalette(c('white','brown3'))(25),
       cluster_rows = F, cluster_cols = F, fontsize_number = 8, number_color = "black",
       number_format = "%.0f", fontsize = 9, angle_col = 90,
       legend = F)


# Jaccard distance matrix ----------------------------------------------
# vegdist calculates the Jaccard distances from the edge matrix
jacPot <- vegdist(edges, method="jaccard", binary=FALSE, diag=FALSE, upper=FALSE,
             na.rm = FALSE)

# save the output as a matrix
distPot <- as.matrix(jacPot)


# Jaccard similarity matrix --------------------------------------------
# subtract the distance from 1 to turn the distance matrix into similarity matrix
simPot <- (1-distPot)

# make export copy where decimals are set to two
exSimPot <- round(simPot, digits = 2)

# write CSV of similarity matrix
write.csv(exSimPot,
        "C:/Users/natme/Desktop/Thesis/Code/similarityPottery.csv",
        fileEncoding="UTF-16LE")


# Histogram of Jaccard similarities ------------------------------------
# plot a histogram to show the distribution of the Jaccard values
hist(simPot, col = "darkslategray3", main = NA,
    breaks = seq(0, 1, by = 0.05), xlim = c(0,1))

#add the median as a red vertical line
abline(v = median(simPot),
      col = "red",
      lwd = 3)


# Thresholding ---------------------------------------------------------
# comment out non-required thresholds
# threshold for low similarity
 simPot[simPot < 0.19] <- 0

# threshold for moderate similarity
# simPot[simPot < 0.5] <- 0
```

```
# threshold for high similarity above
# simPot[simPot < 0.7] <- 0


# Creation of similarity network ----------------------------------------
# weighted = TRUE because the edge weight represents the similarity
potNet <- graph_from_adjacency_matrix(simPot, weighted=T)

# make graph undirected
# choose collapse so that each directed edge will be turned into an undirected
potNet <- as.undirected(potNet, "collapse")


# simplify graph by removing loops (nodes having edges with themselves)
# remove.multiple = F because multiple edges between nodes do not exist
potNet <- simplify(potNet, remove.multiple = F, remove.loops = T)

# make edge widths proportionate to edge weights based on jaccard index
edge.attributes(potNet)$width <- E(potNet)$weight

# add locations as vertex attributes
V(potNet)$Location <- nodes$Location

# create color palette based on unique values for vertex attribute
pal <- brewer.pal(length(unique(V(potNet)$Location)), "Set1")


# Plotting of similarity network ----------------------------------------
# plot network using Fruchterman-Reingold layout
plot(potNet, layout = layout_with_fr,
    vertex.label.color = "black", vertex.size = 3, vertex.label.cex = 0.6,
    vertex.label.dist = 1,
    vertex.label.family = "sans",
    vertex.color = "lightslateblue")

# COMMENT OUT FOR 0.19 and 0.5 JACCARD THRESHOLDS
# plot without Leiden groups and only colored Locations for high Jaccard
plot(potNet, layout = layout_with_fr, vertex.size = 5, vertex.label = NA,
    vertex.color = pal[(vertex_attr(potNet, "Location"))])

# create a legend for the node attribute location
legend("bottomright",
      legend = unique(
        (vertex_attr(potNet, "Location")))[order(unique(
          (vertex_attr(potNet, "Location"))))],
      pch = 19,
      title = "Location clusters", bty = "n",
      col = unique(
        pal[(vertex_attr(potNet, "Location"))])[order(unique(
          (vertex_attr(potNet, "Location"))))])


# Network level metrics -------------------------------------------------
# get number of nodes
gorder(potNet)
```

```
# get number of edges
gsize(potNet)

# get number of isolates
sum(degree(potNet) == 0)

# calculate edge density
edge_density(potNet)

# calculate diameter
diameter(potNet)

# calculate transitivity as global clustering coefficient
transitivity(potNet, type = "global", isolates = "zero")

# calculate assortativity (nominal) pf "Location" attribute to investigate homophily
assortativity_nominal(potNet, (as.factor(V(potNet)$Location)))

# calculate normalized degree centralization
centr_degree(potNet, normalized=T)

# create dataframe holding normalized degree centralities of all nodes
degree <- as.data.frame(degree(potNet, normalized = T))


# COMMENT OUT COMMUNITY DETECTION FOR 0.7 THRESHOLD
# Community detection ------------------------------------------------------
# Leiden clustering
leidenPot <- cluster_leiden(potNet,objective_function = "modularity",
          weights = NULL, resolution_parameter = 1, beta = 0.01,
          initial_membership = NULL, n_iterations = -1, vertex_weights = NULL)

# plot communities Leiden
plot(leidenPot, potNet, mark.groups = communities(leidenPot),
  edge.color = c("black", "red")[crossing(leidenPot, potNet) + 1],
  layout=layout_with_fr,
  vertex.size = 5,
  vertex.label = NA,
  col = pal[(vertex_attr(potNet, "Location"))])

# create a legend for the node attributes "Locations"
legend("bottomright",
     legend = unique(
       (vertex_attr(potNet, "Location")))[order(unique(
         (vertex_attr(potNet, "Location"))))],
     pch = 19,
     title = "Location clusters", bty = "n",
     col = unique(
       pal[(vertex_attr(potNet, "Location"))])[order(unique(
         (vertex_attr(potNet, "Location"))))])

# save community memberships in dataframe
commPot <- data.frame(names = leidenPot$names,
                      membership = leidenPot$membership)
```

```
# write CSV of community memberships
write.csv(commPot,
        "C:/Users/natme/Desktop/Thesis/Code/communitiesPottery.csv",
        fileEncoding="UTF-16LE")


# COMMENT OUT BOTH THRESHOLDS AND RE-RUN BEFORE BACKBONE SECTION
# Backbone ----------------------------------------------------------------
backPot <- disparity(simPot, alpha = 0.05, class = "igraph")

plot(backPot, layout = layout_with_fr,
    vertex.label.color = "black", vertex.size = 5, vertex.label.cex = 0.75,
    vertex.label.dist = 1.5,
    vertex.label.family = "sans",
    vertex.color = "lightslateblue",
    edge.color = "black")


# SELECT 0.19 THRESHOLD AND RE-RUN BEFORE THIS SECTION
# Delete random vertices ----------------------------------------------------
numNodes <- vcount(potNet)
remNodes <- numNodes

# change the value in (numNodes - 5) according to the desired network size
# re-run script entirely for each network size
for (i in 1:(numNodes - 5)) {
  delNodes <- sample(remNodes, size = 1)
  potNet <- delete.vertices(potNet, delNodes)
  remNodes <- remNodes - 1
}

# plot the graph with the remaining nodes
plot(potNet, layout=layout_with_fr,
    vertex.label.color = "black", vertex.size = 5, vertex.label.cex = 0.75,
    vertex.label.dist = 1.5,
    vertex.label.family = "sans",
    vertex.color = "lightslateblue",
    edge.color = "black")
```

Appendix 7 R script for the pottery similarity networks.

```
# Header ----------------------------------------------------------------

# Project name: Thesis - Obsidian Similarity Network
# Contributor:  Natalie Mez
# Institution:  Leiden University - Faculty of Archaeology
# Contact:      natmez1@aol.com


# Code description ------------------------------------------------------

# This code calculates the Jaccard indices for the obsidian matrix using the vegan
# package. A barplot, histogram, and heatmap provide information about the data.
# It also creates a similarity network for the obsidian assemblages.
# The igraph package is used for network analysis and plotting the network.
# The code calculates network-level metrics such as the number of nodes,
# number of edges, density, diameter, clustering coefficient, and assortativity.
# Then, the similarity network is subjected to the Leiden community detection.
# Last, the statistically significant edges in the graph are determined through
# use of the backbone package.


# Load required libraries -----------------------------------------------
# igraph package for network analysis
library(igraph)

# vegan package for Jaccard similarity measure
library(vegan)

# RColorBrewer package for color control in the network plot
library(RColorBrewer)

# backbone package for extracting the statistically significant edges
library(backbone)

# pheatmap package to plot a heatmap including the underlying values
library(pheatmap)


# Data import and preparation -------------------------------------------
# import CSV files with nodes and edges for obsidian dataset
nodes <- read.csv2("C:/Users/natme/Desktop/Thesis/Code/obsidianNodes.csv",
                   header=T, as.is=T)
edges <- read.csv2("C:/Users/natme/Desktop/Thesis/Code/obsidianEdges.csv",
                   header=T, row.names=1)

# convert edges dataset to incidence matrix
edges <- as.matrix(edges)

# remove rows dealing with source as the network will only show sites
nodes <- nodes[!complete.cases(nodes), ]


# Barplot of obsidian source frequencies ----------------------------------
# create barplot of obsidian edges matrix
par(mar = c(7, 2, 2, 2))
```

```
barplot(edges, las = 3, col = "grey70", cex.names = 0.8, ylim = c(0,10))


# Co-occurrences of sources ------------------------------------------------
# transpose matrix
features <- t(edges)

# convert imported incidence to adjacency matrix
print.table(occurences <- tcrossprod(features))
occurences <- as.matrix(occurences)

# create heatmap of source co-occurrences
pheatmap(occurences, display_numbers = T, color = colorRampPalette(c('white','gray47'))(25),
       cluster_rows = F, cluster_cols = F, fontsize_number = 8, number_color = "black",
       number_format = "%.0f", fontsize = 9, angle_col = 90,
       legend = F)


# Jaccard distance matrix --------------------------------------------------
# vegdist calculates the Jaccard distances from the edge matrix
jacObs <- vegdist(edges, method="jaccard", binary=FALSE, diag=FALSE, upper=FALSE,
              na.rm = FALSE)

# save the output as a matrix
distObs <- as.matrix(jacObs)


# Jaccard similarity matrix ------------------------------------------------
# subtract the distance from 1 to turn the distance matrix into similarity matrix
simObs <- (1-distObs)

# make export copy where decimals are set to two
exSimObs <- round(simObs, digits = 2)

# write CSV of similarity matrix
write.csv(exSimObs,
        "C:/Users/natme/Desktop/Thesis/Code/similarityObsidian.csv",
        fileEncoding="UTF-16LE")

# Histogram of Jaccard similarities ----------------------------------------
# plot a histogram to show the distribution of the Jaccard values
hist(simObs, col = "darkslategray3", main = NA,
    breaks = seq(0, 1, by  =0.05), xlim = c(0,1))

#add the median as a red vertical line
abline(v = median(simObs),
      col = "red",
      lwd = 3)


# Thresholding -------------------------------------------------------------
# comment out non-required thresholds
# threshold for low similarity
 simObs[simObs < 0.19] <- 0
```

```
# threshold for moderate similarity
# simObs[simObs < 0.5] <- 0

# threshold for high similarity above
# simObs[simObs < 0.7] <- 0


# Creation of similarity network ----------------------------------------
# weighted = TRUE because the edge weight represents the similarity
obsNet <- graph_from_adjacency_matrix(simObs, weighted=T)

# make graph undirected
# choose collapse so that each directed edge will be turned into an undirected
obsNet <- as.undirected(obsNet, "collapse")


# simplify graph by removing loops (nodes having edges with themselves)
# remove.multiple = F because multiple edges between nodes do not exist
obsNet <- simplify(obsNet, remove.multiple = F, remove.loops = T)

# make edge widths proportionate to edge weights based on jaccard index
edge.attributes(obsNet)$width <- E(obsNet)$weight

# add locations as vertex attributes
V(obsNet)$Location <- nodes$Location

# create color palette based on unique values for vertex attribute
pal <- brewer.pal(length(unique(V(obsNet)$Location)), "Set1")

# create named vector of unique Location values and their corresponding colors
loCol <- setNames(pal, unique(V(obsNet)$Location))


# Plotting of similarity network ----------------------------------------
# plot network using Fruchterman-Reingold layout
plot(obsNet, layout = layout_with_fr, vertex.label.cex = 0.75,
    vertex.label.color = "black", vertex.size = 5, vertex.label.dist = 1.5,
    vertex.label.family = "sans",
    vertex.color = "lightslateblue")


# COMMENT OUT FOR 0.19 and 0.5 JACCARD THRESHOLDS
# plot without Leiden groups and only colored Locations for high Jaccard
plot(obsNet, layout = layout_with_fr, vertex.size = 5, vertex.label = NA,
    vertex.color = loCol[vertex_attr(obsNet, "Location")])

# create a legend for the node attributes location
legend("bottomright",
      legend = unique(vertex_attr(obsNet, "Location"))[order(unique(vertex_attr(obsNet, "Location")))],
      pch = 19,
      title = "Location clusters", bty = "n",
      col = loCol[unique(vertex_attr(obsNet, "Location"))][order(unique(vertex_attr(obsNet, "Location")))])


# Network level metrics -------------------------------------------------
```

```
# get number of nodes
gorder(obsNet)

# get number of edges
gsize(obsNet)

# get number of isolates
sum(degree(obsNet) == 0)

# calculate edge density
edge_density(obsNet)

# calculate diameter
diameter(obsNet)

# calculate transitivity as global clustering coefficient
transitivity(obsNet, type = "global", isolates = "zero")

# calculate assortativity (nominal) pf "Location" attribute to investigate homophily
assortativity_nominal(obsNet, (as.factor(V(obsNet)$Location)))

# calculate normalized degree centralization
centr_degree(obsNet, normalized = T)

# create dataframe holding normalized degree centralities of all nodes
degree <- as.data.frame(degree(obsNet, normalized = T))


# COMMENT OUT COMMUNITY DETECTION FOR 0.7 THRESHOLD
# Community detection ------------------------------------------------------
# Leiden clustering
leidenObs <- cluster_leiden(obsNet,objective_function = "modularity",
                      weights = NULL, resolution_parameter = 1, beta = 0.01,
                     initial_membership = NULL, n_iterations = -1, vertex_weights = NULL)

# plot communities Leiden
plot(leidenObs, obsNet,
   mark.groups = communities(leidenObs),
    edge.color = c("black", "red")[crossing(leidenObs, obsNet) + 1],
    layout=layout_with_fr,
    vertex.label = NA, vertex.size = 5,
    col = loCol[vertex_attr(obsNet, "Location")])

# create a legend for the node attributes "Locations"
legend("bottomright",
     legend = unique(vertex_attr(obsNet, "Location"))[order(unique(vertex_attr(obsNet, "Location")))],
     pch = 19,
     title = "Location clusters", bty = "n",
     col = loCol[unique(vertex_attr(obsNet, "Location"))][order(unique(vertex_attr(obsNet, "Location")))])

# save community memberships in dataframe
commObs <- data.frame(names = leidenObs$names,
                      membership = leidenObs$membership)

# write CSV of community memberships
```

```
write.csv(commObs,
        "C:/Users/natme/Desktop/Thesis/Code/communitiesObsidian.csv",
        fileEncoding="UTF-16LE")


# COMMENT OUT BOTH THRESHOLDS AND RE-RUN BEFORE BACKBONE SECTION
# Backbone ----------------------------------------------------------------

backObs <- disparity(simObs, alpha = 0.05, class = "igraph")
# change alpha to NULL to obtain the underlying p values

plot(backObs, layout = layout_with_fr,
    vertex.label.color = "black", vertex.size = 5, vertex.label.cex = 0.75,
    vertex.label.dist = 1.5,
    vertex.label.family = "sans",
    vertex.color = "lightslateblue",
    edge.color = "black")


# SELECT 0.19 THRESHOLD AND RE-RUN BEFORE THIS SECTION
# Delete random vertices ----------------------------------------------------
numNodes <- vcount(obsNet)
remNodes <- numNodes

# change the value in (numNodes - 5) according to the desired network size
# re-run script entirely for each network size
for (i in 1:(numNodes - 5)) {
  delNodes <- sample(remNodes, size = 1)
  obsNet <- delete.vertices(obsNet, delNodes)
  remNodes <- remNodes - 1
}

# plot the graph with the remaining nodes
plot(obsNet, layout = layout_with_fr,
    vertex.label.color = "black", vertex.size = 5, vertex.label.cex = 0.75,
    vertex.label.dist = 1.5,
    vertex.label.family = "sans",
    vertex.color = "lightslateblue",
    edge.color = "black")
```

Appendix 8 R script for the obsidian similarity networks.

```
# Header ----------------------------------------------------------------

# Project name: Thesis - Bimodal Obsidian Network
# Contributor:  Natalie Mez
# Institution:  Leiden University - Faculty of Archaeology
# Contact:      natmez1@aol.com


# Code description ------------------------------------------------------

# This code creates a bipartite network of archaeological sites and their
# obsidian sources, using the igraph package in R for network analysis.
# The code reads in two CSV files for nodes and edges, and creates an incidence
# matrix from the edge file. The network is then created from the incidence
# matrix, with directed edges from the obsidian sources to the sites.
# Node types are assigned colors and shapes, and the network is plotted.
# Finally, network level metrics such as the number of nodes, edges, and
# isolates are computed.


# Load required libraries -----------------------------------------------
# igraph package for network analysis
library(igraph)

# Data import and preparation -------------------------------------------
# import CSV files with nodes and edges for obsidian dataset
nodes <- read.csv2("C:/Users/natme/Desktop/Thesis/Code/obsidianNodes.csv",
                   header=T, as.is=T)
edges <- read.csv2("C:/Users/natme/Desktop/Thesis/Code/obsidianEdges.csv",
                   header=T, row.names=1)

# save dataset as an incidence matrix
edges <- as.matrix(edges)

# Network creation ------------------------------------------------------
# create graph from incidence matrix, directed TRUE for directed network,
# mode "in" meaning nodes of second kind go to nodes of first kind
obsNet <- graph_from_incidence_matrix(edges, directed = TRUE, mode = "in")

# assing colors and shapes to different node types
V(obsNet)$color <- ifelse(V(obsNet)$type, "grey70", "lightslateblue")
V(obsNet)$shape <- ifelse(V(obsNet)$type, "square", "circle")

# plot network using Fruchterman-Reingold layout
plot(obsNet,vertex.label.color = "black",
    vertex.label.family = "Helvetica", vertex.size = 5, vertex.label.cex = 0.75,
    layout=layout_with_fr,
    vertex.label.dist=1.5, edge.arrow.size = 0.25)


# Network level metrics -------------------------------------------------
# get number of nodes
gorder(obsNet)

# get number of edges
```

```
gsize(obsNet)

# get number of isolates
sum(degree(obsNet) == 0)
```

Appendix 9 R script for the bimodal obsidian network.

```
# Header ----------------------------------------------------------------

# Project name: Thesis - Graph Comparison
# Contributer:  Natalie Mez
# Institution:  Leiden University - Faculty of Archaeology
# Contact:      natmez1@aol.com

# Code description ------------------------------------------------------

# This code creates a subset of pottery data, and then compares the resulting
# graph with an obsidian similarity network. The code imports the required
# packages, prepares the data, subsets it, calculates the similarity of the
# pottery subset, creates graphs, simplifies them, adds attributes,
# calculates network-level metrics, and performs community detection.
# Next, the code exports the similarity matrix and plots the network.
# Finally, a matrix containing all sites that share similarity in obsidian and
# pottery decoration use is created.

# Load required libraries -----------------------------------------------
# igraph package for network analysis
library(igraph)

# vegan package for Jaccard similarity measure
library(vegan)

# RColorBrewer package for color control in the network plot
library(RColorBrewer)

# Data import and preparation -------------------------------------------
# import CSV files with nodes and edges for pottery dataset
nodesPot <- read.csv2("C:/Users/natme/Desktop/Thesis/Code/potteryNodes.csv",
                header=T, as.is=T)
edgesPot <- read.csv2("C:/Users/natme/Desktop/Thesis/Code/potteryEdges.csv",
                header=T)

# import CSV files with nodes and edges for obsidian dataset
nodesObs <- read.csv2("C:/Users/natme/Desktop/Thesis/Code/obsidianNodes.csv",
              header=T, as.is=T)
edgesObs <- read.csv2("C:/Users/natme/Desktop/Thesis/Code/obsidianEdges.csv",
              header=T, row.names=1)


# Subset ----------------------------------------------------------------
# subset pottery nodes to only include sites also in obsidian nodes
nodesPot <- subset(nodesPot,Name%in%nodesObs$Name)

# subset pottery edges to only include sites also in obsidian edges
edgesPot <- subset(edgesPot, X%in%nodesPot$Name)

# set the row names to the values in the "X" column of the same data frame
row.names(edgesPot) <- edgesPot$X

# remove the first row of the "edgesPot" data frame
edgesPot <- edgesPot[-1]
```

```
# sets the row names of the "edgesPot" data frame to the values in the "Name"
# column of the "nodesPot" data frame
row.names(edgesPot) <- nodesPot$Name

# remove rows dealing with source as the network will only show sites
nodesObs <- nodesObs[!complete.cases(nodesObs), ]

# Jaccard distance matrix ----------------------------------------------
# convert edges datasets to incidence matrices
edgesPot <- as.matrix(edgesPot)
edgesObs <- as.matrix(edgesObs)

# vegdist calculates the Jaccard distances from the edge matrices
jacPot <- vegdist(edgesPot, method="jaccard", binary=FALSE, diag=FALSE, upper=FALSE,
         na.rm = FALSE)
jacObs <- vegdist(edgesObs, method="jaccard", binary=FALSE, diag=FALSE, upper=FALSE,
         na.rm = FALSE)

# save the output as a matrix
distPot <- as.matrix(jacPot)
distObs <- as.matrix(jacObs)

# Jaccard similarity matrix --------------------------------------------
# subtract the distance from 1 to turn the distance matrix into similarity matrix
simPot <- (1-distPot)
simObs <- (1-distObs)

# make export copy where decimals are set to two
exedgesPot <- round(edgesPot, digits = 2)

# write CSV of similarity matrix
write.csv(exedgesPot,
      "C:/Users/natme/Desktop/Thesis/Code/similarityPotterySubset.csv",
      fileEncoding="UTF-16LE")


# COMMENT OUT THE THRESHOLDS AN RE-RUN BEFORE GRAPH COMBINATION PART
# Thresholding ---------------------------------------------------------
# comment out non-required thresholds
# threshold for low similarity
  simPot[simPot < 0.19] <- 0

# threshold for moderate similarity
# simPot[simPot < 0.5] <- 0


# Creation of similarity networks --------------------------------------
# weighted = TRUE because the edge weight represents the similarity
potNet <- graph_from_adjacency_matrix(simPot, weighted=T)
obsNet <- graph_from_adjacency_matrix(simObs, weighted=T)

# make graph undirected
# choose collapse so that each directed edge will be turned into an undirected
potNet  <- as.undirected(potNet, "collapse")
obsNet <- as.undirected(obsNet, "collapse")
```

```
# simplify graph by removing loops (nodes having edges with themselves)
# remove.multiple = F because multiple edges between nodes do not exist
potNet <- simplify(potNet, remove.multiple = F, remove.loops = T)
obsNet <- simplify(obsNet, remove.multiple = F, remove.loops = T)

# make edge widths proportionate to edge weights based on Jaccard index
edge.attributes(potNet)$width <- E(potNet)$weight

# add locations as vertex attributes
V(obsNet)$Location <- nodesObs$Location
V(potNet)$Location <- nodesPot$Location

# create color palette based on unique values for vertex attribute
pal <- brewer.pal(length(unique(V(obsNet)$Location)), "Set1")

# create named vector of unique Location values and their corresponding colors
loCol <- setNames(pal, unique(V(obsNet)$Location))


# Plotting of similarity network ----------------------------------------
# plot network using Fruchterman-Reingold layout
plot(potNet, layout = layout_with_fr,
    vertex.label.color = "black", vertex.size = 5,
    vertex.label.dist = 1.5, vertex.label.cex = 0.75,
    vertex.label.family = "sans", vertex.color = "lightslateblue")


# Pottery subset network level metrics ----------------------------------
# get number of nodes
gorder(potNet)

# get number of edges
gsize(potNet)

# get number of isolates
sum(degree(potNet) == 0)

# calculate edge density
edge_density(potNet)

# calculate diameter
diameter(potNet)

# calculate transitivity as global clustering coefficient
transitivity(potNet, type = "global", isolates = "zero")

# calculate assortativity (nominal) pf "Location" attribute to investigate homophily
assortativity_nominal(potNet, (as.factor(V(potNet)$Location)))

# calculate normalized degree centralization
centr_degree(potNet, normalized = T)

# create dataframe holding normalized degree centralities of all nodes
degree <- as.data.frame(degree(potNet, normalized = T))
```

```
# Community detection ------------------------------------------------------
# Leiden clustering
leidenPot <- cluster_leiden(potNet,objective_function = "modularity",
                    weights = NULL, resolution_parameter = 1, beta = 0.01,
                    initial_membership = NULL, n_iterations = -1, vertex_weights = NULL)

# plot communities Leiden
plot(leidenPot, potNet,
    mark.groups = communities(leidenPot),
    edge.color = c("black", "red")[crossing(leidenPot, potNet) + 1],
    layout=layout_with_fr,
     vertex.size = 5, vertex.label = NA,
    col = loCol[vertex_attr(obsNet, "Location")])

# create a legend for the node attributes "Locations"
legend("bottomright",
      legend = unique(vertex_attr(obsNet, "Location"))[order(unique(vertex_attr(obsNet, "Location")))],
      pch = 19,
      title = "Location clusters", bty = "n",
      col = loCol[unique(vertex_attr(obsNet, "Location"))][order(unique(vertex_attr(obsNet, "Location")))])

# save community memberships in dataframe
commPot <- data.frame(names = leidenPot$names,
                    membership = leidenPot$membership)

# write CSV of community memberships
write.csv2(commPot,
        "C:/Users/natme/Desktop/Thesis/Code/communitiesSubsetPottery.csv")


# COMMENT OUT THRESHOLD AND RERUN BEFORE RUNNING THE FOLLOWING SECTION
# Graph isomorphism ---------------------------------------------------------
# check obisidan and pottery subset networks for isomorphism
isomorphic(obsNet, potNet, method = "auto")


# Graph similarity ----------------------------------------------------------
# function for Jaccard similarity of edge sets from Keith McNulty (2022)
# "Handbook of graphs and networks in people analytics", Section 8.3
# adapted to include edge weights in the calculation of the Jaccard index
jaccard_edgeset_similarity <- function(G1, G2) {
  inter <- intersect(E(G1), E(G2))
  common_weight <- sum(E(G1)[inter]$weight)
  unique_weight <- sum(E(G1)$weight) + sum(E(G2)$weight)

  if (unique_weight == 0) {
    return(0)
  } else {
    return(common_weight / unique_weight)
  }
}

# calculate Jaccard similarity for both edge sets
```

```
jaccard_edgeset_similarity(potNet, obsNet)


# Combination matrix ------------------------------------------------------
# binarize data
simObs[simObs > 0] <- 1
simPot[simPot > 0] <- 1

# add matrices to third matrix
edgesTotal <- simObs + simPot

# set all values below 2 to 0 and 2 to 1 to finish binarizing
edgesTotal[edgesTotal < 2] <- 0
edgesTotal[edgesTotal == 2] <- 1

# write CSV of total matrix containing shared edges in both networks
write.csv(edgesTotal,
        "C:/Users/natme/Desktop/Thesis/Code/edgesTotal.csv",
        fileEncoding="UTF-16LE")
```

Appendix 10 R script for the investigation of graph differences.

	Agarak	Alaybeyi Höyük	Ashagi Dasharkh	Aygevan	Duzdağı	Dvin	Erebyengicesi	Franganots	Gegharot
Agarak	1	0.56	0.07	0.43	0	0.36	0.07	0.73	0.41
Alaybeyi Höyük	0.56	1	0.09	0.31	0.09	0.23	0.08	0.53	0.31
Ashagi Dasharkh	0.07	0.09	1	0	0	0.2	0	0.08	0.1
Aygevan	0.43	0.31	0	1	0	0.22	0	0.29	0.23
Duzdağı	0	0.09	0	0	1	0	0	0.08	0
Dvin	0.36	0.23	0.2	0.22	0	1	0	0.42	0.36
Erebyengicesi	0.07	0.08	0	0	0	0	1	0.08	0.09
Franganots	0.73	0.53	0.08	0.29	0.08	0.42	0.08	1	0.38
Gegharot	0.41	0.31	0.1	0.23	0	0.36	0.09	0.38	1
Gökçeli	0.5	0.62	0.1	0.23	0	0.36	0.2	0.47	0.33
Jradzor	0.12	0.15	0	0.11	0.25	0.12	0	0.14	0.17
Jrahovit	0.53	0.43	0.11	0.25	0	0.4	0.1	0.62	0.36
Karnut 1	0.6	0.5	0.1	0.45	0.1	0.36	0.09	0.57	0.43
Khalaj	0.2	0.25	0	0.25	0	0.29	0.2	0.23	0.08
Kohne Pasgah Tepesi	0.07	0.08	0	0	0.5	0.17	0	0.17	0.09
Köhne Shahar	0.38	0.36	0	0.4	0.12	0.3	0.11	0.43	0.2
Kohne Tepesi	0.5	0.4	0.1	0.33	0.1	0.36	0	0.47	0.43
Kul Tepe Jolfa	0.47	0.47	0.07	0.33	0.07	0.36	0	0.53	0.41
Kuli Tepe	0.07	0.08	0	0	0	0.17	0	0.08	0.09
Kültepe 1	0.33	0.31	0.17	0.2	0	0.22	0.33	0.29	0.14
Kültepe 2	0.42	0.5	0.08	0.19	0.08	0.29	0.15	0.39	0.44
Maxta 1	0.56	0.67	0.07	0.43	0.07	0.27	0.14	0.53	0.5
Melekli Höyük	0.25	0.42	0	0.09	0	0.1	0.33	0.2	0.23
Mokhrablur	0.6	0.4	0.1	0.33	0	0.36	0.09	0.69	0.43
Nadir Tepesi	0.07	0.08	0	0	0.5	0.17	0	0.17	0.09
Ovçular Tepesi	0.44	0.43	0	0.36	0.11	0.27	0.22	0.5	0.27

Sadarak	0.29	0.36	0	0.17	0.12	0.3	0.25	0.43	0.29
Shengavit	0.71	0.62	0.07	0.4	0.07	0.33	0	0.69	0.47
Shirakavan	0.33	0.31	0.17	0.5	0.17	0.38	0	0.5	0.23
Shortepe	0.12	0.25	0	0.11	0.25	0.12	0.2	0.23	0.08
Shreshblur	0.21	0.08	0.33	0.12	0	0.6	0	0.25	0.3
Sos Höyük	0.62	0.53	0.08	0.38	0.08	0.42	0	0.6	0.47
Tsaghkalanj	0.6	0.4	0.1	0.23	0.1	0.25	0.09	0.83	0.33
Yakhvali	0	0.09	0	0	1	0	0	0.08	0

	Gökçeli	Jradzor	Jrahovit	Karnut 1	Khalaj	Kohne Pasgah Tepesi	Köhne Shahar	Kohne Tepesi
Agarak	0.5	0.12	0.53	0.6	0.2	0.07	0.38	0.5
Alaybeyi Höyük	0.62	0.15	0.43	0.5	0.25	0.08	0.36	0.4
Ashagi Dasharkh	0.1	0	0.11	0.1	0	0	0	0.1
Aygevan	0.23	0.11	0.25	0.45	0.25	0	0.4	0.33
Duzdağı	0	0.25	0	0.1	0	0.5	0.12	0.1
Dvin	0.36	0.12	0.4	0.36	0.29	0.17	0.3	0.36
Erebyengicesi	0.2	0	0.1	0.09	0.2	0	0.11	0
Franganots	0.47	0.14	0.62	0.57	0.23	0.17	0.43	0.47
Gegharot	0.33	0.17	0.36	0.43	0.08	0.09	0.2	0.43
Gökçeli	1	0.17	0.58	0.33	0.4	0.09	0.5	0.33
Jradzor	0.17	1	0.08	0.08	0	0.5	0.33	0.27
Jrahovit	0.58	0.08	1	0.36	0.18	0.1	0.21	0.27
Karnut 1	0.33	0.08	0.36	1	0.27	0.09	0.38	0.67
Khalaj	0.4	0	0.18	0.27	1	0	0.5	0.27
Kohne Pasgah Tepesi	0.09	0.5	0.1	0.09	0	1	0.25	0.2
Köhne Shahar	0.5	0.33	0.21	0.38	0.5	0.25	1	0.5

Kohne Tepesi	0.33	0.27	0.27	0.67	0.27	0.2	0.5	1
Kul Tepe Jolfa	0.41	0.29	0.35	0.41	0.2	0.14	0.47	0.5
Kuli Tepe	0.09	0	0	0.09	0.2	0	0.11	0.09
Kültepe 1	0.45	0	0.36	0.45	0.43	0	0.27	0.33
Kültepe 2	0.53	0.13	0.38	0.53	0.31	0.15	0.4	0.53
Maxta 1	0.6	0.2	0.44	0.6	0.29	0.07	0.47	0.5
Melekli Höyük	0.6	0.11	0.25	0.14	0.25	0	0.27	0.07
Mokhrablur	0.54	0.08	0.9	0.43	0.17	0.09	0.29	0.33
Nadir Tepesi	0.09	0.5	0.1	0.09	0	1	0.25	0.2
Ovçular Tepesi	0.58	0.3	0.29	0.46	0.44	0.22	0.89	0.46
Sadarak	0.5	0.33	0.31	0.38	0.5	0.25	0.6	0.5
Shengavit	0.47	0.27	0.5	0.47	0.19	0.13	0.44	0.56
Shirakavan	0.23	0.11	0.36	0.6	0.25	0.14	0.4	0.45
Shortepe	0.27	0.14	0.08	0.27	0.6	0.2	0.5	0.27
Shreshblur	0.18	0.17	0.33	0.18	0	0.25	0.1	0.18
Sos Höyük	0.47	0.14	0.5	0.69	0.23	0.17	0.43	0.69
Tsaghkalanj	0.33	0.17	0.58	0.43	0.08	0.2	0.29	0.33
Yakhvali	0	0.25	0	0.1	0	0.5	0.12	0.1

	Kul Tepe Jolfa	Kuli Tepe	Kültepe 1	Kültepe 2	Maxta 1	Melekli Höyük	Mokhrablur	Nadir Tepesi
Agarak	0.47	0.07	0.33	0.42	0.56	0.25	0.6	0.07
Alaybeyi Höyük	0.47	0.08	0.31	0.5	0.67	0.42	0.4	0.08
Ashagi Dasharkh	0.07	0	0.17	0.08	0.07	0	0.1	0
Aygevan	0.33	0	0.2	0.19	0.43	0.09	0.33	0
Duzdağı	0.07	0	0	0.08	0.07	0	0	0.5
Dvin	0.36	0.17	0.22	0.29	0.27	0.1	0.36	0.17
Erebyengicesi	0	0	0.33	0.15	0.14	0.33	0.09	0

Franganots	0.53	0.08	0.29	0.39	0.53	0.2	0.69	0.17
Gegharot	0.41	0.09	0.14	0.44	0.5	0.23	0.43	0.09
Gökçeli	0.41	0.09	0.45	0.53	0.6	0.6	0.54	0.09
Jradzor	0.29	0	0	0.13	0.2	0.11	0.08	0.5
Jrahovit	0.35	0	0.36	0.38	0.44	0.25	0.9	0.1
Karnut 1	0.41	0.09	0.45	0.53	0.6	0.14	0.43	0.09
Khalaj	0.2	0.2	0.43	0.31	0.29	0.25	0.17	0
Kohne Pasgah Tepesi	0.14	0	0	0.15	0.07	0	0.09	1
Köhne Shahar	0.47	0.11	0.27	0.4	0.47	0.27	0.29	0.25
Kohne Tepesi	0.5	0.09	0.33	0.53	0.5	0.07	0.33	0.2
Kul Tepe Jolfa	1	0.07	0.18	0.42	0.56	0.18	0.41	0.14
Kuli Tepe	0.07	1	0	0.07	0.07	0.14	0	0
Kültepe 1	0.18	0	1	0.46	0.33	0.2	0.33	0
Kültepe 2	0.42	0.07	0.46	1	0.5	0.27	0.35	0.15
Maxta 1	0.56	0.07	0.33	0.5	1	0.43	0.5	0.07
Melekli Höyük	0.18	0.14	0.2	0.27	0.43	1	0.23	0
Mokhrablur	0.41	0	0.33	0.35	0.5	0.23	1	0.09
Nadir Tepesi	0.14	0	0	0.15	0.07	0	0.09	1
Ovçular Tepesi	0.44	0.1	0.36	0.47	0.53	0.36	0.36	0.22
Sadarak	0.38	0.11	0.4	0.5	0.47	0.27	0.29	0.25
Shengavit	0.71	0.06	0.17	0.4	0.71	0.24	0.56	0.13
Shirakavan	0.43	0	0.33	0.27	0.43	0	0.45	0.14
Shortepe	0.2	0.2	0.25	0.31	0.29	0.25	0.08	0.2
Shreshblur	0.21	0	0.12	0.14	0.13	0	0.3	0.25
Sos Höyük	0.53	0.08	0.29	0.56	0.62	0.2	0.57	0.17
Tsaghkalanj	0.41	0	0.23	0.28	0.41	0.14	0.67	0.2
Yakhvali	0.07	0	0	0.08	0.07	0	0	0.5

	Ovçular Tepesi	Sadarak	Shengavit	Shirakavan	Shortepe	Shreshblur	Sos Höyük	Tsaghkalanj	Yakhvali
Agarak	0.44	0.29	0.71	0.33	0.12	0.21	0.62	0.6	0
Alaybeyi Höyük	0.43	0.36	0.62	0.31	0.25	0.08	0.53	0.4	0.09
Ashagi Dasharkh	0	0	0.07	0.17	0	0.33	0.08	0.1	0
Aygevan	0.36	0.17	0.4	0.5	0.11	0.12	0.38	0.23	0
Duzdagi	0.11	0.12	0.07	0.17	0.25	0	0.08	0.1	1
Dvin	0.27	0.3	0.33	0.38	0.12	0.6	0.42	0.25	0
Erebyengicesi	0.22	0.25	0	0	0.2	0	0	0.09	0
Franganots	0.5	0.43	0.69	0.5	0.23	0.25	0.6	0.83	0.08
Gegharot	0.27	0.29	0.47	0.23	0.08	0.3	0.47	0.33	0
Gökçeli	0.58	0.5	0.47	0.23	0.27	0.18	0.47	0.33	0
Jradzor	0.3	0.33	0.27	0.11	0.14	0.17	0.14	0.17	0.25
Jrahovit	0.29	0.31	0.5	0.36	0.08	0.33	0.5	0.58	0
Karnut 1	0.46	0.38	0.47	0.6	0.27	0.18	0.69	0.43	0.1
Khalaj	0.44	0.5	0.19	0.25	0.6	0	0.23	0.08	0
Kohne Pasgah Tepesi	0.22	0.25	0.13	0.14	0.2	0.25	0.17	0.2	0.5
Köhne Shahar	0.89	0.6	0.44	0.4	0.5	0.1	0.43	0.29	0.12
Kohne Tepesi	0.46	0.5	0.56	0.45	0.27	0.18	0.69	0.33	0.1
Kul Tepe Jolfa	0.44	0.38	0.71	0.43	0.2	0.21	0.53	0.41	0.07
Kuli Tepe	0.1	0.11	0.06	0	0.2	0	0.08	0	0
Kültepe 1	0.36	0.4	0.17	0.33	0.25	0.12	0.29	0.23	0
Kültepe 2	0.47	0.5	0.4	0.27	0.31	0.14	0.56	0.28	0.08
Maxta 1	0.53	0.47	0.71	0.43	0.29	0.13	0.62	0.41	0.07
Melekli Höyük	0.36	0.27	0.24	0	0.25	0	0.2	0.14	0
Mokhrablur	0.36	0.29	0.56	0.45	0.08	0.3	0.57	0.67	0
Nadir Tepesi	0.22	0.25	0.13	0.14	0.2	0.25	0.17	0.2	0.5

Ovçular Tepesi	1	0.7	0.41	0.36	0.44	0.09	0.4	0.36	0.11
Sadarak	0.7	1	0.35	0.27	0.5	0.1	0.33	0.29	0.12
Shengavit	0.41	0.35	1	0.4	0.19	0.2	0.69	0.56	0.07
Shirakavan	0.36	0.27	0.4	1	0.25	0.29	0.5	0.45	0.17
Shortepe	0.44	0.5	0.19	0.25	1	0	0.23	0.17	0.25
Shreshblur	0.09	0.1	0.2	0.29	0	1	0.25	0.3	0
Sos Höyük	0.4	0.33	0.69	0.5	0.23	0.25	1	0.47	0.08
Tsaghkalanj	0.36	0.29	0.56	0.45	0.17	0.3	0.47	1	0.1
Yakhvali	0.11	0.12	0.07	0.17	0.25	0	0.08	0.1	1

Appendix 11 Adjacency matrix with Jaccard similarities for the pottery dataset.

	Agarak	Aygevan	Dvin	Gegharot	Jrahovit	Karnut 1	Kohne Pasgah Tepesi	Kohne Tepesi	Kul Tepe Jolfa
Agarak	1	0.33	0.33	0.57	0.57	0.17	0	0	0.22
Aygevan	0.33	1	0.67	0.12	0.5	0.09	0	0	0.29
Dvin	0.33	0.67	1	0.12	0.5	0	0	0	0.29
Gegharot	0.57	0.12	0.12	1	0.33	0.22	0	0	0.14
Jrahovit	0.57	0.5	0.5	0.33	1	0.1	0	0	0.33
Karnut 1	0.17	0.09	0	0.22	0.1	1	0	0	0
Kohne Pasgah Tepesi	0	0	0	0	0	0	1	1	0.25
Kohne Tepesi	0	0	0	0	0	0	1	1	0.25
Kul Tepe Jolfa	0.22	0.29	0.29	0.14	0.33	0	0.25	0.25	1
Kuli Tepe	0	0	0	0	0	0	1	1	0.25
Kültepe 1	0.33	0.25	0.43	0.29	0.5	0.09	0.2	0.2	0.5
Mokhrablur	0.5	0.43	0.25	0.5	0.5	0.33	0	0	0.12
Nadir Tepesi	0.12	0.17	0.17	0	0.2	0	0.5	0.5	0.5
Ovçular Tepesi	0.12	0.17	0.17	0	0.2	0	0.5	0.5	0.5
Shengavit	0.29	0.4	0.4	0.2	0.5	0	0	0	0.2
Shirakavan	0.22	0	0	0.14	0.14	0.22	0	0	0
Sos Höyük	0	0	0	0	0	0	0	0	0

	Kuli Tepe	Kültepe 1	Mokhrablur	Nadir Tepesi	Ovçular Tepesi	Shengavit	Shirakavan	Sos Höyük
Agarak	0	0.33	0.5	0.12	0.12	0.29	0.22	0
Aygevan	0	0.25	0.43	0.17	0.17	0.4	0	0
Dvin	0	0.43	0.25	0.17	0.17	0.4	0	0
Gegharot	0	0.29	0.5	0	0	0.2	0.14	0
Jrahovit	0	0.5	0.5	0.2	0.2	0.5	0.14	0
Karnut 1	0	0.09	0.33	0	0	0	0.22	0
Kohne Pasgah Tepesi	1	0.2	0	0.5	0.5	0	0	0
Kohne Tepesi	1	0.2	0	0.5	0.5	0	0	0
Kul Tepe Jolfa	0.25	0.5	0.12	0.5	0.5	0.2	0	0
Kuli Tepe	1	0.2	0	0.5	0.5	0	0	0
Kültepe 1	0.2	1	0.25	0.4	0.4	0.17	0.12	0
Mokhrablur	0	0.25	1	0	0	0.4	0.12	0
Nadir Tepesi	0.5	0.4	0	1	1	0	0	0
Ovçular Tepesi	0.5	0.4	0	1	1	0	0	0
Shengavit	0	0.17	0.4	0	0	1	0	0
Shirakavan	0	0.12	0.12	0	0	0	1	0
Sos Höyük	0	0	0	0	0	0	0	1

Appendix 12 Adjacency matrix with Jaccard similarities for the obsidian dataset.

	Agarak	Aygevan	Dvin	Gegharot	Jrahovit	Karnut 1	Kohne Pasgah Tepesi	Kohne Tepesi	Kul Tepe Jolfa
Agarak	1	0.43	0.36	0.41	0.53	0.6	0.07	0.5	0.47
Aygevan	0.43	1	0.22	0.23	0.25	0.45	0	0.33	0.33
Dvin	0.36	0.22	1	0.36	0.4	0.36	0.17	0.36	0.36
Gegharot	0.41	0.23	0.36	1	0.36	0.43	0.09	0.43	0.41
Jrahovit	0.53	0.25	0.4	0.36	1	0.36	0.1	0.27	0.35
Karnut 1	0.6	0.45	0.36	0.43	0.36	1	0.09	0.67	0.41
Kohne Pasgah Tepesi	0.07	0	0.17	0.09	0.1	0.09	1	0.2	0.14
Kohne Tepesi	0.5	0.33	0.36	0.43	0.27	0.67	0.2	1	0.5
Kul Tepe Jolfa	0.47	0.33	0.36	0.41	0.35	0.41	0.14	0.5	1
Kuli Tepe	0.07	0	0.17	0.09	0	0.09	0	0.09	0.07
Kültepe 1	0.33	0.2	0.22	0.14	0.36	0.45	0	0.33	0.18
Mokhrablur	0.6	0.33	0.36	0.43	0.9	0.43	0.09	0.33	0.41
Nadir Tepesi	0.07	0	0.17	0.09	0.1	0.09	1	0.2	0.14
Ovçular Tepesi	0.44	0.36	0.27	0.27	0.29	0.46	0.22	0.46	0.44
Shengavit	0.71	0.4	0.33	0.47	0.5	0.47	0.13	0.56	0.71
Shirakavan	0.33	0.5	0.38	0.23	0.36	0.6	0.14	0.45	0.43
Sos Höyük	0.62	0.38	0.42	0.47	0.5	0.69	0.17	0.69	0.53

	Kuli Tepe	Kültepe 1	Mokhrablur	Nadir Tepesi	Ovçular Tepesi	Shengavit	Shirakavan	Sos Höyük
Agarak	0.07	0.33	0.6	0.07	0.44	0.71	0.33	0.62
Aygevan	0	0.2	0.33	0	0.36	0.4	0.5	0.38
Dvin	0.17	0.22	0.36	0.17	0.27	0.33	0.38	0.42
Gegharot	0.09	0.14	0.43	0.09	0.27	0.47	0.23	0.47
Jrahovit	0	0.36	0.9	0.1	0.29	0.5	0.36	0.5
Karnut 1	0.09	0.45	0.43	0.09	0.46	0.47	0.6	0.69
Kohne Pasgah Tepesi	0	0	0.09	1	0.22	0.13	0.14	0.17
Kohne Tepesi	0.09	0.33	0.33	0.2	0.46	0.56	0.45	0.69
Kul Tepe Jolfa	0.07	0.18	0.41	0.14	0.44	0.71	0.43	0.53
Kuli Tepe	1	0	0	0	0.1	0.06	0	0.08
Kültepe 1	0	1	0.33	0	0.36	0.17	0.33	0.29
Mokhrablur	0	0.33	1	0.09	0.36	0.56	0.45	0.57
Nadir Tepesi	0	0	0.09	1	0.22	0.13	0.14	0.17
Ovçular Tepesi	0.1	0.36	0.36	0.22	1	0.41	0.36	0.4
Shengavit	0.06	0.17	0.56	0.13	0.41	1	0.4	0.69
Shirakavan	0	0.33	0.45	0.14	0.36	0.4	1	0.5
Sos Höyük	0.08	0.29	0.57	0.17	0.4	0.69	0.5	1

Appendix 13 Adjacency matrix with Jaccard similarities for the subset of the pottery dataset.

	Agarak	Aygevan	Dvin	Gegharot	Jrahovit	Karnut 1	Kohne Pasgah Tepesi	Kohne Tepesi
Agarak	1	1	1	1	1	1	0	0
Aygevan	1	1	1	1	1	1	0	0
Dvin	1	1	1	1	1	0	0	0
Gegharot	1	1	1	1	1	1	0	0
Jrahovit	1	1	1	1	1	1	0	0
Karnut 1	1	1	0	1	1	1	0	0
Kohne Pasgah Tepesi	0	0	0	0	0	0	1	1
Kohne Tepesi	0	0	0	0	0	0	1	1
Kul Tepe Jolfa	1	1	1	1	1	0	1	1
Kuli Tepe	0	0	0	0	0	0	0	1
Kültepe 1	1	1	1	1	1	1	0	1
Mokhrablur	1	1	1	1	1	1	0	0
Nadir Tepesi	1	0	1	0	1	0	1	1
Ovçular Tepesi	1	1	1	0	1	0	1	1
Shengavit	1	1	1	1	1	0	0	0
Shirakavan	1	0	0	1	1	1	0	0
Sos Höyük	0	0	0	0	0	0	0	0

	Kul Tepe Jolfa	Kuli Tepe	Kültepe 1	Mokhrablur	Nadir Tepesi	Ovçular Tepesi	Shengavit	Shirakavan	Sos Höyük
Agarak	1	0	1	1	1	1	1	1	0
Aygevan	1	0	1	1	0	1	1	0	0
Dvin	1	0	1	1	1	1	1	0	0
Gegharot	1	0	1	1	0	0	1	1	0
Jrahovit	1	0	1	1	1	1	1	1	0
Karnut 1	0	0	1	1	0	0	0	1	0
Kohne Pasgah Tepesi	1	0	0	0	1	1	0	0	0
Kohne Tepesi	1	1	1	0	1	1	0	0	0
Kul Tepe Jolfa	1	1	1	1	1	1	1	0	0
Kuli Tepe	1	1	0	0	0	1	0	0	0
Kültepe 1	1	0	1	1	0	1	1	1	0
Mokhrablur	1	0	1	1	0	0	1	1	0
Nadir Tepesi	1	0	0	0	1	1	0	0	0
Ovçular Tepesi	1	1	1	0	1	1	0	0	0
Shengavit	1	0	1	1	0	0	1	0	0
Shirakavan	0	0	1	1	0	0	0	1	0
Sos Höyük	0	0	0	0	0	0	0	0	1

Appendix 14 Adjacency matrix of sites sharing both pottery decorations and obsidian sources.

	Agarak	Alaybeyi Höyük	Ashagi Dasharkh	Aygevan	Duzdagi	Dvin	Erebyengicesi	Franganots	Gegharot	Gökceli	Jradzor	Jrahovit
Agarak	0	277.21	107	33.42	141.86	41.52	108.01	6.33	45.82	34.3	80.93	33.3
Alaybeyi Höyük	277.21	0	345.15	247.47	373.56	303.48	339.58	275.76	281.17	267.73	252.46	293.24
Ashagi Dasharkh	107	345.15	0	115.29	35	65.71	8.91	102.64	148	89.37	187.73	73.92
Aygevan	33.42	247.47	115.29	0	149.81	57.84	113.67	29.81	67.44	25.93	87.29	47.31
Duzdagi	141.86	373.56	35	149.81	0	100.44	36.39	137.59	182	123.88	222.42	108.88
Dvin	41.52	303.48	65.71	57.84	100.44	0	67.39	37.75	83.02	35.86	122.02	10.54
Erebyen-gicesi	108.01	339.58	8.91	113.67	36.39	67.39	0	103.28	150.32	87.77	188.93	74.71
Franganots	6.33	275.76	102.64	29.81	137.59	37.75	103.28	0	52	28	85.88	28.72
Gegharot	45.82	281.17	148	67.44	182	83.02	150.32	52	0	79.02	44.68	77.14
Gökceli	34.3	267.73	89.37	25.93	123.88	35.86	87.77	28	79.02	0	107.79	26.05
Jradzor	80.93	252.46	187.73	87.29	222.42	122.02	188.93	85.88	44.68	107.79	0	114.23
Jrahovit	33.3	293.24	73.92	47.31	108.88	10.54	74.71	28.72	77.14	26.05	114.23	0
Karnut 1	60.9	262.04	167.23	71.92	201.8	101.53	168.7	66.22	24.36	89.89	21.08	94.11
Khalaj	101.72	335.78	9.54	107.87	41.96	61.07	6.33	97.02	144	81.94	182.63	68.42
Kohne Pasgah Tepesi	256.55	509.01	164.22	274.53	136.13	217.71	169.44	254.34	285.2	249.55	329.69	228.05
Köhne Sha-har	124.49	295.25	72.71	111.72	86.25	96.62	63.91	118.25	170.23	91.83	198.61	97.12
Kohne Tepesi	256.75	509.26	164.46	274.75	136.38	217.92	169.69	254.54	285.38	249.77	329.87	228.26
Kül Tepe 1	151.91	386.7	46.15	161.44	13.15	110.4	48.76	147.92	190.77	135.52	232.02	119.3
Kül Tepe 2	152.03	386.91	46.3	161.59	13.38	110.51	48.94	148.04	190.85	135.67	232.12	119.42
Kul Tepe Jolfa	200.84	417.79	93.84	206.75	59.21	159.52	93.53	196.41	241.18	180.97	281.54	167.7
Kuli Tepe	259.79	511.28	166.69	277.48	138.13	220.78	171.77	257.52	288.74	252.42	333.21	231.1
Maxta 1	97.23	337.25	9.85	105.59	44.85	56.04	12.93	92.82	138.58	79.69	178.02	64.11

Melekli Höyük	41.75	260.35	92.79	24.94	126.7	44.02	90.34	35.64	85.06	9.26	110.82	34.69
Mokhrablur	20.69	273.34	93.29	26.2	128.26	31.97	92.98	14.36	66.16	13.95	97.9	21.48
Nadir Tepesi	282.79	547.56	203.79	305.48	181.14	247.63	210.46	281.73	304.29	282.05	348.82	258.17
Ovçular Tepesi	103.27	347.35	8.32	113.86	38.98	61.76	16.84	99.25	143.03	88.11	183.58	70.65
Sadarak	76.74	318.61	31.33	84.07	66.22	36.52	31.28	72.01	119.52	58.2	157.66	43.44
Shengavit	22.98	293.21	84.57	45.74	119.26	18.85	86.12	20.17	64.63	31.02	103.17	13.05
Shirakavan	60.27	240.06	166.45	59.4	201.44	101.59	166.67	63.93	41.45	81.91	29.34	92.59
Shortepe	109.02	342.2	6.57	115.41	34.44	68.15	2.84	104.39	150.95	89.49	189.91	75.75
Shreshblur	10.5	281.48	96.63	34.59	131.53	31.38	97.53	6.63	55.63	27.49	91.41	22.82
Sos Höyük	236.5	41.34	304.09	206.39	332.86	262.2	298.64	234.88	242.34	226.43	216.03	251.99
Tsaghkalanj	10.92	270.13	104.27	23.78	139.27	40.54	104.4	6.05	54.53	24.5	85.73	30.75
Yakhvali	116.87	319.42	42.06	112.79	56.18	81.5	33.15	111.12	162.14	88.74	196	85.26

	Karnut 1	Khalaj	Kohne Pasgah Tepesi	Köhne Shahar	Kohne Tepesi	Kül Tepe 1	Kül Tepe 2	Kul Tepe Jolfa	Kuli Tepe	Maxta 1	Mele-kli Höyük
Agarak	60.9	101.72	256.55	124.49	256.75	151.91	152.03	200.84	259.79	97.23	41.75
Alaybeyi Höyük	262.04	335.78	509.01	295.25	509.26	386.7	386.91	417.79	511.28	337.25	260.35
Ashagi Dasharkh	167.23	9.54	164.22	72.71	164.46	46.15	46.3	93.84	166.69	9.85	92.79
Aygevan	71.92	107.87	274.53	111.72	274.75	161.44	161.59	206.75	277.48	105.59	24.94
Duzdagi	201.8	41.96	136.13	86.25	136.38	13.15	13.38	59.21	138.13	44.85	126.7
Dvin	101.53	61.07	217.71	96.62	217.92	110.4	110.51	159.52	220.78	56.04	44.02
Erebyengicesi	168.7	6.33	169.44	63.91	169.69	48.76	48.94	93.53	171.77	12.93	90.34
Franganots	66.22	97.02	254.34	118.25	254.54	147.92	148.04	196.41	257.52	92.82	35.64
Gegharot	24.36	144	285.2	170.23	285.38	190.77	190.85	241.18	288.74	138.58	85.06
Gökceli	89.89	81.94	249.55	91.83	249.77	135.52	135.67	180.97	252.42	79.69	9.26
Jradzor	21.08	182.63	329.69	198.61	329.87	232.02	232.12	281.54	333.21	178.02	110.82
Jrahovit	94.11	68.42	228.05	97.12	228.26	119.3	119.42	167.7	231.1	64.11	34.69

Karnut 1	0	162.38	308.76	181.55	308.94	211.23	211.33	260.97	312.26	157.57	93.95
Khalaj	162.38	0	173.44	64.74	173.68	53.97	54.14	99.64	175.86	7.75	84.8
Kohne Pasgah Tepesi	308.76	173.44	0	220.54	0.27	123	122.77	109.34	4.13	172.69	254.69
Köhne Shahar	181.55	64.74	220.54	0	220.8	98.8	99.05	122.58	222.14	71.36	87.81
Kohne Tepesi	308.94	173.68	0.27	220.8	0	123.26	123.03	109.61	4.09	172.92	254.92
Kül Tepe 1	211.23	53.97	123	98.8	123.26	0	0.25	51.31	124.99	55.91	138.72
Kül Tepe 2	211.33	54.14	122.77	99.05	123.03	0.25	0	51.28	124.76	56.05	138.89
Kul Tepe Jolfa	260.97	99.64	109.34	122.58	109.61	51.31	51.28	0	109.66	103.61	182.77
Kuli Tepe	312.26	175.86	4.13	222.14	4.09	124.99	124.76	109.66	0	175.26	257.47
Maxta 1	157.57	7.75	172.69	71.36	172.92	55.91	56.05	103.61	175.26	0	83.34
Melekli Höyük	93.95	84.8	254.69	87.81	254.92	138.72	138.89	182.77	257.47	83.34	0
Mokhrablur	78.98	86.85	249.49	104.08	249.7	139.22	139.35	186.49	252.52	83.45	22.41
Nadir Tepesi	328.57	213.33	57.28	267.35	57.04	168.57	168.32	164.31	58.61	210.92	288.46
Ovçular Tepesi	162.9	15.12	162.97	79.79	163.2	48.67	48.79	98.18	165.6	10.3	92.3
Sadarak	137.48	25.01	192.85	70.14	193.08	77.45	77.6	124.54	195.54	21.55	62.18
Shengavit	82.68	79.8	234.17	110.01	234.38	129.1	129.2	178.37	237.36	74.89	40.28
Shirakavan	23.68	160.48	315.79	171.12	315.98	211.86	211.97	260.07	319.12	156.61	83.76
Shortepe	169.59	7.55	166.85	66.6	167.1	46.58	46.76	92.16	169.2	12.67	92.27
Shreshblur	71.39	91.24	247.71	115.26	247.91	141.71	141.82	190.45	250.89	86.84	36.05
Sos Höyük	224.17	294.75	468.08	255.71	468.32	345.97	346.19	378.05	470.39	296.11	219.02
Tsaghkalanj	66.74	98.2	257.97	115.96	258.18	149.92	150.04	197.8	261.1	94.42	
Yakhvali	177.12	35.11	191.96	31.46	192.22	69.13	69.37	100.51	193.81	42.47	

	Mokhrablur	Nadir Tepesi	Ovçular Tepesi	Sadarak	Shengavit	Shirakavan	Shortepe	Shreshblur	Sos Höyük	Tsaghkalanj	Yakhvali
Agarak	20.69	282.79	103.27	76.74	22.98	60.27	109.02	10.5	236.5	10.92	116.87
Alaybeyi Höyük	273.34	547.56	347.35	318.61	293.21	240.06	342.2	281.48	41.34	270.13	319.42
Ashagi Dasharkh	93.29	203.79	8.32	31.33	84.57	166.45	6.57	96.63	304.09	104.27	42.06
Aygevan	26.2	305.48	113.86	84.07	45.74	59.4	115.41	34.59	206.39	23.78	112.79
Duzdagi	128.26	181.14	38.98	66.22	119.26	201.44	34.44	131.53	332.86	139.27	56.18
Dvin	31.97	247.63	61.76	36.52	18.85	101.59	68.15	31.38	262.2	40.54	81.5
Erebyengicesi	92.98	210.46	16.84	31.28	86.12	166.67	2.84	97.53	298.64	104.4	33.15
Franganots	14.36	281.73	99.25	72.01	20.17	63.93	104.39	6.63	234.88	6.05	111.12
Gegharot	66.16	304.29	143.03	119.52	64.63	41.45	150.95	55.63	242.34	54.53	162.14
Gökceli	13.95	282.05	88.11	58.2	31.02	81.91	89.49	27.49	226.43	24.5	88.74
Jradzor	97.9	348.82	183.58	157.66	103.17	29.34	189.91	91.41	216.03	85.73	196
Jrahovit	21.48	258.17	70.65	43.44	13.05	92.59	75.75	22.82	251.99	30.75	85.26
Karnut 1	78.98	328.57	162.9	137.48	82.68	23.68	169.59	71.39	224.17	66.74	177.12
Khalaj	86.85	213.33	15.12	25.01	79.8	160.48	7.55	91.24	294.75	98.2	35.11
Kohne Pasgah Tepesi	249.49	57.28	162.97	192.85	234.17	315.79	166.85	247.71	468.08	257.97	191.96
Köhne Shahar	104.08	267.35	79.79	70.14	110.01	171.12	66.6	115.26	255.71	115.96	31.46
Kohne Tepesi	249.7	57.04	163.2	193.08	234.38	315.98	167.1	247.91	468.32	258.18	192.22
Kül Tepe 1	139.22	168.57	48.67	77.45	129.1	211.86	46.58	141.71	345.97	149.92	69.13
Kül Tepe 2	139.35	168.32	48.79	77.6	129.2	211.97	46.76	141.82	346.19	150.04	69.37
Kul Tepe Jolfa	186.49	164.31	98.18	124.54	178.37	260.07	92.16	190.45	378.05	197.8	100.51
Kuli Tepe	252.52	58.61	165.6	195.54	237.36	319.12	169.2	250.89	470.39	261.1	193.81
Maxta 1	83.45	210.92	10.3	21.55	74.89	156.61	12.67	86.84	296.11	94.42	42.47
Melekli Höyük	22.41	288.46	92.3	62.18	40.28	83.76	92.27	36.05	219.02	31.24	87.86
Mokhrablur	0	279.47	90.82	62.06	20.37	73.85	94.35	13.65	232.19	12.24	98.19
Nadir Tepesi	279.47	0	200.68	228.96	261.86	339.21	207.68	275.18	506.28	286.2	237.13
Ovçular Tepesi	90.82	200.68	0	30.11	80.51	163.19	14.8	93.04	306.18	101.31	49.68

Sadarak	62.06	228.96	30.11	0	55.05	135.53	32.41	66.26	277.35	73.26	47.96
Shengavit	20.37	261.86	80.51	55.05	0	83.25	86.95	13.54	252.12	24.34	98.18
Shirakavan	73.85	339.21	163.19	135.53	83.25	0	167.93	70.22	201.63	62.28	170.65
Shortepe	94.35	207.68	14.8	32.41	86.95	167.93	0	98.56	301.23	105.66	35.7
Shreshblur	13.65	275.18	93.04	66.26	13.54	70.22	98.56	0	240.53	11.4	106.66
Sos Höyük	232.19	506.28	306.18	277.35	252.12	201.63	301.23	240.53	0	229.2	279.11
Tsaghkalanj	12.24	286.2	101.31	73.26	24.34	62.28	105.66	11.4	229.2	0	110.42
Yakhvali	98.19	237.13	49.68	47.96	98.18	170.65	35.7	106.66	279.11	110.42	0

Appendix 15 Distance matrix of all sites (in km).

References

Abedi, A., & Omrani, B. (2015). Kura-Araxes culture and North-Western Iran: New perspectives from Kul Tepe Jolfa (Hadishahr). *Paléorient*, *41*(1), 55–68. https://doi.org/10.3406/paleo.2015.5655

Abedi, A., Orange, M., & Thomalsky, J. (in press). *Late prehistoric interregional networks in Iranian Azerbaijan (North-western Iran): New insights from the reconstruction of obsidian exploitation patterns*.

Abedi, A., Shahidi, H. K., Chataigner, C., Niknami, K., Eskandarani, N., Kazempour, M., Pirmohammadi, A., Hosseinzadeh, J., & Ebrahimi, G. (2014). Excavation at Kul Tepe (Hadishahr), North-Western Iran, 2010: First preliminary report. *Ancient Near Eastern Studies*, *51*, 33–165.

Achino, K., Duboscq, S., Morell, B., & Gibaja, J. F. (2017). Comparing in archaeology through a quantitative approach: Dealing with similarity and dissimilarity issues. In A. Vale, J. Alves-Ferreira, & I. Garcia-Rovira (Eds.), *Rethinking comparison in archaeology* (pp. 74–89). Cambridge Scholars Publishing.

Alizadeh, K., Eghbal, H., & Samei, S. (2015). Approaches to social complexity in Kura-Araxes culture: A view from Köhne Shahar (Ravaz) in Chaldran, Iranian Azerbaijan. *Paléorient*, *41*(1), 37–54. https://doi.org/10.3406/paleo.2015.5654

Alizadeh, K., Maziar, S., & Mohammadi, M. R. (2018). The end of the Kura-Araxes culture as seen from Nadir Tepesi in Iranian Azerbaijan. *American Journal of Archaeology*, *122*(3), 463–477. https://doi.org/10.3764/aja.122.3.0463

Andrade, C. (2019). The P Value and Statistical Significance: Misunderstandings, Explanations, Challenges, and Alternatives. *Indian Journal of Psychological Medicine*, *41*(3), 210–215. https://doi.org/10.4103/IJPSYM.IJPSYM_193_19

Anuar, S. H. H., Abas, Z. A., Yunos, N. M., Zaki, N. H. M., Hashim, N. A., Mokhtar, M. F., Asmai, S. A., Abidin, Z. Z., & Nizam, A. F. (2021). Comparison between Louvain and Leiden Algorithm for Network Structure: A Review. *Journal of Physics: Conference Series*, *2129*(1), 12028. https://doi.org/10.1088/1742-6596/2129/1/012028

Ashurov, S. (2002). *Naxçıvanın ilk tunc dövrü keramikası*. Nafta Press.

Ashurov, S., Hüseynova, S., & Aliyeva, F. (2020). *Maxta ilk tunc dövrü abidesi: I kitab*. Apostrof A.

Badalyan, R. (2010). Obsidian in the Southern Caucasus: The use of raw materials in the Neolithic to Early Iron Ages. In I. Motzenbacker, A. Hauptmann, & S. Hansen (Eds.), *Kolloquien zur Vor- und Frühgeschichte: Vol. 13. Von Majkop bis Trialeti: Gewinnung und Verbreitung von Metallen und Obsidian in Kaukasien im 4.-2. Jt. v. Chr.* (pp. 27–28).

Badalyan, R. (2014). New data on the periodization and chronology of the Kura-Araxes culture in Armenia. *Paléorient*, *40*(2), 71–92. https://doi.org/10.3406/paleo.2014.5636

Badalyan, R. (2021). The exploitation of mineral resources in Armenia in the Early Bronze Age: Obsidian, metal, bitumen, and salt. In C. Marro & T. Stöllner (Eds.), *On salt, copper and gold* (pp. 425–444). MOM Éditions.

Badalyan, R., & Avetisyan, P. (2007). *Bronze and Early Iron Age archaeological sites in Armenia*. *BAR international series: Vol. 1697*. Archaeopress.

Badalyan, R., Chataigner, C., & Kohl, P. (2004). Trans-Caucasian obsidian: The exploitation of the sources and their distribution. In A. Sagona (Ed.), *Ancient Near Eastern Studies: Vol. 12. A view from the highlands: Archaeological studies in honour of C. Burney* (pp. 437–465). Peeters.

Badalyan, R., Smith, A. T., Lindsay, I., Harutyunyan, A., Greene, A., Marshall, M., Monahan, B., & Hovsepyan, R. (2014). A preliminary report on the 2008, 2010, and 2011 investigations of Project ArAGATS on the Tsaghkahovit plain, Republic of Armenia. *Archäologische Mitteilungen Aus Iran Und Turan*, *46*, 149–222.

Bakhshaliyev, V., & Seyidov, A. (2013a). New findings from the settlement of Sadarak (Nakhchivan-Azerbaijan). *Anatolia Antiqua*, *21*(1), 1–21. https://doi.org/10.3406/anata.2013.1337

Bakhshaliyev, V., & Seyidov, A. (2013b). Şortepe yaşayış yerinin erken tunc dövrü keramikası. *Azerbaycan Milli Elmler Akademiyası Naxçıvan Bölmesinin*, *1*, 57–66.

Barabási, A.-L. (2016). *Network science*. Cambridge University Press.

Barge, O., Azizi Kharanaghi, H., Biglari, F., Moradi, B., Mashkour, M., Tengberg, M., & Chataigner, C. (2018). Diffusion of Anatolian and Caucasian obsidian in the Zagros Mountains and the highlands of Iran: Elements of explanation in 'least cost path' models. *Quaternary International*, *467*, 297–322. https://doi.org/10.1016/j.quaint.2018.01.032

Batiuk, S., Rothman, M., Samei, S., & Hovsepyan, R. (2022). Unravelling the Kura-Araxes cultural tradition across space and time. *Ancient Near Eastern Studies*, *59*, 217–449. https://doi.org/10.2143/ANES.59.0.3291195

Birch, J., & Hart, J. P. (2021). Conflict, population movement, and microscale social networks in Northern Iroquoian archaeology. *American Antiquity*, *86*(2), 350–367. https://doi.org/10.1017/aaq.2021.5

Boyd, A. T., & Rocconi, L. M. (2021). Formatting data for one and two mode undirected social network analysis. *Practical Assessment, Research, and Evaluation*, *26*, 1–10. https://doi.org/10.7275/22895861

Box, G. E. P. (1979). Robustness in the strategy of scientific model building. In R. L. Launer & G. N. Wilkinson (Eds.), Robustness in statistics. Academic Press.

Brennan, P. V. (2000). Obsidian from volcanic sequences and recent alluvial deposits, Erzurum District, North-Eastern Anatolia: Chemical characterisation and archaeological implications. *Ancient Near Eastern Studies*, *37*, 128–152.

Brughmans, T., & Peeples, M. A. (2023). *Network science in archaeology*. *Cambridge manuals in archaeology*. Cambridge University Press. https://doi.org/10.1017/9781009170659

Carlson, D. L. (Ed.). (2017). *Quantitative Methods in Archaeology Using R*. Cambridge University Press. https://doi.org/10.1017/9781139628730

Chataigner, C., & Barge, O. (2008). Quantitative Approach to the Diffusion of Obsidian in the Ancient Northern Near East. In A. Posluschny, K. Lambers, & I. Herzog (Eds.), *Kolloquien zur Vor- und Frühgeschichte: Vol. 10. Layers of Perception: Proceedings of the 35th International Conference on Computer Applications and Quantitative Methods in Archaeology (CAA), Berlin, Germany, April 2–6, 2007* (pp. 374–380). Dr. Rudolf Habelt.

Chataigner, C., & Gratuze, B. (2014). New data on the exploitation of obsidian in the Southern Caucasus (Armenia, Georgia) and Eastern Turkey: Part 2: Obsidian procurement from the Upper Palaeolithic to the Late Bronze Age. *Archaeometry*, *56*(1), 48–69. https://doi.org/10.1111/arcm.12007

Collar, A., Coward, F., Brughmans, T., & Mills, B. J. (2015). Networks in archaeology: Phenomena, abstraction, representation. *Journal of Archaeological Method and Theory*, *22*(1), 1–32. https://doi.org/10.1007/s10816-014-9235-6

Csárdi, G., & Nepusz, T. (2006). The igraph software package for complex network research. *InterJournal*, *Complex Systems*, 1965.

Daems, D., Coco, E., Gillreath-Brown, A., & Kafetzaki, D. (2023). The Effects of Time-Averaging on Archaeological Networks. *Journal of Archaeological Method and Theory*, 1–34. https://doi.org/10.1007/s10816-023-09608-7

Dawson, H. (2020). Networks in archaeology. *ETopoi. Journal for Ancient Studies*, *7*, 74–86. https://doi.org/10.17169/refubium-28211

de Groot, B. G. (2019). A diachronic study of networks of ceramic assemblage similarity in Neolithic Western Anatolia, the Aegean and the Balkans (c.6600–5500 bc). *Archaeometry*, *61*(3), 600–613. https://doi.org/10.1111/arcm.12450

Düring, M. (2015). *Cheat Sheet: Social Network Analysis for Humanists*. https://cvcedhlab.hypotheses.org/106

Earley-Spadoni, T. (2015). Landscapes of warfare: Intervisibility analysis of Early Iron and Urartian fire beacon stations (Armenia). *Journal of Archaeological Science: Reports*, *3*, 22–30. https://doi.org/10.1016/j.jasrep.2015.05.008

Fabian, L. (2018). Moving in the mountains: GIS and mapping the phenomenology of travel through the South Caucasus. In W. Anderson, K. Hopper, & A. Robinson (Eds.), *Oriental and European Archaeology: Vol. 8. Landscape archaeology in Southern Caucasia: Finding common ground in diverse environments proceedings of the workshop held at 10th ICAANE in Vienna, April 2016* (pp. 23–36). Verlag der Österreichischen Akademie der Wissenschaften.

Fortunato, S., & Barthélemy, M. (2007). Resolution limit in community detection. *Proceedings of the National Academy of Sciences of the United States of America*, *104*(1), 36–41. https://doi.org/10.1073/pnas.0605965104

Fruchterman, T. M. J., & Reingold, E. M. (1991). Graph drawing by force-directed placement. *Software: Practice and Experience*, *21*(11), 1129–1164. https://doi.org/10.1002/spe.4380211102

Golitko, M., & Feinman, G. M. (2015). Procurement and distribution of Pre-Hispanic Mesoamerican obsidian 900 BC–AD 1520: A Social Network Analysis. *Journal of Archaeological Method and Theory*, *22*(1), 206–247. https://doi.org/10.1007/s10816-014-9211-1

Habiba, H., Athenstädt, J. C., Mills, B. J., & Brandes, U. (2018). Social networks and similarity of site assemblages. *Journal of Archaeological Science*, *92*, 63–72. https://doi.org/10.1016/j.jas.2017.11.002

Haroutunian, S. (2016). A GIS analysis of Early Bronze Age settlement patterns in Armenia. *Quaternary International*, *395*, 95–103. https://doi.org/10.1016/j.quaint.2015.07.023

Hart, J. P., & Engelbrecht, W. (2012). Northern Iroquoian ethnic evolution: A social network analysis. *Journal of Archaeological Method and Theory*, *19*(2), 322–349. https://doi.org/10.1007/s10816-011-9116-1

Hayrapetyan, A. (2008). Some technical aspects of the pottery of the Early Bronze Age site of Gegharot (Armenia). In K. S. Rubinson & A. Sagona (Eds.), *Ancient Near Eastern studies. Supplement: Vol. 27. Ceramics in transitions: Chalcolithic through Iron Age in the highlands of the Southern Caucasus and Anatolia.* Peeters.

Iserlis, M. (2010). Bet Yerah, Aparan III and Karnut I: Preliminary observations on Kura-Araks homeland and diaspora ceramic technologies. *Turkish Academy of Sciences Journal of Archaeology*, *13*, 245–262.

Iserlis, M., Goren, Y., Hovsepyan, I., & Greenberg, R. (2015). Early Kura-Araxes ceramic technology in the fourth millennium BCE site of Tsaghkasar, Armenia. *Paléorient*, *41*(1), 9–23. https://doi.org/10.3406/paleo.2015.5652

Isern, N., Fort, J., Carvalho, A. F., Gibaja, J. F., & Ibañez, J. J. (2014). The Neolithic transition in the Iberian Peninsula: Data analysis and modeling. *Journal of Archaeological Method and Theory*, *21*(2), 447–460. https://doi.org/10.1007/s10816-013-9193-4

Işıklı, M. (2019). Chalcolithic and Early Bronze Age levels of Alaybeyi Höyük, Erzurum Plain. In G. Altunkaynak (Ed.), *Karaz'dan Büyük İskender'e Erzurum Ovası'nda yeni bir keşif Alaybeyi Höyük* (pp. 139–182). Bilgin Kültür Sanat Yayınları.

Juharyan, A. K. (2018). The principles of choice of Armenian obsidian sources in Bronze Age, obtained by pXRF analysis. *Yerevan State University Scientific Bulletin - Geology and Geography*, *52*(1), 20–26.

Kanters, H., Brughmans, T., & Romanowska, I. (2021). Sensitivity analysis in archaeological simulation: An application to the MERCURY model. *Journal of Archaeological Science: Reports*, *38*, 102974. https://doi.org/10.1016/j.jasrep.2021.102974

Khademi Nadooshan, F., Abedi, A., Glascock, M. D., Eskandari, N., & Khazaee, M. (2013). Provenance of prehistoric obsidian artefacts from Kul Tepe, northwestern Iran using X-ray fluorescence (XRF) analysis. *Journal of Archaeological Science*, *40*(4), 1956–1965. https://doi.org/10.1016/j.jas.2012.12.032

Khatchadourian, L., Badalyan, R., & Smith, A. T. (2023). *Project ArAGATS data portal*. https://aragats.gorgesapps.us/search

Kibaroğlu, M., Sagona, A., & Satir, M. (2011). Petrographic and geochemical investigations of the late prehistoric ceramics from Sos Höyük, Erzurum (Eastern Anatolia). *Journal of Archaeological Science*, *38*(11), 3072–3084. https://doi.org/10.1016/j.jas.2011.07.006

Kleiss, W., & Kroll, S. (1979). Ravaz und Yakhvali: Zwei Befestigte Plätze des 3. Jahrtausends. *Archäologische Mitteilungen Aus Iran*, *12*, 27–47.

Kroll, S. (2006). Southern Armenian survey (Syunik) 2000-2003. *Aramazd*, *1*, 19–49.

Ladefoged, T. N., Gemmell, C., McCoy, M., Jorgensen, A., Glover, H., Stevenson, C., & O'Neale, D. (2019). Social network analysis of obsidian artefacts and Māori interaction in northern Aotearoa New Zealand. *PloS One*, *14*(3), e0212941. https://doi.org/10.1371/journal.pone.0212941

Longford, C. (2015). *Plant economy of the Kura-Araxes: A comparative analysis of agriculture in the Near East from the Chalcolithic to the Middle Bronze Age* [Doctoral dissertation, University of Sheffield]. White Rose eTheses Online. https://etheses.whiterose.ac.uk/10675/

Manoukian, N., Whelton, H. L., Dunne, J., Badalyan, R., Smith, A. T., Simonyan, H. Y., Rothman, M., Bobokhyan, A., Hovsepyan, R., Avetisyan, P., Evershed, R. P., & Pollard, A. M. (2022). Diverse

dietary practices across the Early Bronze Age 'Kura-Araxes culture' in the South Caucasus. *PloS One*, *17*(12), e0278345. https://doi.org/10.1371/journal.pone.0278345

Marro, C. (2021). The functions of Kura-Araxes ceramic containers in Caucasian early mining. In C. Marro & T. Stöllner (Eds.), *On salt, copper and gold* (pp. 79–100). MOM Éditions. https://doi.org/10.4000/books.momeditions.12472

Marro, C., Bakhshaliyev, V., & Ashurov, S. (2009). Excavations at Ovçular Tepesi (Nakhchivan, Azerbaijan): First preliminary report: The 2006-2008 seasons. *Anatolia Antiqua*, *17*(1), 31–87. https://doi.org/10.3406/anata.2009.1276

Marro, C., Bakhshaliyev, V., Berthon, R., & Thomalsky, J. (2019). New light on the late prehistory of the South Caucasus: Data from the recent excavation campaigns at Kültepe I in Nakhchivan, Azerbaijan (2012-2018). *Paléorient*, *45*(1), 81–113. https://doi.org/10.4000/paleorient.589

Marro, C., & Özfirat, A. (2003). Pre-classical survey in eastern Turkey. First preliminary report: The Ağrı Dağ (Mount Ararat) Region. *Anatolia Antiqua*, *11*(1), 385–422. https://doi.org/10.3406/anata.2003.1012

Marro, C., & Stöllner, T. (Eds.). (2021). *On salt, copper and gold*. MOM Éditions. https://doi.org/10.4000/books.momeditions.12257

Maziar, S. (2010). Excavations at Kohne Pasgah Tepesi, the Araxes Valley, northwest Iran: First preliminary report. *Ancient Near Eastern Studies*, *47*, 165–193.

Maziar, S. (2015). Settlement dynamics of the Kura-Araxes culture: An overview of the Late Chalcolithic and Early Bronze Age in the Khoda Afarin Plain, North-Western Iran. *Paléorient*, *41*(1), 25–36. https://doi.org/10.3406/paleo.2015.5653

Maziar, S. (2019). Iran and the Kura-Araxes cultural tradition, so near and yet so far. In J.-W. Meyer, E. Vila, M. Mashkour, M. Casanova, & R. Vallet (Eds.), *The Iranian plateau during the Bronze Age* (pp. 51–74). MOM Éditions. https://doi.org/10.4000/books.momeditions.7986

Maziar, S. (2021). Geographical proximity and material culture: The interplay between Syunik and the southern part of the Araxes River Basin in the 6th to the 3rd Millennium BC. *Quaternary International*, *579*, 42–58. https://doi.org/10.1016/j.quaint.2020.03.055

Maziar, S., & Glascock, M. D. (2017). Communication networks and economical interactions: Sourcing obsidian in the Araxes River Basin. *Journal of Archaeological Science*, *14*, 31–37. https://doi.org/10.1016/j.jasrep.2017.05.021

Maziar, S., & Zalaghi, A. (2021). Exploring beyond the river and inside the valleys: Settlement development and cultural landscape of the Araxes River Basin through time. *Iran*, *59*(1), 36–56. https://doi.org/10.1080/05786967.2019.1708207

McNulty, K. (2022). *Handbook of graphs and networks in people analytics: With examples in R and Python*. Chapman and Hall.

Mills, B. J. (2017). Social network analysis in archaeology. *Annual Review of Anthropology*, *46*(1), 379–397. https://doi.org/10.1146/annurev-anthro-102116-041423

Mills, B. J., Clark, J. J., Peeples, M. A., Haas, W. R., Roberts, J. M., Hill, J. B., Huntley, D. L., Borck, L., Breiger, R. L., Clauset, A., & Shackley, M. S. (2013). Social Networks in the distant past. *Archaeology Southwest Magazine*, *27*(2), 3–24.

Nahm, F. S. (2017). What the p values really tell us. *The Korean Journal of Pain*, *30*(4), 241–242. https://doi.org/10.3344/kjp.2017.30.4.241

Neal, Z. P. (2022). Backbone: An R package to extract network backbones. *PloS One*, *17*(5), e0269137. https://doi.org/10.1371/journal.pone.0269137

Neuwirth, E. (2022). *RColorBrewer: ColorBrewer Palettes* [Computer software]. https://CRAN.R-project.org/package=RColorBrewer

Nocaj, A., Ortmann, M., & Brandes, U. (2015). Untangling the hairballs of multi-centered, small-world online social media networks. *Journal of Graph Algorithms and Applications*, *19*(2), 595–618. https://doi.org/10.7155/jgaa.00370

Ognyanova, K. (2016). *Network analysis and visualization with R and igraph: NetSciX 2016 School of Code workshop, Wroclaw, Poland*. https://kateto.net/netscix2016.html

Oksanen, J., Simpson, G., Blanchet, F., Kindt, R., Legendre, P., Minchin, P., O'Hara, R., Solymos, P., Stevens, M., Szoecs, E., Wagner, H., Barbour, M., Bedward, M., Bolker, B., Borcar, D., Carvalho, G., Cirico, M., Caceres, M. de, & Durand, S. (2022). *vegan: Community Ecology Package* [Computer software]. https://CRAN.R-project.org/package=vegan

Orange, M., Abedi, A., Le Bourdonnec, F.-X., Vosough, B., Ebrahimi, G., Razani, M., & Marro, C. (2021a). Consuming local: The new obsidian source of Ideloo (northwestern Iran) and first evidence of use by neighbouring prehistoric communities. *Geoarchaeology*, *36*(2), 266–282. https://doi.org/10.1002/gea.21829

Orange, M., Le Bourdonnec, F.-X., Berthon, R., Mouralis, D., Gratuze, B., Thomalsky, J., Abedi, A., & Marro, C. (2021b). Extending the scale of obsidian studies: Towards a high-resolution investigation of obsidian prehistoric circulation patterns in the Southern Caucasus and north-western Iran. *Archaeometry*, *63*(5), 923–940. https://doi.org/10.1111/arcm.12660

Östborn, P., & Gerding, H. (2014). Network analysis of archaeological data: A systematic approach. *Journal of Archaeological Science*, *46*, 75–88. https://doi.org/10.1016/j.jas.2014.03.015

Palumbi, G. (2008). *The red and black: Social and cultural Interaction between the Upper Euphrates and Southern Caucasus communities in the fourth and third millennium BC*. *Studi di preistoria*

orientale: Vol. 2. Sapienza Università di Roma, Dipartimento di scienze storiche archeologiche e antropologiche dell'antichità.

Palumbi, G. (2017). Push or pull factors? The Kura-Araxes expansion from a different perspective: the Upper Euphrates Valley. In E. Rova & M. Tonussi (Eds.), *Subartu: Vol. 38. At the northern frontier of Near Eastern archaeology* (pp. 113–132). Brepols.

Palumbi, G., & Chataigner, C. (2014). The Kura-Araxes culture from the Caucasus to Iran, Anatolia and the Levant: Between unity and diversity. *Paléorient*, *40*(2), 247–260. https://doi.org/10.3406/paleo.2014.5645

Perkins, A. D., & Langston, M. A. (2009). Threshold selection in gene co-expression networks using spectral graph theory techniques. *BMC Bioinformatics*, *10*(11), S4. https://doi.org/10.1186/1471-2105-10-S11-S4

Prignano, L., Morer, I., & Diaz-Guilera, A. (2017). Wiring the past: A network science perspective on the challenge of archeological similarity networks. *Frontiers in Digital Humanities*, *4*, Article 13. https://doi.org/10.3389/fdigh.2017.00013

Riris, P., & Oliver, J. (2019). Patterns of style, diversity, and similarity in Middle Orinoco rock art assemblages. *Arts*, *8*(2), 48. https://doi.org/10.3390/arts8020048

Ristvet, L., Bakhshaliyev, V., & Ashurov, S. (2011). Settlement and society in Naxçivan: 2006 excavations and survey of the Naxçivan Archaeological project. *Iranica Antiqua*, *46*, 1–53. https://doi.org/10.2143/IA.46.0.2084412

Rothman, M. (2015). Early Bronze Age migrants and ethnicity in the Middle Eastern mountain zone. *Proceedings of the National Academy of Sciences of the United States of America*, *112*(30), 9190–9195. https://doi.org/10.1073/pnas.1502220112

Rothman, M. (2016). Explaining the Kura-Araxes. In K. O. Weber, E. Hite, L. Khatchadourian, & A. T. Smith (Eds.), *Fitful histories and unruly publics: Rethinking temporality and community in Eurasian archaeology* (pp. 217–257). Brill. https://doi.org/10.1163/9789004325470_011

Rothman, M. (2018). Modelling the Kura-Araxes cultural tradition. In A. Batmaz, G. Bedianashvili, A. Michalewicz, & A. Robinson (Eds.), *Orientalia Lovaniensia Analecta: Vol. 268. Context and connection: Studies on the archaeology of the ancient Near East in honour of Antonio Sagona* (pp. 125–146). Peeters.

Rothman, M. (2022). *Database of diagnostic pottery analysis.* https://doi.org/10.48512/XCV8472172

Rova, E. (2020). A unified terminology for the South-Caucasian "Early Bronze Age": A worthy and achievable target? In M. Kašuba, S. Reinhold, & J. J. Piotrovskij (Eds.), *Archäologie in Iran und Turan: Vol. 19. Der Kaukasus zwischen Osteuropa und Vorderem Orient in der Bronze- und Eisenzeit: Dialog der Kulturen, Kultur des Dialoges* (pp. 353–374). Dietrich Reimer.

Sacco, A. (2021). *More than people and pots: Identity and regionalization in Ancient Egypt during the second intermediate period, ca. 1775-1550 BC* [Doctoral dissertation, Leiden University]. Leiden University Scholarly Publications. https://hdl.handle.net/1887/3192232

Sagona, A. (1998). Social identity and religious ritual in the Kura-Araxes cultural complex: Some observations from Sos Höyük. *Mediterranean Archaeology*, *11*, 13–25.

Sagona, A. (2000). Sos Höyük and the Erzurum region in late prehistory: A provisional chronology for northeast Anatolia. In C. Marro & H. Hauptmann (Eds.), *Varia Anatolica: Vol. 11. Chronologies des pays du Caucase et de l'Euphrate aux IVe-IIIe millenaires* (pp. 329–373). De Boccard.

Sagona, A. (2018). *The archaeology of the Caucasus: From the earliest settlements to the Iron Age*. *Cambridge world archaeology*. Cambridge University Press.

Sattarnezhad, S., Esmaili Atiq, H., Parvin, S., & Azizi, S. (2020). The Iron Age period at the Sarand necropolis in northwestern Iran. *Materiale Şi Cercetãri Arheologice*, *16*(1), 119–127. https://doi.org/10.3406/mcarh.2020.2127

Schmidt, S. C., Martini, S., Staniuk, R., Quatrelivre, C., Hinz, M., Nakoinz, O., Bilger, M., Roth, G., Laabs, J., & Plath, R. V. (2022). *Tutorial on classification in archaeology: Distance matrices, clustering methods and validation*. Zenodo. https://doi.org/10.5281/zenodo.6325372

Schubert, L., Tsitsipas, A., & Donnellan, L. (2019). Statistics in archaeological social network analysis. In A. Trník & I. Medved (Eds.), *AIP Conference Proceedings, Central European Symposium on Thermophysics 2019 (CEST).* AIP Publishing. https://doi.org/10.1063/1.5114035

Seyidov, A., Bakhshaliyev, V., & Mahmudova, V. (2010). *Xalac*. Elm.

Sharp, K. (2016). Fuzzy classification of Gallinazo and Mochica ceramics in the North Coast, Peru using the Jaccard coefficient. In S. Campana, R. Scopigno, G. Carpentiero, & M. Cirillo (Eds.), *CAA2015. Keep the Revolution Going: Proceedings of the 43rd Annual Conference on Computer Applications and Quantitative Methods in Archaeology* (pp. 463–471). Archaeopress.

Skeates, R. (2009). Trade and interaction. In B. Cunliffe, C. Gosden, & R. Joyce (Eds.), *The Oxford Handbook of Archaeology* (pp. 555–578). Oxford University Press.

Smith, A. T. (2005). Prometheus unbound: Southern Caucasia in prehistory. *Journal of World Prehistory*, *19*(4), 229–279. https://doi.org/10.1007/s10963-006-9005-9

Traag, V. A., Waltman, L., & van Eck, N. J. (2019). From Louvain to Leiden: Guaranteeing well-connected communities. *Scientific Reports*, *9*(1), 5233. https://doi.org/10.1038/s41598-019-41695-z

Valeriola, S. de (2021). Can historians trust centrality?, *6*(1). https://doi.org/10.25517/jhnr.v6i1.105 (Journal of Historical Network Research).

Voloshin, V. I. (2009). *Introduction to graph theory*. Nova Science Publishers.

Wehner, D. (2019). *Artefakt-Netzwerke im östlichen Mitteleuropa an der Schwelle zum hohen Mittelalter: Zur Quantifizierung, Visualisierung und Beschaffenheit überregionaler Kommunikations- und Austauschbeziehungen*. *Universitätsforschungen zur prähistorischen Archäologie: Vol. 329*. Dr. Rudolf Habelt.

Weidele, D., van Garderen, M., Golitko, M., Feinman, G. M., & Brandes, U. (2016). On graphical representations of similarity in geo-temporal frequency data. *Journal of Archaeological Science*, *72*, 105–116. https://doi.org/10.1016/j.jas.2016.05.013

Yardimciel, A., Özdermir, A. M., & Işıklı, M. (2018). A survey project on the borderlands of Turkey – Armenia – Nakhchivan – North-western Iran: Preliminary report of the 2014-2016 surveys on the Middle Araxes Basin. In W. Anderson, K. Hopper, & A. Robinson (Eds.), *Oriental and European Archaeology: Vol. 8. Landscape archaeology in Southern Caucasia: Finding common ground in diverse environments proceedings of the workshop held at 10th ICAANE in Vienna, April 2016* (pp. 67–82). Verlag der Österreichischen Akademie der Wissenschaften.

Zalaghi, A., Maziar, S., Aghalari, B., Mashkour, M., & Jayez, M. (2021). Kohne Tepesi: A Kura-Araxes and Parthian settlement in the Araxes River Basin, Northwest Iran. *Journal of Iran National Museum*, *2*(1), 75–100.

Abstract

This master's thesis approaches similarities in pottery decorations and obsidian procurement among Kura-Araxes sites in the Araxes River Basin using Social Network Analysis (SNA). The methodology combines the Jaccard similarity statistic with SNA to create networks based on quantified inter-site similarities in the R software environment. The study processed data from published research and applied SNA to Maziar's (2021) article "Geographical proximity and material culture: The interplay between Syunik and the southern part of the Araxes River Basin in the 6th to the 3rd Millennium BC". Methodological hurdles to overcome included using data from diverse publications for SNA.

The study answered the research question of how similar the sites are regarding their pottery decoration and shared obsidian sources. The results show that the sites are generally dissimilar in their use of pottery decorations and choice of obsidian sources, indicating cultural and economic inhomogeneity in the study area. The obsidian network displays a low influence of location, and the pottery network shows none, indicating a partial tendency toward regionalism for obsidian procurement. The lack of regional standardization could hint at a decentralized nature of the Kura-Araxes cultural horizon regarding pottery decorations. Various obsidian source choices could indicate differing access to and preferences for raw materials. The results of the pottery networks diverge from Maziar's (2021) findings, as higher similarities between sites in the southern part of the Araxes Basin exist. The obsidian similarity networks created in this study align with Maziar's (2021) previous assessment that the shared use of obsidian sources north and south of the Araxes hints at possible communication routes.

The overarching methodological research question was also answered to what limit previously researched case studies are adaptable for SNA. For Maziar's example, the general framework was suitable for SNA, but the data selection required significant changes in site selection. Methodological choices, such as the choice of similarity measure and the integration of the two networks, had to be made. The lack of a clear supra-regional typology for Kura-Araxes ceramics made applying SNA challenging. Furthermore, the data collection revealed that to properly investigate ceramic ASN for the Kura-Araxes period, a unified typology or an extensive supra-regional study is needed to improve such meta-analyses performed.

There are many possibilities to continue the SNA of Kura-Araxes sites. The geographic scope could be expanded toward Lake Urmia. The lake and Araxes River are located in the larger region of

northwestern Iran. Multiple well and less well-studied Kura-Araxes settlements are located around Lake Urmia. The new data can also be utilized as a robustness test since introducing new nodes and edges into the networks challenges structural stability. Regarding the methodology, the present study could benefit from a mixed methods approach of GIS and SNA to better integrate physical and social space because a sizeable spatial expansion through diverse terrain defines the Kura-Araxes cultural horizon. Also, GIS would enable a more thorough investigation of the relationship between material culture similarity and geographical proximity, especially using least-cost paths.